Development of a Knowledge-Based Engineering Application to Support Conceptual Fuselage Design

T.S.L.M. Smeets

Technische Universiteit Delft

TU Delft Delft University of Technology

Challenge the future

Development of a Knowledge-Based Engineering Application to Support Conceptual Fuselage Design

by

T.S.L.M. Smeets

in partial fulfillment of the requirements for the degree of

Master of Science
in Aerospace Engineering

at the Delft University of Technology,
to be defended publicly on Thursday December 7^{th}, 2017 at 14:00.

Student number:	4490428	
Thesis registration number:	167#17#MT#FPP	
Thesis committee:	Prof. dr. ir. L.L.M. Veldhuis,	TU Delft, Chairman
	Dr. ir. G. La Rocca,	TU Delft, Supervisor
	Dr. ir. W.J.C. Verhagen,	TU Delft

Source cover front picture: the Lockheed BoxWing Jet, by Nick Kaloterakis, http://www.kollected.com/
An electronic version of this thesis is available at http://repository.tudelft.nl/.

TU Delft Delft University of Technology

ACKNOWLEDGEMENTS

This Master thesis is the result of ten months of hard work in order to obtain my Master of Science in Aerospace Engineering degree. Throughout these ten months I have been surrounded by people who have helped me achieve this goal and thus I would like to thank them all here.

First of all, I would like to thank my thesis supervisor, Dr.ir Gianfranco La Rocca, for his continuous help throughout my thesis project. His feedback and guidance have been very useful to me to get to where I am today. I would also like to thank Prof.dr.ir. Leo Veldhuis and Dr.ir. Wim Verhagen to have accepted to be on my thesis committee and to assess my thesis work.

Furthermore, I would like to thank Dr.ir. Roelof Vos and Ir. Imco van Gent for their feedback on my work during the project, especially for the green light meeting.

I would also like to thank both my parents, Nathalie and Lucas Smeets, for their support during these two intensive years. Finally I would like to thank my boyfriend Thomas and my friend Laura for being there for me in good times and especially in bad. These two years in Delft would have been a lot harder without them.

T.S.L.M. Smeets
December 2017

SUMMARY

Air travel will significantly grow over the coming years. This is why the world is now entering a challenging period for the Aerospace Industry to meet the requirements for the future of airt ravel. Within Europe, short-medium range flights are of large interest as a transportation system to connect the european regions. On these flights, the focus is turned to reducing turnaround time and increasing passenger comfort. Aircraft design will play a role in meeting the requirements for the future of air travel. Focusing on fuselage design could reduce turnaround time and increase passenger comfort. Turnaround time could be reduced by increasing the aisle width and passenger comfort could be increased by allowing passengers to bring two carry-on luggage instead of one. The geometrical impact of bringing two carry-on luggage is a shift of cargo hold volume to the overhead storage compartments. The impact of these geometrical modifications on the fuselage performances, meaning the fuselage drag and weight, will have to be assessed. Because research is turning its focus to innovative aircraft, it would be interesting to look at the impact of meeting the requirements for the future of air travel on conventional and novel fuselages such as the Oval fuselage or the fuselage of the Prandtl Plane. In fact, the aim of this research is to develop an advanced design tool that supports the conceptual design of conventional and novel fuselages to enable the generation of parametric models of such fuselages. The development of this advanced design tool, called ParaFuse, will allow to perform fuselage performance studies. Hence, this thesis project aims at answering the following question: to what extend can the turnaround time be reduced and passenger's comfort be enhanced by conventional and novel fuselages? What would be the opportunities offered by a Prandtl Plane configuration on the reduction of turnaround time and enhancement of passenger's comfort?

For the purpose of this research, a parametric fuselage model called ParaFuse has been extended and improved. ParaFuse is part of the Multi-Model Generator in the Aircraft Design and Engineering Engine at the TU Delft. In fact, before the start of this master thesis, ParaFuse, which can be referred to as ParaFuse 1.0, could only generate the outer geometry and the cabin configuration of conventional fuselages. This new version of ParaFuse, ParaFuse 2.0, can generate oval fuselages and double deck fuselages. The size and shape of the overhead storage compartments have been modified in order to make the overhead storage compartments more realistic and the continuous cargo holds have been implemented for the Prandtl Plane fuselage. Moreover, ParaFuse has been coupled to the Initiator which is another component of the Design and Engineering Engine that gives starting values to the Multi-Model Generator to generate parametric models of aircraft components. The Initiator has a Fuselage Weight estimation module which is useful to calculate the weight of the fuselage generated in ParaFuse. Following the extension and improvement of ParaFuse as well as the coupling between ParaFuse and the Initiator, a verification and validation of the parametric fuselage model has been performed to gain confidence in the model before performing the fuselage performance studies. The fuselage of an Airbus A320-200, a typical medium range aircraft, has been generated. The generation of the fuselage showed the same fuselage height and width than the reference aircraft. It showed however a slightly shorter fuselage and a much thicker floor due to an innacurate rule used to calculate the floor thickness. From this verification and validation, case studies have been performed for the A320-200 and the Prandtl Plane. The fuselages of both aircraft have been applied four different cross sections: circular, elliptical, oval and double bubble and the fuselage performances have been calculated when increasing the aisle width and shifting cargo hold volume to the overhead storage compartments. Increasing the aisle width results in an increase in fuselage wetted area and form factor thus leading to an increase in fuselage drag area and weight for the A320-200 and the Prandtl Plane. The increase in fuselage drag area and weight is larger for the Prandtl Plane than for the A320-200. Shifting cargo hold volume to the overhead bins results in a decrease in fuselage wetted area and form factor thus leading to a decrease in fuselage drag area and fuselage weight for each cross section type. Combining both geometrical modifications leads to a decrease in fuselage drag area and weight but the decrease is less than when only the cargo hold volume shift is applied to the fuselages. In the end, a comparison between the best Prandtl Plane fuselage and the best Airbus A320-200 fuselage is performed in terms of fuselage performances. The Prandtl Plane fuselage contains 56.79% more passengers than the A320-200 fuselage for a fuselage length only 4.56% larger. Per passenger, the drag area and the weight are lower for the Prandtl Plane than for the conventional fuselage. For a medium range conventional aircraft,

the best fuselage cross section is the elliptical cross section in terms of fuselage performances and the worst cross section is the oval cross section.

ParaFuse has been extended and improved and can now generate conventional and novel fuselages such as the oval fuselage or the Prandtl Plane. This tool has enabled case studies on fuselage performances for conventional and novel fuselages in order to answer the research question. Increasing the aisle width results in higher fuselage drag and weight whereas shifting cargo hold volume to the overhead bins results in lower fuselage drag and weight.

CONTENTS

List of Figures

List of Tables

NOMENCLATURE

ABBREVIATIONS

Acronym	Definition
BWB	Blended Wing Body
BWS	Best Wing System
CAD	Computer-Aided Design
CM	Capability Module
CS	Certification Specifications
DEE	Design and Engineering Engine
EASA	European Aviation Safety Agency
GUI	Graphical User Interface
HLP	High-Level Primitive
ICAO	International Civil Aviation Organization
KBE	Knowledge-Based Engineering
MDO	Multidisciplinary Design Optimization
MMG	Multi-Model Generator
OHSC	Overhead Storage Compartment
TLR	Top-Level Requirements
ULD	Unit Load Device
UML	Unified Modeling Language
XML	eXtensible Markup Language

LIST OF SYMBOLS

LATIN SYMBOLS

Symbol	Description	Unit
a	Speed of sound	$[m/s]$
C_f	Friction coefficient	$[-]$
D	Drag area	$[m^2]$
d	Diameter	$[m]$
h	height	$[m]$
k	Form factor	$[-]$
L	length	$[m]$
M	Cruise Mach number	$[-]$
Re	Reynolds number	$[-]$
S	Area	$[m^2]$
W	Weight	$[kg]$
w	width	$[m]$

GREEK SYMBOLS

Symbol	Description	Unit
μ	Dynamic viscosity	$[kg/(s.m)]$
ρ	Air density	$[kg/m^3]$

SUBSCRIPTS

Symbol	Description
p	parasite
wet	wetted

1

INTRODUCTION

The story of human kind with commercial air travel started in 1914 with only one passenger [11]. Since then, over 65 billion passengers have been using air transport. This number is predicted to double within the next fifteen years on short and long range flights [12]. This rapid increase of passengers inevitably poses new challenges, imperatives and requirements for the future of air travel. These challenges are detailed in the report "Flightpath 2050 Europe's Vision for Aviation" ([13], p.1). The Vice-President of the European Commission and Commissioner for Transport, Siim Kallas, and the Commissioner for Research, Innovation and Science, Máire Geoghegan-Quinn, have regrouped stakeholders of the Aerospace Industry from the "air traffic management, airports, airlines, energy providers and the research community" ([13], p.3) to determine the path for air travel in 2050. In the coming years, air travel will have to comply to very restrictive requirements in terms of costs, emissions, quality, safety and security [13]. These challenging requirements leave no choice to the Aerospace Industry but to drastically improve the aircraft's performances.

Although aircraft have evolved over the years from simple machines to very complex structures, one aircraft configuration has been dominating the Aerospace industry for the past sixty years: the tube-and-wing (TAW) configuration [14]. From propeller airplanes to wide-body jets, this configuration has stood the test of time, as figure 1.1 illustrates. As Dr. Thomas Enders, the Chief Executive Officer of Airbus Group, once said, "if you look at the design of commercial aircraft, we still look like the 60's".

An overview of the development of air travel in terms of key performance indicators can be found in figure 1.2. This graph shows the increase in passengers in air travel, as well as the increase in CO_2 emissions and productivity between 1990 and 2011. It also shows the decrease in specific fuel consumption and fatal accidents during the aforementioned year range. These trends combined with the fact that aircraft design has almost not evolved for the last sixty years show why the focus of the research in civil aviation is now turned to highly innovative designs in terms of aircraft configuration [15].

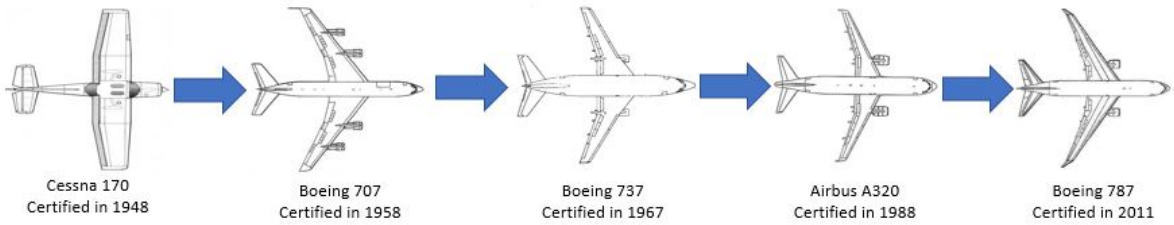

Figure 1.1: Evolution of aircraft over the years

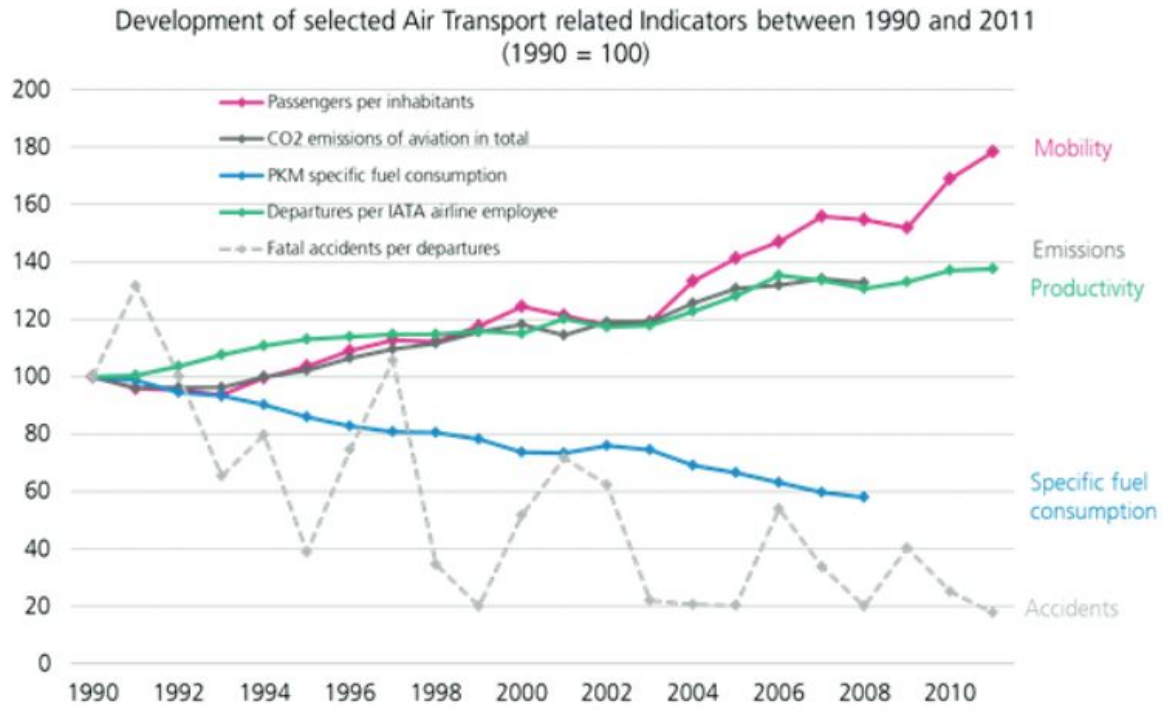

Figure 1.2: Development of Key Air Transport Performance Indicators between 1990 and 2011 [1]

1.1. CHALLENGES OF FUTURE AIR TRAVEL

The future of air travel is at our door and awaits the next technological improvement. With more and more passengers using air travel as a means of transportation each year, the air transportation system must evolve. However this evolvement is constrained by numerous requirements and limitations. A report identifying those requirements has been published by the European commission on "Europe's vision for Aviation" for 2050 [13]. This report focuses on long haul flights but also on short haul flights. In fact, short haul flights are of large interest for the European Aerospace Industry as a transportation system to connect the european regions. Air transport remains the fastest and most direct transportation system to connect the various countries and regions in Europe.

On short haul flights, the focus is turned to reducing turnaround time and increasing passenger's comfort. Turnaround time can be defined as 'the time required to unload an airplane after its arrival at the gate and to prepare it for departure again' [16]. Once the plane lands, two main operations occur: the cabin operations and the ramp operations. The cabin operations are mainly composed of the disembarking of passengers and then of boarding of passengers. The ramp operations mainly consist of unloading and loading the cargo holds. A reduction of the time of these operations would reduce the turnaround time of the aircraft. Increasing passenger's comfort is of interest both in the aircraft and in the airport. In the airport, the focus is turned to offering more services to passengers and to improving the quality of those services. Inside the aircraft, the focus is turned to allocating more space to passengers within the cabin and allowing passengers to board the plane with more carry-on luggage. In fact, especially on short haul flights, passengers tend to not check-in their luggage but rather bring it with them on the plane. This is done mainly to save time upon arrival. The question then arises: how can this turnaround time be reduced and how can passenger's comfort be increased within an aircraft?

1.2. AIRCRAFT DESIGN TO REDUCE TURNAROUND TIME AND INCREASE PASSENGER'S COMFORT

Aircraft design will play a role in meeting the requirements for the future of air travel. As stated in the previous section, the focus is turned to reducing turnaround time and increasing passenger's comfort on short haul flights. Thus, which components of an aircraft play a role in reducing turnaround time and increasing passenger's comfort?

As stated in the previous section, turnaround time essentially focuses on the luggage and the passengers. Passengers and luggage are located in the fuselage. As for passenger's comfort, passengers are located in the fuselage. Thus the main focus for both requirements would be the fuselage. The specific features of the fuselage that impact the fulfillment of both requirements are detailed below.

One of the most time consuming steps in the turnaround time operations is the boarding and disembarking of passengers [16]. A recurring issue when boarding and disembarking a plane is that two passengers cannot cross or at least have difficulties to cross in an aisle. A minimum requirement is set for an aisle width depending on the number of seats abreast [17] for safety reasons. However there is no recommendation for a minimum aisle width so that two passengers can cross. A proper aisle width where two passengers can cross would avoid the recurrent issue of passengers loading and unloading carry-on luggage into the overhead bins which results in blocking the aisle for other passengers. This would reduce the boarding and disembarking time, thus in the end reduce the turnaround time. On short haul flights, passengers have a willingness to bring more carry-on luggage and less check-in luggage. This would mean that there is less luggage volume needed in the cargo holds and more luggage volume needed in the overhead bins. Currently, most major airlines allow passengers to bring one carry-on luggage [1]. Passenger's comfort would then be increased if passenger's were allowed to bring for example two carry-on luggage.

Focusing on fuselage design could allow the aircraft to fulfill some of the requirements of the future of air travel. But then the question arises: which fuselages should be investigated? Only conventional fuselages or also novel fuselages? According to Frediani et al. [18], research to tackle these requirements has to turn its focus to innovative aircraft design configurations.

1.3. FUSELAGE DESIGN: CONVENTIONAL AND UNCONVENTIONAL FUSELAGES

The last two sections have shown the requirements for future air travel and the need to focus on fuselage design to tackle the reduction of turnaround time and increase of passenger's comfort. Key authors in the field of aircraft design such as Torenbeek ([19], [20]) and Frediani ([15], [21]) have expressed their motivation to study innovative aircraft designs as an answer to the requirements set for the future of air travel as well as the current limitations faced for conventional aircraft configurations. Research in innovative aircraft design configurations is driven by the importance of enhancing aerodynamic performances. In the last decades, several new innovative aircraft configurations have been proposed as figure 1.3 depicts.

Numerous research programs are or have been looking into these unconventional configurations [22]. These research programs mainly focus on enhancing the aerodynamic performances of the wings. The fuselage either has a very simple shape (a circular cross section) like the canard, the tandem, the three surface or the C-wing, or is fully integrated in the wing system like the flying wing or the blended wing body. Section 1.2 has shown that the fuselage design is of importance to help meet the reduction of turnaround time and the increase in passenger's comfort thus the focus of the following subsections will be on research programs that have been looking into new fuselage configurations. These new fuselage configurations are the Oval fuselage and the fuselage of the Prandtl Plane. But before detailing these research, it is important to define what a conventional fuselage is.

1.3.1. CONVENTIONAL FUSELAGE

A conventional aircraft is a passenger aircraft that is certified under the European Aviation Safety Agency Certification Specifications 25 [23]. Thus, a conventional fuselage is the fuselage component of a conventional aircraft. Typical short-medium range conventional aircraft are the Airbus A320 and the Boeing B737, depicted in figures 1.4 and 1.5. In general aviation, the cross section of a conventional fuselage can mainly be circular,

[1] https://www.klm.com

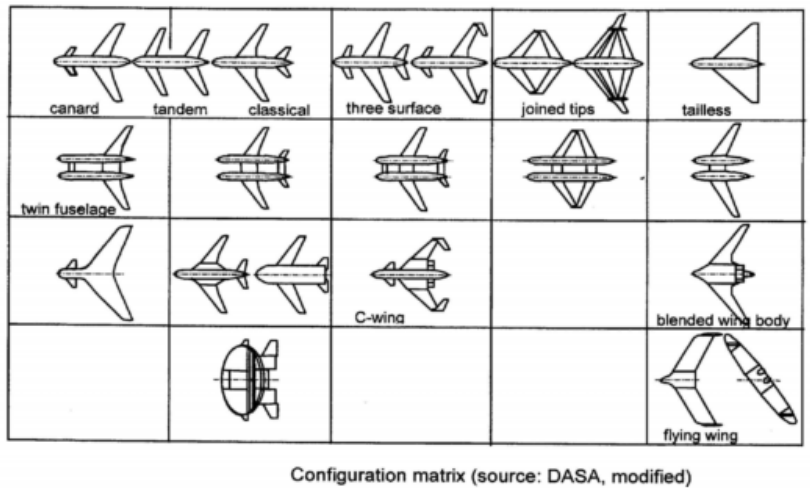

Figure 1.3: Innovative aircraft configurations matrix [2]

Figure 1.4: Airbus A320

Figure 1.5: Boeing B737

elliptical, double bubble or quadrangular. These cross sections are depicted in figure 1.6. Nowadays most airliners have a pressurized cabin thus circular, elliptical and double bubble cross sections are preferred to a quadrangular cross section. A conventional fuselage is usually a single deck aircraft but double deck aircraft have appeared in the last decades such as the Airbus A380 and the Boeing B747. Finally, the cargo holds of a conventional fuselage are divided into a front and an aft cargo holds due to the crossing of the wings in the fuselage, as figure 1.7 depicts.

1.3.2. OVAL FUSELAGE

The concept of the oval fuselage was first introduced as a solution for non-cylindrical pressurized cabins [24]. The oval fuselage concept is a concept used in the investigation of unconventional configurations such as the Blended Wing Body [4]. The oval fuselage does not have a conventional cross section that is depicted in figure 1.6. In fact, the oval fuselage is defined by a single trapezoidal structure [8]. A single arc spans over the top of the box, a single arc spans over the bottom to include the cargo bay and two arcs at each side of the box form the sides. The oval fuselage is depicted in figure 1.8. The structural complexity of this cross section compared to a circular cross section could result in lengthy computational times using the current aircraft design process. The oval fuselage has already been parameterized in two master thesis research projects ([8], [4]).

1.3.3. PRANDTL PLANE FUSELAGE

The Prandtl Plane is a concept dating back from 1999 initiated by Prof. Aldo Frediani. Frediani defines the Prandtl Plane as an aircraft configuration that has been provided with the 'Best Wing System' [25]. Numerous other definitions have been given in open literature. According to Rizzo, the PrandtlPlane is "a new aircraft concept based on the general aim to reduce induced drag" ([26], p.1). As for Thiede, the PrandtlPlane is "a non conventional aircraft with a box shaped wing front view based on the Prandtl's best wing system con-

Figure 1.6: Cross sections of conventional aircraft

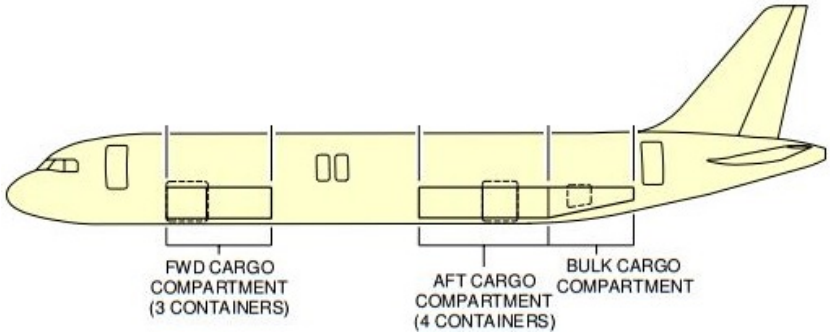

Figure 1.7: Front and aft cargo compartments in the short-medium range aircraft A320-200 [3]

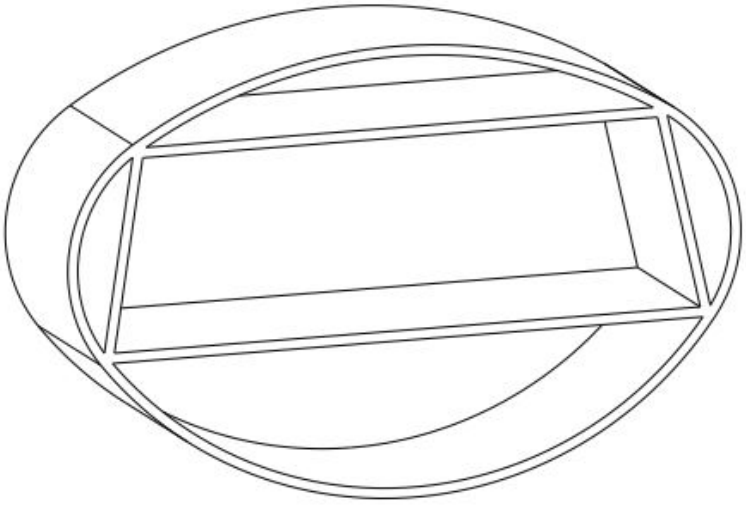

Figure 1.8: The oval fuselage [4]

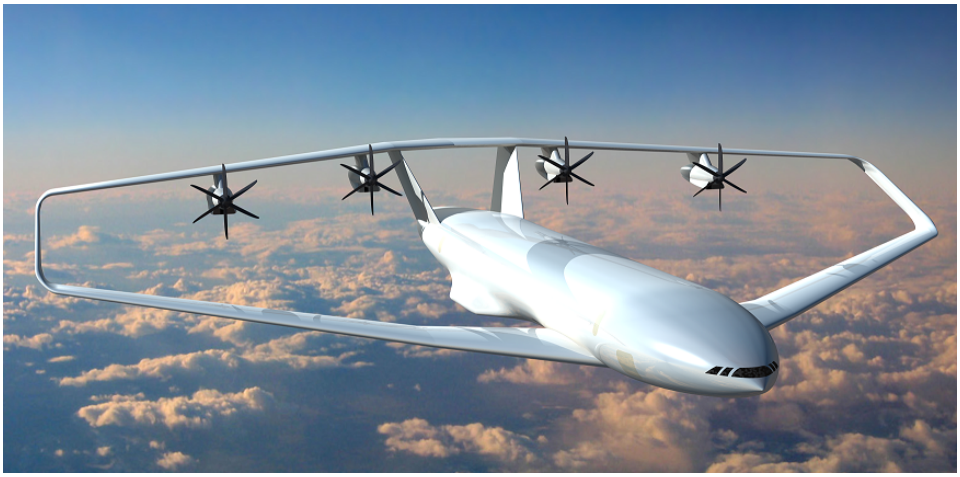

Figure 1.9: Artistic view of PrandtlPlane, *https://commons.wikimedia.org/*

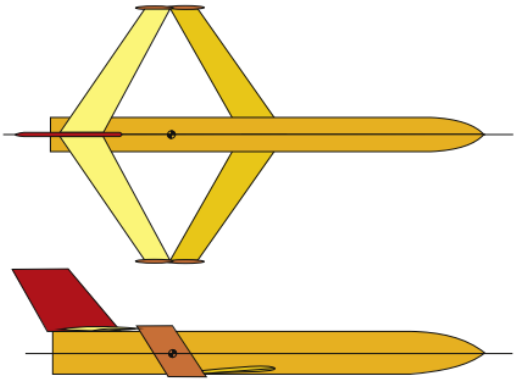

Figure 1.10: Artistic representation of a plane with box shaped wings [5]

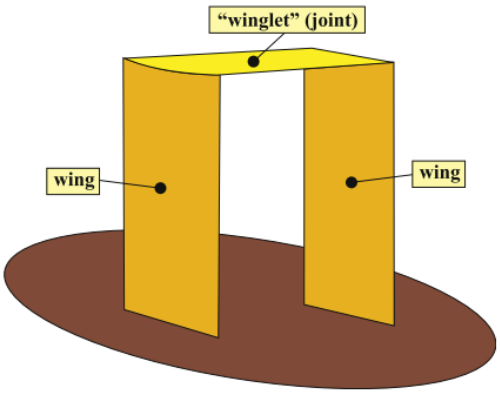

Figure 1.11: Artistic representation of a box shaped wing [5]

cept" ([27], p.316). Finally according to Torenbeek, the PrandtlPlane is an aircraft "conceived to fulfil all the requirements which define a sustainable growth in the civil aviation of the future" ([19], p.139). An artistic view of the Prandtl Plane can be found in figure 1.9. As Frediani stated [25], the main motivation behind the Prandtl Plane's concept is the wing system which was first introduced by Ludwig Prandtl in 1924 [28]. This wing system was called the 'Best Wing System' by Prandtl [28]. Integrating a Best Wing System to an aircraft can lead to an induced drag reduction of up to 30% [5].The box shaped wing configuration is represented in figures 1.10 and in 1.11 [5].

The Prandtl Plane fuselage can be seen as a doubly supported beam with the wings as support as figure 1.10 depicts. The main features of the Prandtl Plane fuselage which make it an unconventional fuselage are its continuous cargo hold and the possibility to have a higher payload capacity than a conventional aircraft with the same fuselage length. This is all enabled by the wing system of the Prandtl Plane. In fact, the front wing of the box shaped wing crosses under the cargo floor in case of a low-wing configuration [18] thus allowing a continuous cargo hold. The higher payload capacity is also enabled by the wing system of the Prandtl Plane. In fact, increasing the payload capacity of an aircraft leads to an increase in wingspan. Indeed, the additional weight caused by the increase in payload implies that more lift needs to be generated by the aircraft. The main lifting surfaces of an aircraft are the wings thus increasing the wingspan will increase the lift and counteract the additional weight. However, increasing the wingspan has numerous negative consequences; a further increase in wingspan leads to additional forces acting on the wing root. This can be balanced with a thicker wing root. However at a certain point the wing root becomes so thick that an incompability appears between the wing root and the dimensions of the fuselage for conventional aircraft [15]. Moreover wingspans cannot be indefinitely increased due to the airport gate dimensions. The box shaped wing system generates

more lift than a conventional wing system because of its two wings generating positive lift. Thus an increase in payload would result in less wingspan increase for a Prandtl Plane than for a conventional aircraft.

The Prandtl Plane is now since May 2017 at the heart of a european project called PARSIFAL. PARSIFAL stands for PrandtlPlane ARchitecture for the Sustainable Improvement of Future AirpLanes. The main goal of the project is to introduce an aircraft with the same dimensions as the Airbus A320 or Boeing 737 but with a higher efficiency and a higher payload capacity. A recent report [10] has been published by the Parsifal project with preliminary designs of a single deck and a double deck fuselage which could be used as a start to look at the reduction of turnaround time and the increase in passenger comfort.

In conclusion, the Aerospace industry is expecting a fast growth in air travel. Within Europe, this growth will mostly impact the short-medium haul flights which are widely used to connect countries and regions. Challenges for the future of air travel have been set to be tackled by 2050. For short-medium haul flights, important requirements are the reduction of turnaround time and the increase in passenger's comfort. These requirements will be mostly tackled by looking at fuselage designs because the main targets of those requirements are the passengers and the luggage that are located in the fuselage of the aircraft. The turnaround time could be reduced by increasing the aisle width which would allow a passenger to pass with his carry-on luggage while another passenger is loading the overhead storage compartment with his carry-on luggage. The passenger's comfort could be increased by allowing passengers to bring two carry-on luggage instead of one on short-medium haul flights. But then arises the question: which tool could be used to increase the aisle width and the overhead storage compartment size on fuselage designs in order to meet the requirements for the future of air travel for short-medium range aircraft?

1.4. PARAFUSE: A PARAMETRIC FUSELAGE MODEL FOR CONVENTIONAL FUSELAGES

The department of Flight Performance and Propulsion at the faculty of Aerospace Engineering at the Delft University of Technology has developed as part of a master thesis project a parametric fuselage model for conventional fuselages at a conceptual design level [9]. This parametric model is part of the Multi-Model Generator which is part of the Design and Engineering Engine (DEE), a Multidisciplinary Optimization approach for complex products with a special focus on aircraft design. The motivation behind the development of the DEE lies in the limitations to the traditional aircraft design process.

1.4.1. LIMITATIONS TO AIRCRAFT DESIGN PROCESS

The aircraft design process is divided into three main phases: the conceptual design phase, the preliminary design phase and the detail design phase. ParaFuse generates parametric fuselage models at a conceptual design level thus the main focus will be on the conceptual design phase. In current practice, the conceptual design phase is too short to find an optimal design solution. Most attention is given to aerodynamics and propulsion in this phase, while other engineering disciplines are only taken into account later. The conceptual design tools are not designed to produce reliable data for unconventional, more complex configurations. They use simple relations and parameters, based on legacy data and experience and are used to compare the performance characteristics for concepts of conventional aircraft configurations. At the end of the conceptual design phase, only a few of the most promising concepts are chosen for further evaluation in the preliminary design phase. Thousands of hours of wind tunnel testing are logged in the preliminary design phase; since it is so time consuming and expensive, only a few models can be tested, and the design can only be modified to a limited degree. Considering the large financial risk of developing a new aircraft, the tendency for the manufacturers is to stick to known configurations, even though new configurations might provide significant performance benefits. Moreover, the traditional design approach is too much dependent on the legacy of previous programs and loses most of its validity as soon as the new design starts deviating too much from reference designs [22].

All these limitations show the need for a new approach to aircraft design. To this end a new approach has been developed: the Multidisciplinary Design Optimization.

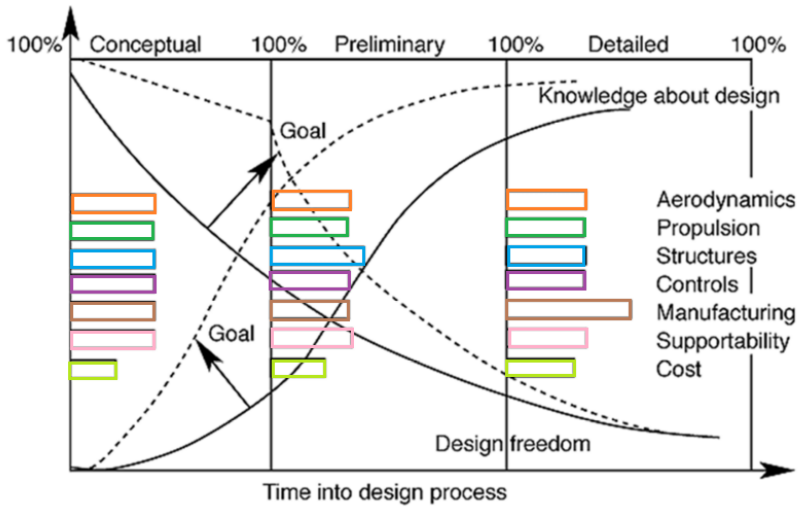

Figure 1.12: Aircraft design process improvements, adapted from [6]

1.4.2. MULTIDISCIPLINARY DESIGN OPTIMIZATION

Multidisciplinary Design Optimization (MDO) is an iterative process which optimizes various disciplines simultaneously in a reduced time. This process allows the designer to acquire more knowledge faster on the design without loosing design freedom. Many different definitions of Multidisciplinary Design Optimization (MDO) can be found in open literature. According to Torenbeek, MDO can be described as "a methodology for the optimum design of systems where the interaction between several functional groups must be considered and where a designer in one functional group is free to significantly affect the performance in other disciplines and at the system level" ([20], p.215). Finally, Sobieszczanski defines multidisciplinary optimization as "a methodology for the design of systems in which strong interaction between disciplines motivates designers to simultaneously manipulate variables in several disciplines" ([29], p.1). Finally, according to La Rocca, the goal of MDO is "to reduce the overall design process duration or allow in the typical time lap the evaluation and optimization of more design configurations" ([22], p.28). An overview of the aircraft design process improvements thanks to MDO can be found in figure 1.12. The first observation that can be made from figure 1.12 is that at each design phase all the disciplines are present and thus necessary to the process. The second observation concerns the curves present in figure 1.12. The dashed line projection from the "Knowledge about Design" shows that more knowledge is required earlier than in the traditional process. The dashed line projection from the "Design Freedom" curve reflects the need to keep more design freedom as the design process progresses.

The goals of such a new design approach are to:

- Increase the knowledge of the design early in the design process,
- Increase design freedom during the design process ,
- Reduce development time and cost,
- Increase per-person productivity,
- Capture the knowledge of the engineering processes.

A technique that is able to provide in the needs described in the previous paragraph is Knowledge-Based Engineering (KBE). The next section will introduce KBE and show how KBE can have a role in supporting the demands of MDO.

1.4.3. KNOWLEDGE BASED ENGINEERING

Numerous key authors in the field of Multidisciplinary Design Optimization have given definitions of Knowledge Based Engineering. At the Delft University of Technology, a course of Knowledge Based Engineering

is taught by Dr.ir. Gianfranco La Rocca and he gives the following definition of KBE: 'Knowledge based engineering (KBE) is engineering using product and process knowledge that has been captured and stored by means of specialized software tools, called KBE systems, to enable its direct exploitation and systematic reuse in the design of new products and variants' [2]. Other definitions have also been given and are quoted below in a chronological order.

According to Chapman, KBE is "an engineering method that represents a merging of object oriented programming (OOP), Artificial Intelligence (AI) techniques and computer-aided design technologies, giving benefit to customised or variant design automation solutions" ([30], p.259). Sainter says that a KBE system can be regarded as a "type of knowledge-based system that performs tasks related to engineering. KBE systems do not express designs with specific data instances, as ordinary CAD systems do, but with sets of rules that enable the design to apply to large classes of similar parts" ([31], p.7). In a later report Chapman gives new definitions of KBE based on the point of view of the person dealing with KBE. For a company manager, KBE is "a technology to compress product development time and cut engineering costs", whereas the user of a KBE system sees it as a" particular kind of programming tool" [32]. Cooper describes KBE as "the use of dedicated software language tools (i.e. KBE systems) in order to capture and reuse product and process engineering knowledge in a convenient and maintainable fashion" ([33], p.1). As for Milton, KBE is "a set of new computer-based techniques and tools that provide a richer and more intelligent use of information technology" ([34], p.13). Other extensive definitions of KBE can be found in [35].

In conclusion it can be said that KBE can be seen as an enabler of MDO, when a generative model is placed within the optimization loop. The knowledge capturing and reusing mechanism of KBE allows for the generation of robust parametric models, which can be used to represent the aircraft at any stage in the design process. Furthermore, KBE is able to record both geometrical and non-geometrical information, so that the translation of the product model to data sets required for various analysis modules can be automated. The faculty of Aerospace Engineering has been working on the development of a MDO system, called the Design and Engineering Engine (DEE), which will be introduced in the following section.

1.4.4. THE DESIGN AND ENGINEERING ENGINE CONCEPT

At the Faculty of Aerospace Engineering, an MDO approach for complex products is being developed, with a special focus on aircraft design. This approach makes use of a so-called Design Engineering Engine (DEE). It supports and accelerates the design process of these complex structures "through the automation of non-creative and repetitive design activities" ([7], p.2). An overview of the Design and Engineering Engine process can be found in figure 1.13. The DEE has four main components: the Initiator, the Multi-Model Generator, the Analysis tools, and the Converger & Evaluator. These main components of the DEE are detailed below:

- Initiator: Provides viable starting values in order to instantiate parametric models of the complex structures,
- Multi-Model Generator (MMG): Instantiates the parametric model and extracts different views of the model into report files to facilitate the Analysis expert tools,
- Analysis (Expert) tools: Evaluates numerous aspects of the design such as the aerodynamic performances,
- Converger & Evaluator: checks the convergence of the design solution and whether the solution meets the design requirements.

Initiator

The Initiator component of the Aircraft DEE is a MATLAB application used to give starting values to the MMG to generate parametric models of aircraft components. The Initiator uses as inputs top level requirements which are then used in a process to provide the initial geometry of the different aircraft components. The Initiator architecture is as follows: it contains an initialization module, a geometry model generator, analysis modules and an optimizer. Among the many analysis modules, the Initiator has a Class II Weight

[2] Quote taken from lecture notes of course AE 4-204 Knowledge Based Engineering, TU Delft.

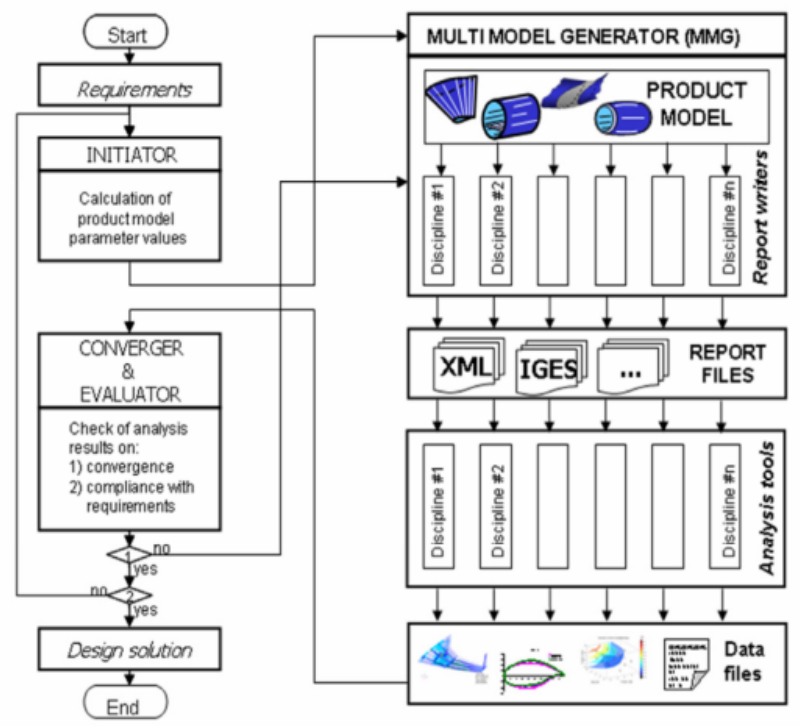

Figure 1.13: The Design and Engineering Engine [7]

Estimation module which estimates the aircraft components' weight with empirical methods. The Initiator also has a Class II.V Weight Estimation which can calculate the wing weight and the fuselage weight more accurately. The fuselage weight estimation can only be performed for conventional circular fuselages and for oval fuselages [4].

Multi-Model Generator

The Multi-Model Generator is a KBE application developed with the two-fold intent of "providing designers with a parametric modeling environment to define generative models of conventional and novel aircraft configurations" and "feeding various analysis tools with dedicated aircraft model abstractions, as required for the verification of the generated design" ([22], p.vi). To meet these objectives, two types of functional blocks have been developed, which constitute the main ingredients of the MMG: the High Level Primitives (HLPs) and the Capability Modules (CMs) [22]. The High Level Primitives are parametric models of the wing, the fuselage and the engine. They can be seen as separate blocks to be assembled to create the geometry of an aircraft concept [22]. Each HLP has been developed in a KBE environment thus allowing them to automatically generate new shapes if the set of inputs would change. The parametric fuselage model is called ParaFuse and has been developed in the KBE environment called ParaPy. It can only generate conventional fuselages. ParaFuse seems like a good candidate to perform the necessary geometrical modifications on fuselage designs to meet the requirements for the future of air travel for short-medium range aircraft. However ParaFuse has limitations that will need to be overcome in order to perform this study.

1.5. LIMITATIONS IN PARAFUSE

ParaFuse generates parametric models of fuselages for conventional aircraft [9]. The scope of ParaFuse is limited to conventional, low-wing, single-deck, passenger aircraft certified under CS 25 airworthiness regulations [23]. To support the design of fuselages of passenger aircraft an inside-out fuselage sizing and outside-in cabin configuration methods have been implemented. The aim of the inside-out fuselage sizing method is to enable the user to evaluate the resulting fuselage dimensions based on top level requirements such as passenger capacity and cargo type, whereas the outside-in cabin configuration method can be used to perform cabin configuration studies on a fuselage with fixed dimensions or a fixed shape. Both methods allow the

designer to specify different levels of passenger comfort. This means ParaFuse can model fuselages with variable seat class distributions, aisle widths, seat spacing and clearance constraints in the cabin. Furthermore, the user can specify the required amount of lavatories and galleys in the cabin.

Many limitations remain for the application ParaFuse in order to perform the study on fulfilling the requirements for the future of air travel for short-medium range aircraft. The first limitation of ParaFuse is the fact that it can only generate conventional fuselages. In fact, the only cross sections that can be generated in ParaFuse are circle, ellipse, double bubble and free form. Free form is a more general cross section shape that is defined with the Class function/Shape function transformation (CST) method proposed by Kulfan ([36], [37]).Thus, currently there is no possibility to investigate an oval fuselage. Implementing the oval fuselage in ParaFuse would be a first step towards the generation of a Blended Wing Body in ParaFuse. Moreover, ParaFuse only allows the generation of single deck aircraft. There is no possibility to generate double deck aircraft. Furthermore, the overhead storage compartments in the cabin have not a properly defined shape. They are generated at the end of the fuselage design process and are drawn based on all the remaining available space in the cabin. No check is performed to verify that the overhead bins can fit the required amount of carry-on luggage. Finally, the cargo holds are generated based on the location of the wing. It is not possible to generate continuous cargo holds without eliminating the wing crossing. Thus, continuous cargo holds could be generated but this would remove an important information on the wing location in case a parametric wing model would be coupled to the parametric fuselage model. Continuous cargo holds are an important feature of the Prandtl Plane fuselage as well as the wing location thus a proper definition of continuous cargo holds has to be implemented.

Once these limitations will be overcome, conventional, oval and Prandtl Plane fuselages will be able to be generated in ParaFuse. Geometrical modifications on the aisle width and the overhead bins size will be performed. The next step of the study will be to evaluate the impact of such modifications on the fuselage performances.

1.6. FUSELAGE PERFORMANCES

The fuselage performances are the fuselage drag area and the fuselage weight. The fuselage drag area corresponds to the drag coefficient multiplied by the reference area. The fuselage drag area is calculated as follows:

$$D_{p,fuselage} = k * C_f * S_{wet} \tag{1.1}$$

This formula accounts for both the friction drag and the form drag which can both be referred to as parasite drag. However no induced drag due to lift is assumed because the fuselage is considered a non-lifting body. The parameter k in equation 1.1 is the form factor and is related to the slenderness of the fuselage [38]. The slenderness ratio is obtained by dividing the fuselage length with the fuselage diameter, both extracted from ParaFuse. The relation between k and the fuselage slenderness $\frac{L}{D}$ is:

$$k = -0.0016 * \left(\frac{L}{D}\right)^3 + 0.0442 * \left(\frac{L}{D}\right)^2 - 0.4131 * \frac{L}{D} + 2.4632 \tag{1.2}$$

This equation was found thanks to a polynomial trendline generated with the data found in [38]. It has a correlation of $R^2 = 0.9995$ which shows a strong correlation between the trendline and the data from [38]. C_f is the skin friction coefficient and is calculated with the logarithmic fit by Von Karman [39]:

$$C_f = \frac{0.455}{log_{10}Re^{2.58}} \tag{1.3}$$

The Reynolds number is obtained with the cruise conditions and the fuselage length. Thus, the fuselage wetted area, length and diameter are necessary to calculate the fuselage drag area. These three parameters can be extracted from ParaFuse.

The fuselage weight is calculated in two ways depending on the cross section shape of the fuselage. If the fuselage is circular or oval, the fuselage weight is calculated thanks to the Class II.V Weight estimation module of the Initiator. However the Initiator cannot calculate the weight of elliptical or double bubble fuselages. Thus, the fuselage weight of elliptical and double bubble fuselages is calculated thanks to the fuselage weight estimation method derived in [40]. The problem is that currently the Initiator and the Multi-Model

Generator currently work sequentially and cannot interoperate. A rethinking of the Design and Engineering Engine process would allow the Initiator to call ParaFuse and calculate the weight of the fuselage generated in ParaFuse. Currently the DEE works sequentially as it is shown in figure 1.13. It is a rigid framework. At the Delft University of Technology in the faculty of Aerospace Engineering, there is a willingness to rethink the process defined in figure 1.13 by enabling a service-oriented approach rather than a sequential approach for the DEE. For this master thesis project, the possibility for the Initiator to call ParaFuse and use it to generate the fuselage geometry instead of using the fuselage configurator module built in the Initiator would allow the calculation of the weight of the fuselage generated in ParaFuse.

1.7. THESIS GOALS

In the context of fast growth of air travel in the years to come, requirements have been set to be tackled by the Aerospace industry by 2050. Short-medium range flights are used widely within Europe to connect the different countries/regions. For these flights, important requirements are the reduction of turnaround time and the increase in passenger's comfort. Reducing turnaround time could be achieved by increasing the aisle width within the fuselage and the increase in passenger's comfort could be achieved by increasing the space allocated to carry-on luggage in the overhead bins. Because research is now looking at novel aircraft designs, it is necessary to study those geometrical modifications on conventional fuselages but also on novel fuselages such as the oval fuselage or the fuselage of the Prandtl Plane. The impact of these geometrical modifications on the fuselage performances will have to be assessed. Thus, the goal of this master thesis is:

the development of an advanced design tool that supports the conceptual design of conventional and novel fuselages to enable the generation of parametric models of such fuselages.

The development of ParaFuse will allow to perform fuselage performance studies. Hence, this thesis project aims at answering the following question:

To what extend can the turnaround time be reduced and passenger's comfort be enhanced by conventional and novel fuselages? What would be the opportunities offered by a Prandtl Plane configuration on the reduction of turn around time and enhancement of passenger's comfort?

Sub-questions are derived from these two research questions:

- What is the impact of varying the number of seats abreast on the fuselage performances while maintaining the same number of passengers?
- What is the impact of increasing the aisle width on the fuselage performances?
- What is the impact of shifting cargo hold volume to the overhead bins on the fuselage performances?
- What is the impact of using different fuselage concepts like the Prandtl Plane on the fuselage performances?

1.8. OUTLINE OF THE REPORT

The structure of this report is as follows. Chapter 2 discusses the extension of the parametric fuselage model ParaFuse. It details the improvements made to ParaFuse which are necessary to conduct the fuselage performance study. A verification and validation of the parametric fuselage model is performed in chapter 3 for a medium range aircraft: the Airbus A320-200. Chapter 4 presents the results of the fuselage performance studies on conventional and oval fuselages. The same studies are performed on the Prandtl Plane fuselage in chapter 5 to which circular, elliptical and oval cross sections are applied. Finally, chapter 6 answers the research question and draws conclusions with respect to the improvements made to ParaFuse and the case studies performed. Recommendations are also presented in chapter 6.

2

EXTENSION OF A PARAMETRIC FUSELAGE MODEL: PARAFUSE

This chapter presents the improvements made to the parametric fuselage model ParaFuse in order to perform the fuselage performance studies to answer the research question. First, section 2.1 describes the architecture of the tool ParaFuse. Section 2.2 describes the necessary improvements made to ParaFuse in order to perform the fuselage performance studies. It details the implementation of these improvements in ParaFuse. Finally, section 2.3 explains the link made between ParaFuse and the Initiator to allow a more service oriented approach of the Design and Engineering Engine which will then be useful in the study cases to calculate the fuselage weight. For clarity purposes, the version of ParaFuse prior to this thesis project will be referred to as ParaFuse 1.0 and the new version of ParaFuse (meaning after this thesis project) will be referred to as ParaFuse 2.0. Thus, ParaFuse 1.0 refers to the work of de Jonge [9] and ParaFuse 2.0 refers to the work in the thesis project described in this report.

2.1. PARAFUSE ARCHITECTURE

ParaFuse is a Knowledge Based Engineering application that generates parametric fuselage models. The application has been developed in a KBE environment called ParaPy. ParaPy is an object oriented programming language built on top of the Python programming language. The version of ParaPy used in this thesis project is version 1.0.7. During the last months of the thesis project, a new version of ParaPy was released, version 2.0, but it was not used in this thesis project.

ParaFuse is made of classes which have inputs, attributes and parts. An example of an input can be found in figure 2.1. An input in ParaFuse and more generally in the programming language ParaPy is first defined by the decorator @Input. Then a name is given to the input: here it is the 'number_of_aisles' input of the class CrossSectionInitiator. A description of the input is given with the type of input. It then returns a value of the type defined in the description, in this case an integer. An example of an attribute can be found in figure 2.2. It is built the same way as an input but with the decorator @Attribute instead. The main difference between an input and an attribute appears after ParaFuse has been run. When ParaFuse is run, a Graphical User Interface (GUI) appears where all the inputs, attributes and parts can be found. An input can be modified by the user in the GUI whereas an attribute cannot. The GUI can then show the impact of modifying an input on the fuselage geometry. Finally an example of a part can be found in figure 2.3. It is defined by the decorator @Part. Again a name is given to the part with a description and the type of part. A part does not return a value like a integer in case of an input or attribute. Instead, it returns a type of class, in this case a PointCloud. The class PointCloud is a class defined within ParaPy which visualizes a group of points effectively as one.

Because of the architecture of ParaFuse, a UML diagram (Unified Modelling Language) has been created in order to grasp the structure of the code. This UML diagram, built in Microsoft Visio, shows all the classes with their inputs, attributes and parts as well as the links between all the classes. The main class is the Fuselage class which contains all the parts, attributes and inputs necessary to generate a fuselage. Each part in the Fuselage class is defined by a type of class which contains other parts, attributes and inputs. For example,

```
@Input
def number_of_aisles(self):
    """Number of aisles in the main cabin as per CS 25 requirements. If :py:attr:`~number_of_seats_abreast` is
    larger than 6 an additional aisle should be positioned in the cabin.

    :rtype: int
    :source: EASA CS 25.817"""
    return 1 if self.number_of_seats_abreast <= 6 else 2
```

Figure 2.1: Example of an input in ParaFuse

```
@Attribute
def max_half_width(self):
    """Maximum half width of the outer cross section

    :rtype: float
    :unit: [m]"""
    return self.max_width_point.y
```

Figure 2.2: Example of an attribute in ParaFuse

```
@Part
def constraints(self):
    """Constraints of the main cabin cross section

    :rtype: PointCloud"""
    return PointCloud(points=self.upper_cross_section_constraints + self.lower_cross_section_constraints
                             if self.lower_cross_section_constraints else self.upper_cross_section_constraints,
                      color='red',
                      hidden=True if self.multiple_deck_configuration else False)
```

Figure 2.3: Example of a part in ParaFuse

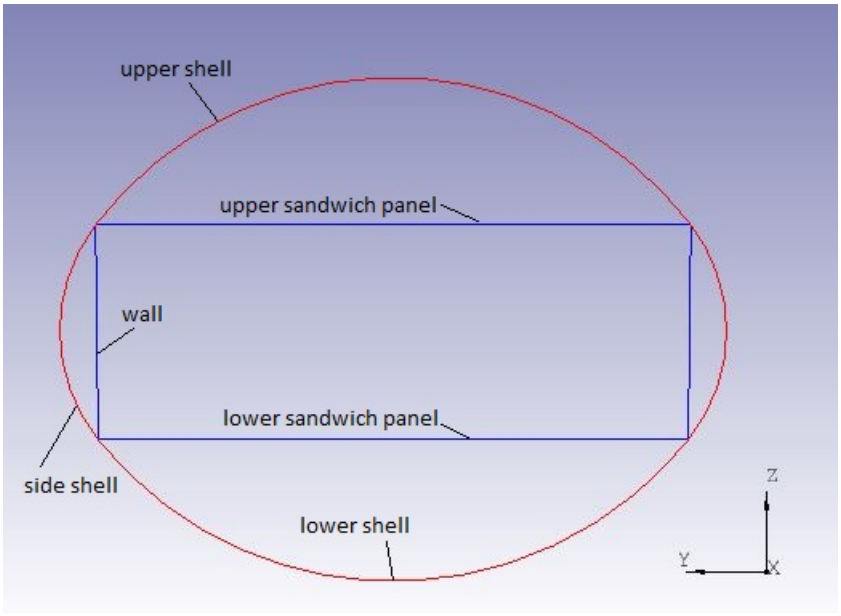

Figure 2.4: Sketch of the oval main cross section, generated in ParaFuse

ParaFuse has a class CargoBay that generates the cargo holds of the fuselage. This CargoBay class is composed of a part cargo which can be defined by two different types of classes: BulkCargo or ContainerizedCargo. The complete list of inputs and attributes of the CargoBay class can be found in appendix A.

2.2. NECESSARY EXTENSIONS AND IMPROVEMENTS TO PERFORM THE FUSELAGE PERFORMANCE STUDIES

This section describes the necessary extensions and improvements made to ParaFuse in order to perform the fuselage performance studies. Each extension and each improvement is allocated a subsection. The extensions presented in this chapter are:

- The oval cross section,
- The double deck fuselage,

The improvements presented in this chapter are:

- The more realistic size and shape of the overhead bins,
- The continuous cargo holds for the Prandtl Plane fuselage.

2.2.1. OVAL CROSS SECTION

In order to study the fuselage performances on the oval fuselage, ParaFuse must be able to generate fuselages with an oval cross section. Thus, the oval cross section has to be implemented in ParaFuse. The oval fuselage has been defined and parameterized in two Master theses at the TU Delft, first by M.F.M. Hoogreef [8] in 2012 and then by K. Schmidt [4] in 2014. These master theses focused on the oval fuselage for the blended wing body. Both parameterizations will be used in this thesis project with alterations for the parameterization made by M.F.M. Hoogreef [8]. The oval fuselage is defined with an outer surface and an inner box. The outer surface is composed of four arcs tangent to one another. These tangency points make up the extreme points of the inner box. This inner box made of an upper sandwich panel, a lower sandwich panel and two walls is necessary because the main cross section is non-cylindrical thus resulting in higher stresses at the four tangency points due to the pressurized cabin. The outer surface and the inner box are defined in figure 2.4. If the upper shell and the lower shell have the same radius, both walls are perfectly vertical.

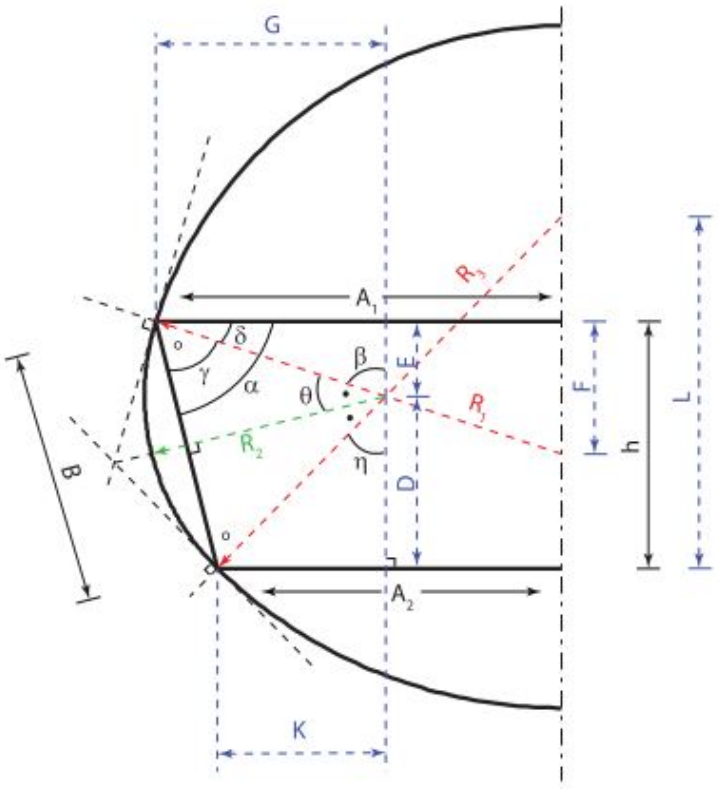

Figure 2.5: Parameterization of oval cross section ([8], p.29)

IMPLEMENTATION OF THE OVAL CROSS SECTION IN THE INSIDE-OUT APPROACH

Before detailing the parameterizations of the oval cross section in the inside-out approach, it is important to describe how the cross section is generated in ParaFuse using the inside-out approach. The inside-out approach follows two main steps: a main cross section sizing procedure followed by a cabin configuration procedure. The generation of the main cross section in ParaFuse is an optimization process which is implemented in the main cross section sizing procedure. A detailed description of the main cross section sizing procedure in the inside-out approach can be found in [9].

Cross section optimization process

The generation of a circular, elliptical, double bubble or free form cross sections in the inside-out approach implemented in ParaFuse is based on an optimization process with a set of design variables. The optimization process aims at minimizing the area of the main cross section. The cross section shape is fitted within constraint points and the cross sectional area is calculated. The set of design variables is modified until the minimum cross sectional area is reached.

For the oval cross section, the optimization process has one design variable: it can be A_2 the floor width or R_2 the radius of the side arc, defined in figure 2.5. In fact, two optimization processes are possible when generating an oval cross section in ParaFuse. The main difference between both optimizations is the set of constraint points. Constraints points are made of upper constraint points and lower constraint points. Upper constraint points are defined by the aisle height h and the floor width A_2, which are defined in figure 2.5. These constraints are the side wall clearance and the eye clerance constraint and are shown in figure 2.6. The side wall clearance is an input given by the user to specify a minimum space between the seats and the sidewall. The eye clearance constraint is calculated thanks to two inputs. The values of these inputs are given in table 5.3. The sitting eye height corresponds to a measurement from buttocks to eyes of the 95th percentile US male [41]. The eye clearance radius is given by Torenbeek in [40] page 71. The eye clearance constraint corresponds to the eye clearance radius added to the sitting eye height.

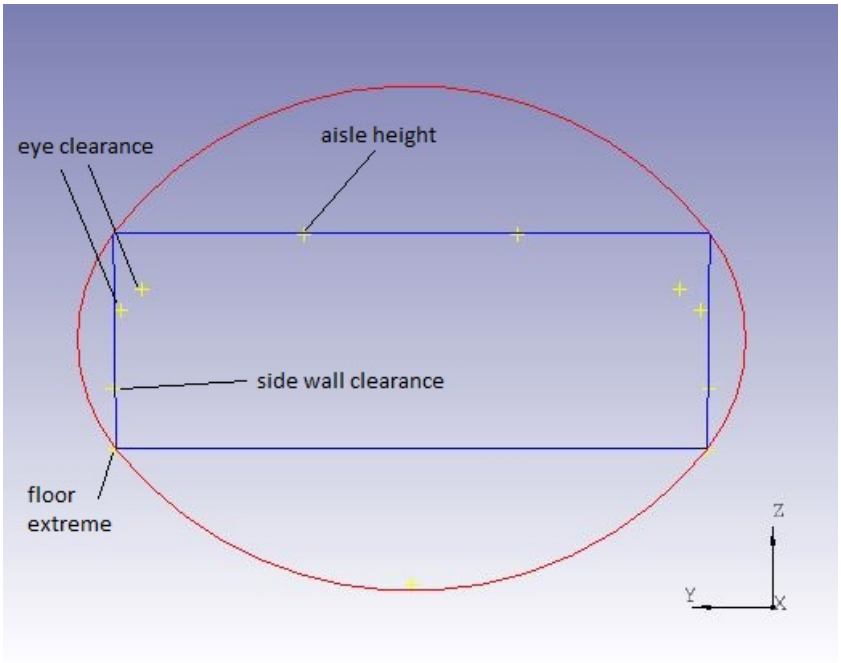

Figure 2.6: Upper constraints used to define the main cross section

Table 2.1: Inputs used to calculate the eye clearance constraints

Input	Unit	Value
Sitting eye height [41]	$[m]$	0.89
Eye clearance constraint [40]	$[m]$	0.25

Lower constraint points correspond to the cargo extreme points which are defined in figure 2.7. The blue dots represent the cargo extreme points. These are defined by the height and the width of the cargo hold. The height and width of the cargo hold are inputs given by the user. If no height and width in specified by the user, then the cargo hold extreme points are not taken into account when fitting the cross section. Thus, if the set of constraint points is only made of the upper constraints, the design variable of the optimization process is R_2. However, if the set of constraint points is made of the upper and the lower constraints, then the design variable is A_2. The parameterization of the oval cross section varies between the two optimization processes.

Parameterization of the oval cross section

The parameterization of M.F.M. Hoogreef [8] is used for the inside-out approach. This parameterization

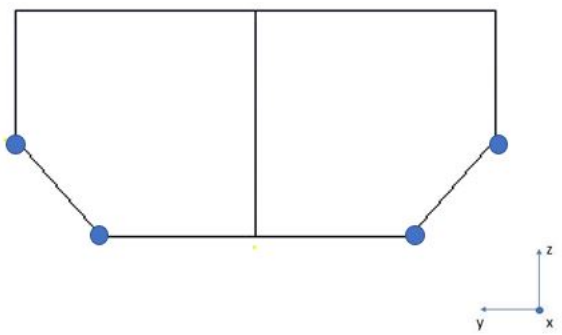

Figure 2.7: Definition of cargo extreme points

is defined in figure 2.5. The parameterization of K. Schmidt [4] needs far less computations than the one of Hoogreef but is not suitable for an inside-out approach because it needs parameters which would fix the outer shape which goes against the foundation of an inside-out approach.

The generation of the oval cross section in the inside-out approach makes use of different calculations whether the user specifies a height and a width for the cargo holds or not. If no dimensions for the cargo holds are defined, the following calculations are performed in order to determine the oval cross section. First, four parameters need to be defined: h, $A1$, $A2$ and $R2$. The height of the inner box, h, is defined by the aisle height which is given as input in the inside-out approach. Then, $A1$, the length of the upper sandwich panel of the inner box is defined based on the upper constraints of the main cross section. $A1$ is defined as the maximum y-coordinate of these points. $A2$, the floor width, is then defined as the y-coordinate of the floor extreme point. From these three parameters, the parameter B, the length of the side wall, can be defined in equation 2.1.

$$B = \sqrt{h^2 + (A1 - A2)^2} \tag{2.1}$$

However these three parameters are not enough to determine all the oval cross section parameters. A last parameter needs to be defined which is $R2$, the radius of the side shell arc. This value is guessed and will be the design variable of the cross section optimization process. Once the four parameters aforementioned are determined, all the other parameters depicted in figure 2.5 can be computed:

$$\alpha = atan\left(\frac{h}{A1 - A2}\right) \tag{2.2}$$

$$\theta = asin\left(\frac{B}{2 * R2}\right) \tag{2.3}$$

$$\gamma = acos\left(\frac{B}{2 * R}\right) \tag{2.4}$$

$$\delta = \alpha - \gamma \tag{2.5}$$

$$\beta = \frac{\pi}{2} - \delta \tag{2.6}$$

$$\eta = \pi - 2 * \theta - \beta \tag{2.7}$$

Calculation of R1 and R3

$$R1 = \frac{A1}{cos(\delta)} \tag{2.8}$$

$$R3 = \frac{A2}{sin(\eta)} \tag{2.9}$$

Find location of center of circle R1 and R3

$$F = R1 * sin(\delta) \tag{2.10}$$

$$L = R3 * cos(\eta) \tag{2.11}$$

Find location of center of circle R2

$$G = R2 * cos(\delta) \tag{2.12}$$

$$E = R2 * sin(\delta) \tag{2.13}$$

From the parameters F, L, G and E the positions of the centers of the four arcs can be defined. The parameter $R2$, the design variable of the optimization process, is chosen in order to reach the minimum cross sectional area.

This parameterization is only suitable when there is no dimensions for the cargo holds are defined. If a height and a width for the cargo holds are defined, for example in order to fit LD3 type Unit Load Devices (ULDs), then the parameterization needs to be modified. Indeed, fixing all four parameters h, $A1$, $A2$ and $R2$ results in an inconsistency if the height of the cargo is to be fixed as well. In fact fixing the cargo height as well as h, $A1$, and $A2$ results in a dependency between these variables and R2. There is no optimization possible. A new parameterization is then needed. The cargo hold height is either the height of a specific unit

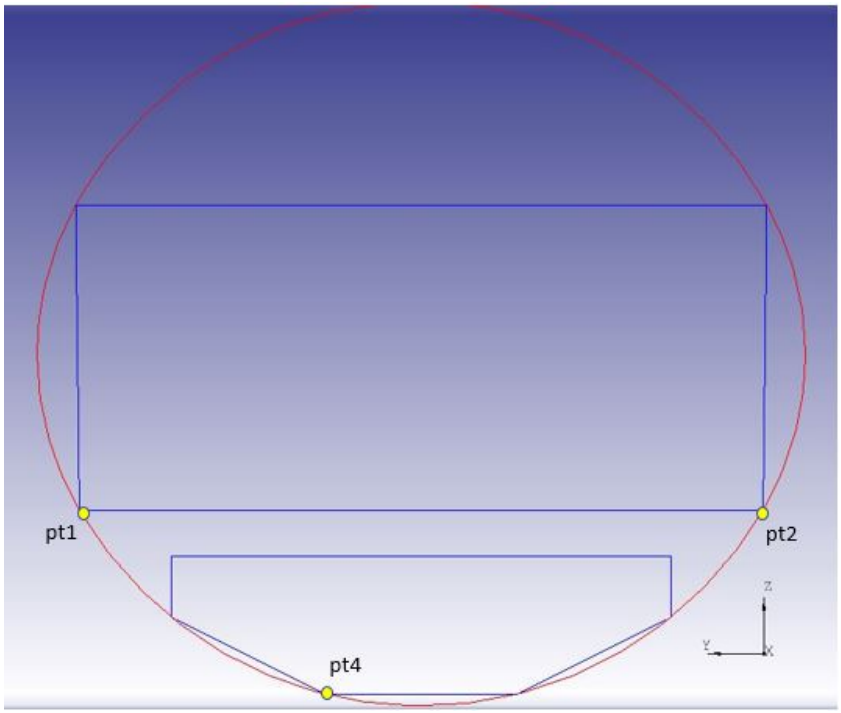

Figure 2.8: Definition of extreme cargo points in main cross section, generated in ParaFuse

load device or the input minimum_bulk_bay_height given by the user in case of bulk cargo.

This new parameterization has a different design variable. Instead of fixing $A2$, the floor width, the optimization process defines $A2$ as the design variable and sets its lower bound as the y-coordinate of the floor extreme point defined in figure 2.5. The parameters h and $A1$ are defined as in the previous parameterization. After fixing these three parameters ($A2$ can be considered as fixed as it is the design variable and will vary at every loop in order to reach the minimum cross sectional area), the first step is to find R3 and the center of the bottom shell. To do so, the points depicted in figure 2.8 are defined.

The arc of the bottom shell can be defined as detailed below. The equation of an arc is defined as follows:

$$Ax^2 + Ay^2 + Bx + Cy + D = 0 \tag{2.14}$$

Before going further, for clarity purposes, the coordinates of the points in figure 2.8 are allocated new names:

$$\begin{aligned} x_1 &= y_{pt1} \\ y_1 &= z_{pt1} \\ x_2 &= y_{pt2} \\ y_2 &= z_{pt2} \\ x_3 &= y_{pt4} \\ y_3 &= z_{pt4} \end{aligned} \tag{2.15}$$

Thus, after substituting the coordinates of the three points in equation 2.14, the set of equations found can be defined as the following determinant:

$$\begin{bmatrix} x^2+y^2 & x & y & 1 \\ x_1^2+y_1^2 & x_1 & y_1 & 1 \\ x_2^2+y_2^2 & x_2 & y_2 & 1 \\ x_3^2+y_3^2 & x_3 & y_3 & 1 \end{bmatrix} \tag{2.16}$$

In order to determine coefficients A, B, C and D from equation 2.14, the following determinants must be solved:

$$A = \begin{bmatrix} x_1 & y_1 & 1 \\ x_2 & y_2 & 1 \\ x_3 & y_3 & 1 \end{bmatrix} \tag{2.17}$$

$$B = -\begin{bmatrix} x_1^2 + y_1^2 & y_1 & 1 \\ x_2^2 + y_2^2 & y_2 & 1 \\ x_3^2 + y_3^2 & y_3 & 1 \end{bmatrix} \tag{2.18}$$

$$C = \begin{bmatrix} x_1^2 + y_1^2 & x_1 & 1 \\ x_2^2 + y_2^2 & x_2 & 1 \\ x_3^2 + y_3^2 & x_3 & 1 \end{bmatrix} \tag{2.19}$$

$$D = \begin{bmatrix} x_1^2 + y_1^2 & x_1 & y_1 \\ x_2^2 + y_2^2 & x_2 & y_2 \\ x_3^2 + y_3^2 & x_3 & y_3 \end{bmatrix} \tag{2.20}$$

Then R3 and the center of the bottom shell can be computed using equations 2.21 and 2.22. The center is defined by two coordinates x and y defined in equation 2.22.

$$R3 = \sqrt{\frac{B^2 + C^2 - 4AD}{4A^2}} \tag{2.21}$$

$$\begin{aligned} x &= \frac{-B}{2A} \\ y &= \frac{-C}{2A} \end{aligned} \tag{2.22}$$

The main difference with the previous parameterization is the fact that the difference between $A1$ and $A2$ can be positive or negative. In other words, the floor width can either be higher, lower or equal to the ceiling width. In order to distinguish both cases, figure 2.9 has been created. This figure shows the differences between two cases: if $A1 > A2$ or if $A1 < A2$.

From this figure, σ, a, B, c and g can be immediately calculated and are independent on the case:

$$\begin{aligned} \sigma &= acos\left(\frac{A2}{R3}\right) \\ a &= 2 * A1 \\ c &= 2 * A2 \\ B &= \sqrt{h^2 + (A1 - A2)^2} \\ g &= \frac{|a - c|}{2} \end{aligned} \tag{2.23}$$

Then depending on whether $A1 > A2$ or $A1 < A2$, λ and α can be calculated:
If A1 > A2:

$$\begin{aligned} \alpha &= acos\left(\frac{g^2 + B^2 - h^2}{2 * g * B}\right) \\ \lambda &= \pi - \alpha \end{aligned} \tag{2.24}$$

If A1 < A2:

$$\begin{aligned} \lambda &= acos\left(\frac{g^2 + B^2 - h^2}{2 * g * B}\right) \\ \alpha &= \pi - \lambda \end{aligned} \tag{2.25}$$

It is then possible to calculate the radius of the side shell $R2$:

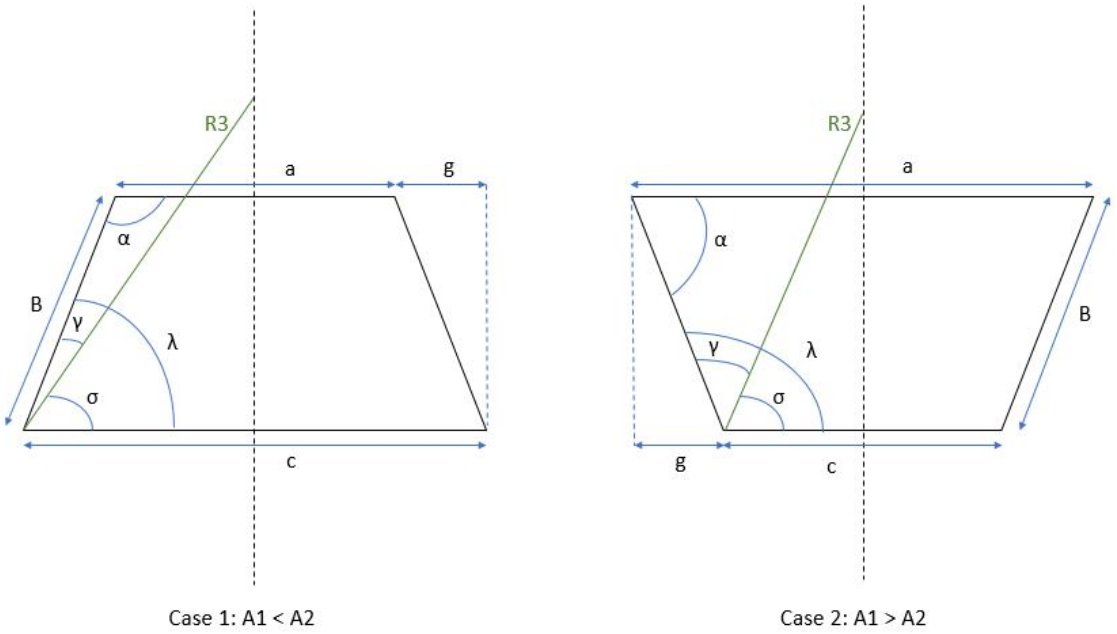

Figure 2.9: Inner box shape dependent on the floor and ceiling widths

$$\begin{aligned} \gamma &= \lambda - \sigma \\ R2 &= \frac{B}{cos(\eta)} \end{aligned} \tag{2.26}$$

The other parameters are then calculated as in the previous parameterization and the oval cross section can be generated.

IMPLEMENTATION OF THE OVAL CROSS SECTION IN THE OUTSIDE-IN APPROACH

The implementation of the oval cross section in the outside-in approach does not make use of an optimization process because the outer shape is already defined by the user. The outside-in approach follows the same steps as the inside-out approach but the steos themselves are different. In fact, for the outside-in approach, it is the parameterization of K. Schmidt which has been chosen [4]. Indeed, this parameterization needs far less computations than the one of M.F.M. Hoogreef [8] and is suitable for the outside-in approach. It uses parameters to first define the outer shape and then use this outer shape to define the cabin configuration which is the foundation of the outside-in approach. A detailed description of the outside-in approach can be found in [9].

In order to generate the oval cross section, a new class named 'Oval' is created. The class uses as inputs the parameters defined in figure 2.10: $h1$, $h2$, $h3$, and wf. The parameterization defined in [4] results in solving equation 2.27:

$$tan^{-1}\left(\frac{wf}{h3}\right) - tan^{-1}\left(\frac{wc}{h1}\right) - tan^{-1}\left(\frac{wc - wf}{h2}\right) = 0 \tag{2.27}$$

Solving this equation results in finding the ceiling width wc. $h1$, $h2$, $h3$, wf, and wc are then known. The top and bottom arcs are thus defined by three points making it possible to find the radius and the center of each arc. Finally, as in the previous parameterization, the radius and the center of the side arc are found thanks to the tangency with the bottom and top arcs at the box corners.

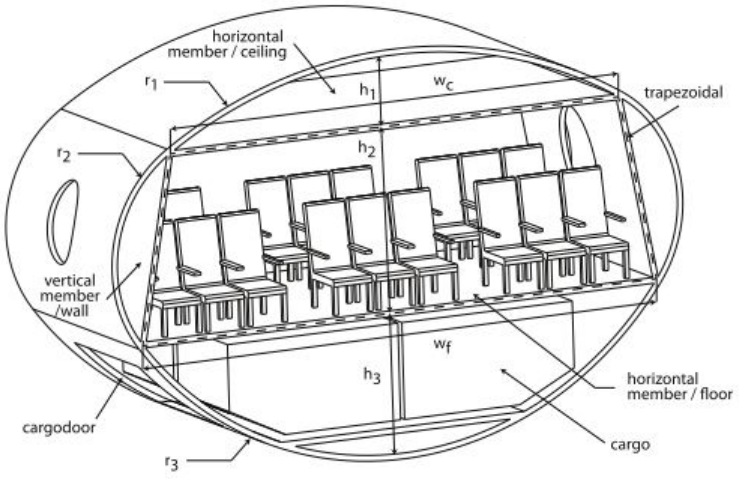

Figure 2.10: The oval cross section, based on Schmidt's parameterization [4]

Table 2.2: Differences in input files between single deck and double deck fuselage

Input	Modified input	Missing input	Additional input
multiple_deck	x		
percentage_first		x	
percentage_business		x	
percentage_premium_economy		x	
number_of_seats_abreast		x	
Lower deck parameters			x
Upper deck parameters			x

2.2.2. DOUBLE DECK AIRCRAFT

The capability to generate double deck aircraft has only implemented for the inside-out approach. The generation of the double deck fuselage follows the same general inside-out procedure as the single deck fuselage: generation of the main cross section and then generation of the cabin configuration. In order to understand how this double deck fuselage has been implemented, it is important to show first the differences in the input files between a single deck and a double deck fuselage. The differences are summarized in table 2.2. The input multiple_deck is a setting that can be set to True or False. If this setting is set to False, the fuselage is a single deck. If the setting is set to True, the fuselage is a double deck. The inputs percentage_first, percentage_business, percentage_premium_economy and number_of_seats_abreast have been removed from the input file for double deck fuselages and have been relocated under lower deck and upper deck parameters.

The first step in the generation of a double deck fuselage using the inside-out approach is the generation of the main cross section. The process of the generation of the main cross section can be found in figure 2.11. The first task is to read the inputs. Table 2.2 has already shown the differences in input file between a single deck and a double deck fuselage. The second task is to determine the number of seats abreast and the number of aisles. This task is performed independently for each deck. Indeed, each deck has a certain number of passengers and a percentage of seat classes. The number of seats abreast can be specified per deck or can be calculated per deck based on the number of passengers with the statistical relation derived by Nita and Scholz [42]. The number of aisles is then derived from the number of seats abreast according to the CS 25 requirements [23]. The third task is to determine the constraints of the upper section. In the case of a double deck fuselage, the constraints of the upper section are the constraints of the upper section of the lower and the upper deck. The constraints of the upper section for the single deck and the double deck fuselages can be found respectively in figures 2.12 and 2.13. The fourth task is to determine the constraints of the lower section. The determination of these constraints does not vary between a single deck and a double deck fuselage. The constraints have already been defined in figure 2.7. The last tasks are performed as for a single deck fuselage.

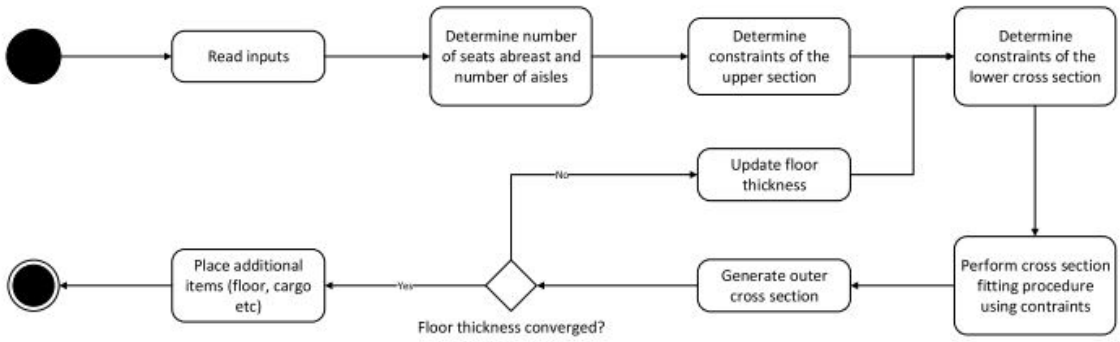

Figure 2.11: Generation of the main cross section in the inside-out approach, based on [9]

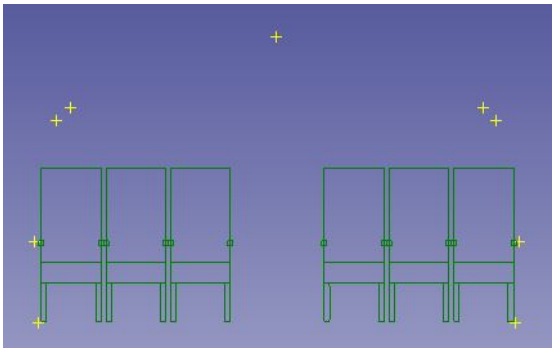

Figure 2.12: Constraints of the upper section for a single deck fuselage

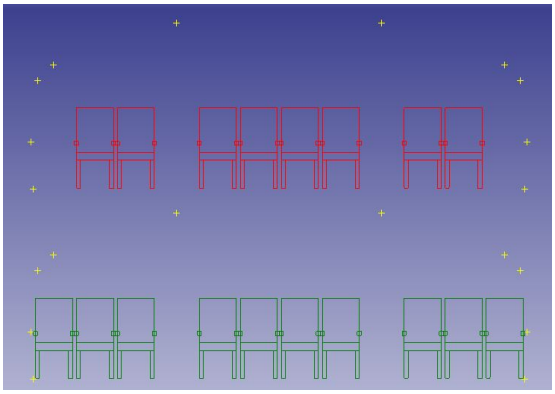

Figure 2.13: Constraints of the upper section for a double deck fuselage

Once the main cross section has been generated, it is used to generate the nose and tail cone surface. The cabin configuration process can then start. This cabin configuration process is performed independently between the lower and the upper deck. In fact, two new classes have been introduced into ParaFuse: a lower deck class and an upper deck class. Each class follows the process described in figure 2.14. The number of exits, lavatories and galleys is calculated independently for the lower and upper decks based on the number of passengers on each deck. The positioning of the emergency exits is also performed independently per deck. Thus, there is currently no rule implemented in ParaFuse to stagger the emergency exits of both decks. An assumption has been made when defining the double deck aircraft: there are no seats in the nose cone on the upper deck. This choice has been made in order to allocate space for the stairs and any other storage compartments such as crew resting, coat storage and passenger lounges as in the Airbus A380.

ParaFuse can now generate double deck fuselages thanks to this improvement. This will be useful for the study with the Prandtl Plane on fuselage performances. In fact, as it was mentioned in section 1.3.3, a report [10] was recently released with the preliminary design of a single deck and a double deck fuselage. Double deck fuselages can however only be generated using the inside-out approach currently. The implementation of the double deck fuselage in the outside-in approach would require modifications on the generation of the cross section step and the class that generates the main cabin. In fact, the cabin configuration process of the outside-in approach uses the same classes for the generation of the nose and the tail cone as the inside-out approach thus these classes have already been adapted for double deck fuselages.

2.2.3. OVERHEAD STORAGE COMPARTMENTS

ParaFuse 1.0 [9] did not take into account the size of the overhead storage compartments (OHSC) in the sizing process of the main cross section. In order to study the possibility of increasing passenger comfort by allowing passengers to bring two carry-on luggage instead of one, it is necessary to account for the OHSC

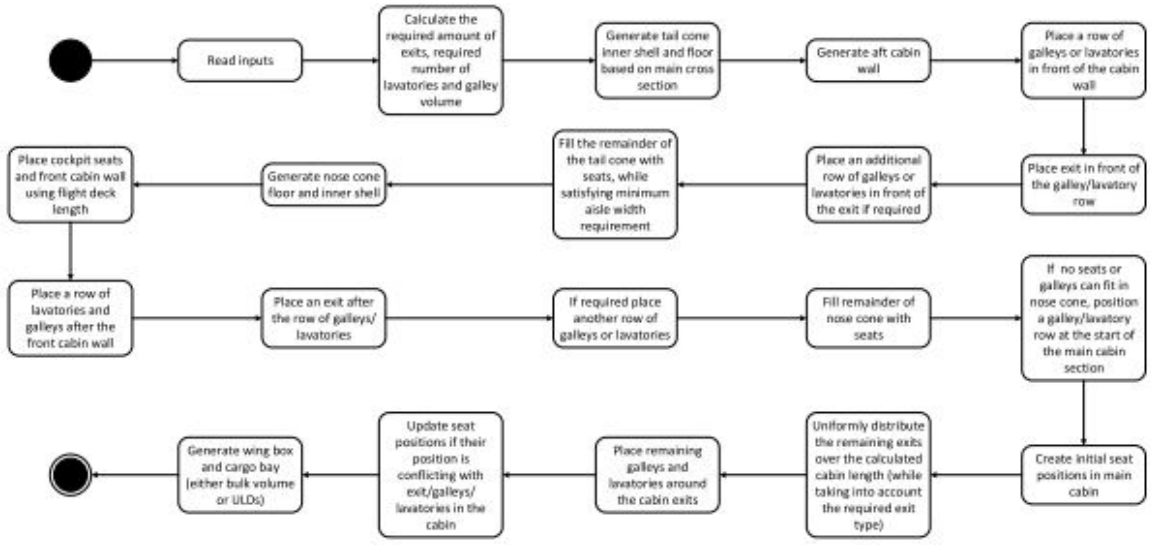

Figure 2.14: Cabin configuration process in the inside-out approach, based on [9]

dimensions.

The size of the OHSC has been integrated in the sizing process of the main cross section in the inside-out approach and is used to determine the shape of the main cross section. It has been integrated by defining a minimum height of the OHSC. This minimum height is a user defined input parameter in ParaFuse to ensure that at least one carry-on luggage can fit inside the OHSC. A carry-on luggage has a size of 55x35x25 cm according to most of the major airlines [1]. Carry-on luggage are placed horizontally in the overhead bins thus a minimum height of 25 cm has been set by default in ParaFuse. But specifying a minimum height for the overhead bins is not enough to ensure that at least one carry-on luggage can be brought per passenger. A volume check has been implemented after the generation of the OHSCs. This volume check verifies that the volume of the OHSCs is equal to or higher than the volume of the number of passengers multiplied by the volume of one carry-on luggage.

The shape of the OHSC has also been modified. Two main improvements have been added to the shape of the overhead bins. The first improvement is the fact that the OHSC cannot extend higher than the aisle height. As can be seen in figure 2.15, the overhead storage compartments depicted in light red generated with ParaFuse 1.0 extend up to the ceiling whereas the overhead storage compartments depicted in blue generated with ParaFuse 2.0 extend up to the aisle height which is shown with the black arrow. Secondly, the OHSCs never extend up to the aisle because there would not be enough space to open the doors of both overhead bins at the same time. The distance between both OHSCs is calculated so that there is enough space to open both doors at the same time. This distance is computed as twice the OHSC height. An example of the OHSC height and the distance between both OHSCs is given in figure 2.15. The red arrows show the lengths in ParaFuse 1.0 and the blue arrows show the lengths in ParaFuse 2.0. In ParaFuse 1.0, the OHSC height is 1.01 m and the distance between both OHSC is 0.76 m. It is not possible to open both doors simultaneously and not even possible to fully open one door. In ParaFuse 2.0, the OHSC height is 0.64 m and the distance between both OHSC is 1.28 m. This distance is exactly twice the OHSC height because it is the rule that has been implemented in ParaFuse. Both doors can open simultaneously in ParaFuse 2.0. Finally, a simple rounded shape was added to where the door is located in the overhead bins.

All these adjustments have been performed by looking at many different cross sections of commercial aircraft. The actual volume of the overhead bins is not provided by the aircraft manufacturer but the shape of the overhead bin is given in the report on 'Aircraft Characteristics Airport and Maintenant Planning' [3]. Thus, to prove that the overhead bin shape in figure 2.15 is realistic, an overlap of the cross section of the A320-200 given in the report [3] with the cross section of the A320-200 generated in ParaFuse can be found in figure 2.16.

[1] www.klm.com

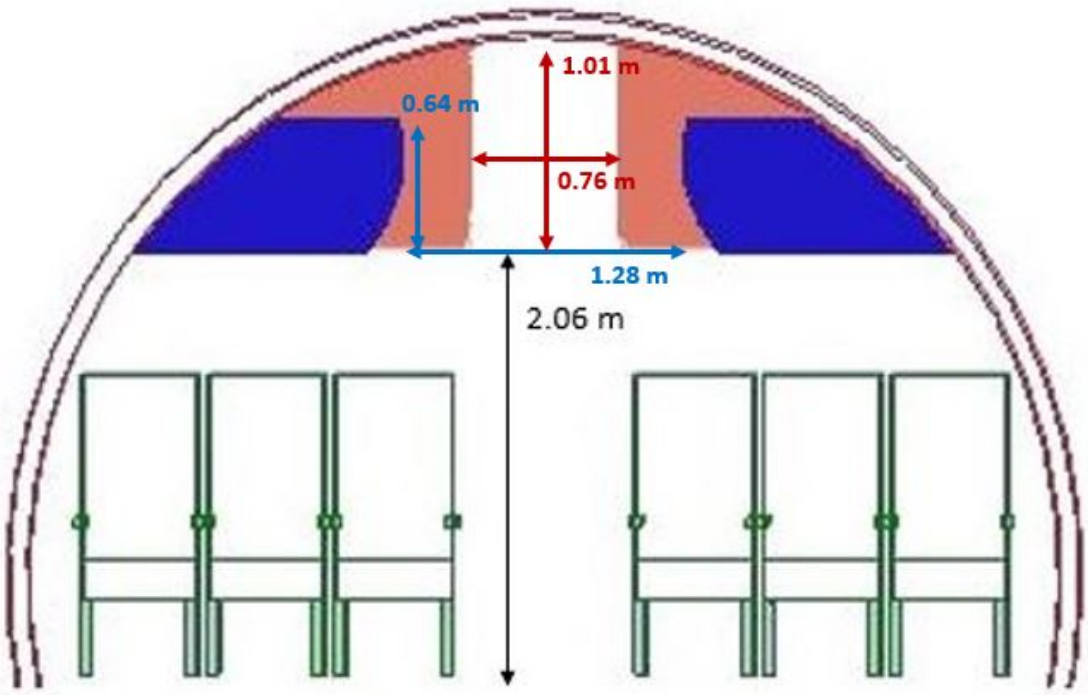

Figure 2.15: Overlap of overhead storage compartments from ParaFuse 1.0 and ParaFuse 2.0

Finally, the overhead bins show discontinuities after being generated. These discontinuities are shown by red arrows in figure 2.17. These discontinuities can be explained by two causes. First, the OHSCs are generated based on the location of the different seat classes. Thus, each OHSC is generated based on a seat class hence the discontinuity presented by arrow number 2. Secondly, the overhead bins are generated independently in the nose cone, the tail cone and the main cabin, hence the discontinuities presented by arrows number 1 and 3. The discontinuity issue was resolved by calculating the volume in the discontinuity and adding it to the total volume of the overhead bins.

ParaFuse can now generate overhead bins with a realistic size and shape. Thanks to this feature, it is possible to increase the overhead bin size so that passengers can bring not one but two carry-on luggage in order to increase passenger comfort. It will then be possible to perform the study on fuselage performances when increasing passenger comfort.

2.2.4. CARGO HOLDS

To perform the study on increasing passenger comfort, the overhead bin size has to be increased. In this thesis project, comfort is defined by the possibility for passengers to bring more than one carry-on luggage in the cabin. An assumption is made in this thesis: passengers tend to check-in their luggage less and less. This means that less and less luggage is stored in the cargo holds. Thus, while increasing the overhead bin size, a reduction in cargo hold volume would be useful. But for that, it is necessary to allow ParaFuse to modify the cargo hold size. It is not possible to modifiy the size of Unit Load Devices (ULD) because the various ULDs have fixed dimensions. However, it is possible to vary the size of bulk cargo. Thus, the definition of bulk cargo holds is extended by adding a minimum bulk bay height requirement. A minimum of 50 cm is required according to Torenbeek [40]. If a minimum of less than 50 cm is given by the user, a warning alerts the user that the minimum bulk bay height has been increased to 50 cm to comply with aircraft design requirements.

Another extension is added to ParaFuse: the possibility to generate continuous cargo holds. Continuous cargo holds is an important feature of the Prandtl Plane fuselage. Having a continuous cargo hold means that

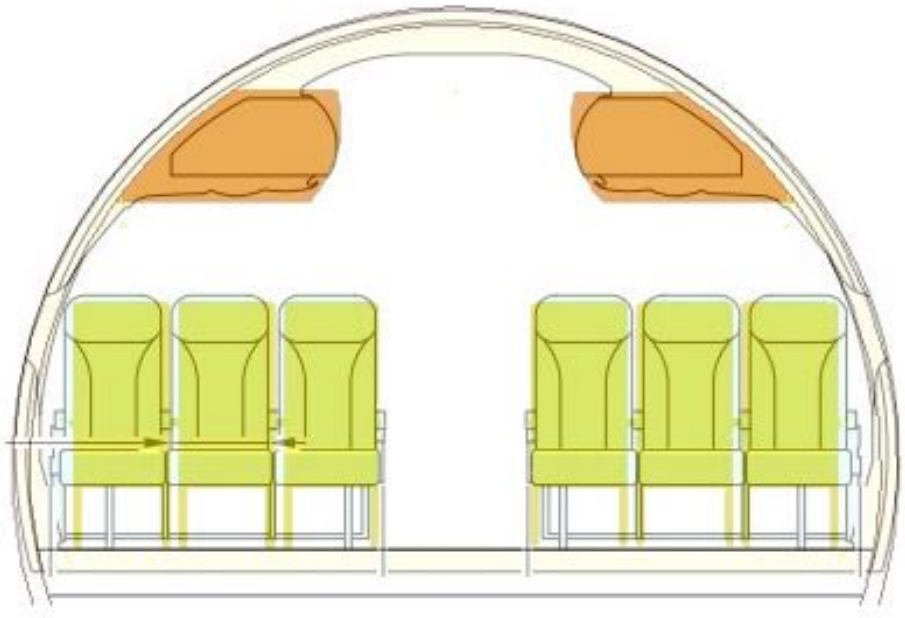

Figure 2.16: A320-200 cross section with 6 seats abreast overlap of reference aircraft [3] and ParaFuse

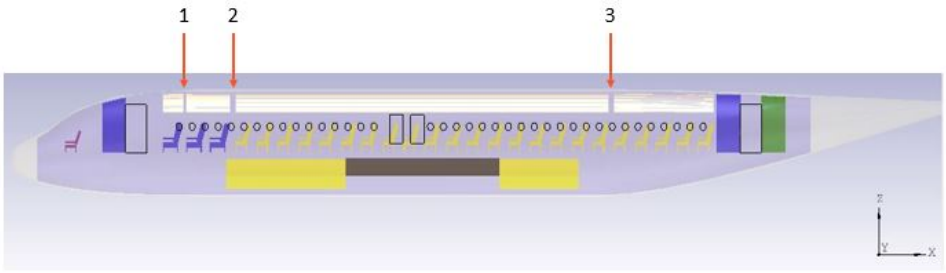

Figure 2.17: Discontinuities in overhead bins

the cargo hold is not divided into two holds due to the crossing of the wing in the fuselage. It is important to note that these continuous cargo holds would also be useful in case of a high wing configuration fuselage. A side view of a Prandtl Plane fuselage can be found in figure 2.18. A bottom view of a Prandtl Plane fuselage can be found in figure 2.19. The design of this Prandtl Plane is taken from the Parsifal technical report [10].

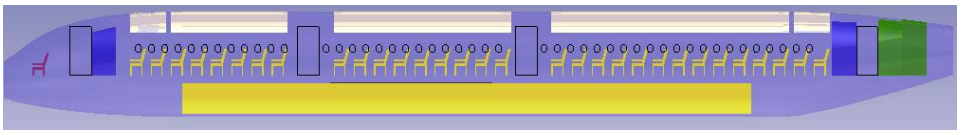

Figure 2.18: Side view of a Prandtl Plane with 248 passengers and a continuous cargo hold

The size of bulk cargo holds can now be modified and the continuous cargo holds have been implemented in ParaFuse. Both features will be useful when performing the fuselage performance studies for conventional and for Prandtl Plane fuselages.

ParaFuse can now generate oval fuselages and double deck fuselages. It also generates overhead storage compartments with a more realistic size and shape and can modify the size of bulk cargo holds and generate continuous cargo holds. Other capabilities have also been added to ParaFuse by identifying opportunities for improvement. These are listed and briefly discussed in appendix B. ParaFuse is almost ready to be used to perform the studies that will help answer the research question: To what extend can the turnaround time be

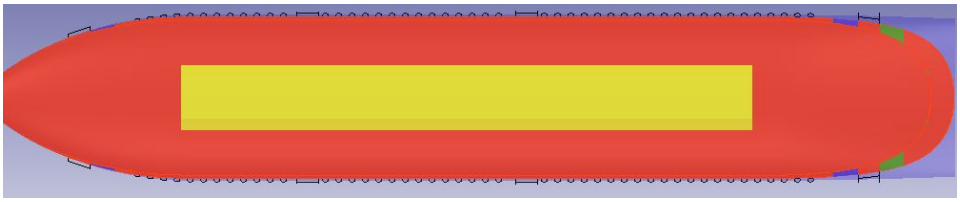

Figure 2.19: Bottom view of a Prandtl Plane with 248 passengers and a continuous cargo hold

reduced and passenger's comfort be enhanced by conventional and novel fuselages? What would be the opportunities offered by a Prandtl Plane configuration on the reduction of turn around time and enhancement of passenger's comfort? One last improvement must be performed to calculate the fuselage weight: coupling ParaFuse with the Initiator.

2.3. COUPLING PARAFUSE TO THE INITIATOR

In order to do the fuselage performance studies, it is necessary to calculate the fuselage weight. The fuselage weight can be obtained by running the Initiator. But before this thesis project, the Initiator would run prior to the Multi-Model Generator. There was no possibility to call ParaFuse within the Initiator to generate the fuselage geometry and then use that fuselage geometry to calculate the fuselage weight.

This thesis project has made it possible for the Initiator to invoke ParaFuse as a service. It bypasses the module @FuselageConfigurator used in the Initiator to generate the fuselage outer geometry and cabin configuration. To enable the use of ParaFuse and the bypass of @FuselageConfigurator, a setting input called 'UseParaFuse' has been added to the settings file of the Initiator. If set to 0, the Initiator uses the module @FuselageConfigurator. But if set to 1, the Initiator bypasses the module @FuselageConfigurator and launches ParaFuse.

The data exchange diagram can be found in figure 2.20. The Initiator is launched and the process goes through the @GeometryEstimation module. The setting UseParaFuse is extracted from the Initiator input file and if the setting is set to 1, then ParaFuse is called using a batch file and the module @FuselageConfigurator is bypassed. The inputs required for ParaFuse are then written in an XML file. ParaFuse is run and writes the parameters necessary for the Initiator into a XML output file. The Initiator then extracts the data from the XML output file of ParaFuse and the results for the fuselage outer geometry and cabin configuration are obtained.

Coupling ParaFuse to the Initiator is the last improvement necessary in order to perform the studies to answer the research question presented in section 1.7. But coupling ParaFuse to the Initiator can also be useful for Initiator users. The results of the cabin configuration of an A320-200 using @FuselageConfigurator and using ParaFuse within the Initiator are presented respectively in figures 2.21 and 2.22. The same top level requirements are used. The first difference observed is a more detailed visualization of the space allocated to galleys and lavatories in figure 2.22 than in figure 2.21. ParaFuse generates galleys and lavatories by taking into account the aisle width which is not the case in the Initiator. ParaFuse makes the distinction between galleys and lavatories but the Initiator does not which is why galleys and lavatories are allocated the same color in figure 2.22. Moreover, the number of emergency exits is different between figures 2.21 and 2.22. Using ParaFuse, there are four exits type '1' and four exits type '3'. Using @FuselageConfigurator, there are four exits type '1' but only two exits type '3'. In ParaFuse, the required number of exits are determined for a high density configuration. This number is specified in the EASA CS 25.807 airworthiness requirements [23]. A fuselage with 12 first class passengers and 144 economy class passengers requires four exits type '1' and four exits type '3'.

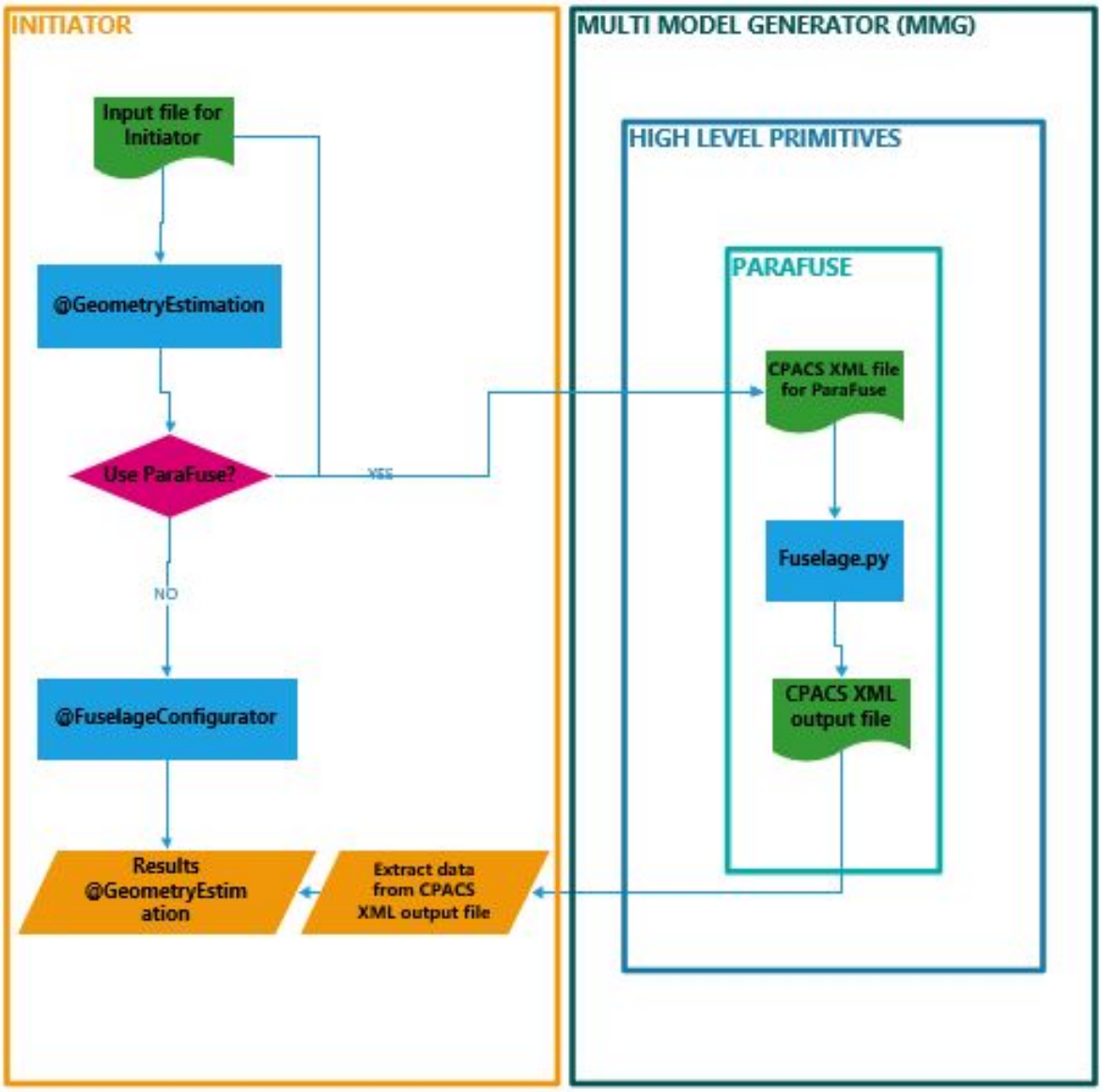

Figure 2.20: Data exchange diagram between the Initiator and ParaFuse

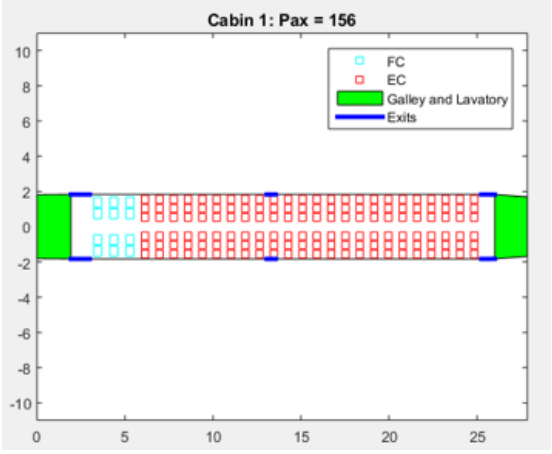

Figure 2.21: Cabin configuration using @FuselageConfigurator in the Initiator

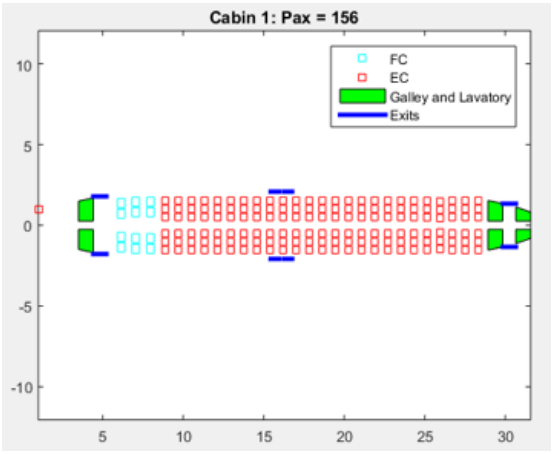

Figure 2.22: Cabin configuration using ParaFuse in the Initiator

3

VERIFICATION AND VALIDATION OF MODEL

A verification and validation of the parametric fuselage model ParaFuse is performed for the fuselage of medium range aircraft. The thesis project focuses on medium range fuselages thus the generation of such fuselages is necessary in order to gain confidence in the fuselage models generated by ParaFuse. The fuselage generated here is the A320-200 aircraft, a medium range aircraft part of the Airbus A320 family.

3.1. INPUT PARAMETERS FOR INSIDE-OUT APPROACH

The input parameters used in the inside-out approach are defined in table 3.1. The number of passengers, the aisle width, the cargo and uld types and the number of seats abreast are given in the report on 'Aircraft Characteristics Airport and Maintenant Planning' [3] for the A320-200. The percentage of passengers in first class is calculated based on the number of first class passengers and the total number of passengers given in [3]. The elliptical cross section shape is chosen because the reference aircraft has a larger fuselage height than width.

Table 3.1: Input parameters to generate A320-200 fuselage in ParaFuse using the inside-out approach

Parameter	Value	Unit
Number of passengers	150	[−]
Aisle width	0.64	[m]
Percentage of passengers in first class	8 %	[−]
Cargo type	Containerized	[−]
ULD type	LD3-45W	[−]
Cross section shape	Ellipse	[−]
Number of seats abreast	3 + 3	[−]

3.2. GENERATION OF A320-200 FUSELAGE IN PARAFUSE

The results for the fuselage of the medium range aircraft A320-200 extracted from ParaFuse can be found in table 3.2. Table 3.2 also presents the data from the actual aircraft taken from the report on 'Aircraft Characteristics Airport and Maintenance Planning' [3]. The fuselage height and the fuselage width in ParaFuse are equal to the ones of the reference aircraft. Thus, the equivalent diameter is also the same. The fuselage length in ParaFuse is 4.37% shorter than the reference aircraft. This shorter fuselage is first due to the fact that the seating arrangement in ParaFuse does not take into account a larger seat pitch at the overwing emergency exits. Secondly, the seat pitch between two seat classes is not increased to mark out the seat class change. The larger seat pitch at the overwing emergency exits and the larger seat pitch between first and economy class seats are shown in figure 3.1. The floor thickness in ParaFuse is more than twice as thick as the floor thickness in the reference aircraft. The rule used to calculate the floor thickness for the reference aircraft is unknown thus a default rule had to be applied in ParaFuse. The floor thickness is calculated with an iterative

loop which continues until the floor thickness is larger or equal to the floor thickness factor multiplied by the main cross section diameter. The initial floor thickness value is set to 0.200 meters which is a typical value for an Airbus aircraft according to Nita and Scholz [42]. According to Torenbeek [40], this floor thickness factor should be equal to 5% of the main cross section diameter. The floor thickness for the reference fuselage and the fuselage in ParaFuse should then be at least equal to $0.202m$ which is the result obtained in ParaFuse as table 3.2 shows.

There is the same number of economy class and first class passengers in the reference aircraft and in ParaFuse. This result was expected as the number of passengers is given as an input in ParaFuse. There is also the same number of exits per exit type: four exits type '1' and four exits type '3'. The number and type of exits are directly derived from the number of passengers in single class thus it was also expected to obtain the same number and type of exits. The number of lavatories is also the same. The number of lavatories is directly derived from the number of passengers per class. Because there is the same number of passengers per class in the reference aircraft and in the ParaFuse aircraft, the same number of lavatories was expected. Finally, there is the same number of galleys in the reference aircraft as in ParaFuse. As for the number of lavatories, the galley volume is directly derived from the number of passengers per class.

Table 3.2: A320-200 fuselage characteristics extracted from reference [3] and from ParaFuse

Parameter	Unit	Reference aircraft [3]	ParaFuse aircraft	Difference
Fuselage height	$[m]$	4.14	4.14	0.0%
Fuselage width	$[m]$	3.95	3.95	0.0%
Equivalent diameter	$[m]$	4.04	4.04	0.0%
Fuselage length	$[m]$	37.57	35.93	-4.37%
Floor thickness	$[m]$	0.095	0.202	112.63%
Economy class passengers	$[-]$	138	138	-
First class passengers	$[-]$	12	12	-
Total number of passengers	$[-]$	150	150	-
Exit type and number	$[-]$	['1', 4], ['3', 4]	['1', 4], ['3', 4]	-
Lavatories	$[-]$	3	3	-
Galleys	$[-]$	3	3	-

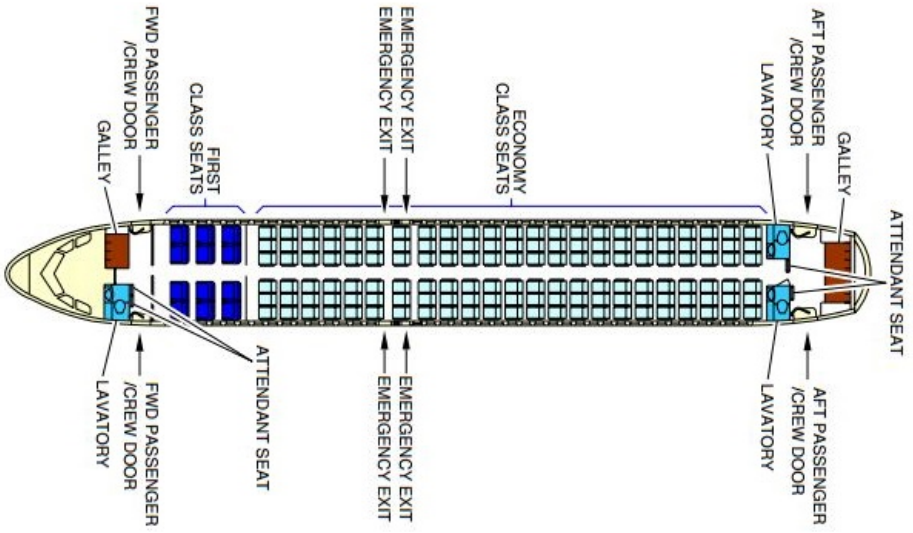

Figure 3.1: A320-200 seating arrangement [3]

3.3. VISUAL COMPARISON BETWEEN PARAFUSE AND REFERENCE AIRCRAFT

A visual comparison of the fuselage generated in ParaFuse with the reference aircraft is also performed. The figures depicting the results from ParaFuse are screenshots taken from the Graphical User Interface (GUI) of ParaPy. The overlap of the seating arrangement is depicted in figure 3.2. The fuselage nose cone in top view of ParaFuse perfectly overlaps with the reference fuselage nose cone. The galley and lavatory present in the nose cone also overlap perfectly as well as the first class seats in blue. However the economy class seats (in yellow in ParaFuse and in ligh blue in the reference aircraft) do not perfectly overlap due to the gap present between the last row of the first class seats and the first row of the economy class seats and the larger seat pitch at the overwing emergency exits in the reference aircraft. This mismatch in the economy class seats leads to a slight shift for the lavatories and galleys in the tail cone.

The overlap of the fuselage side views is shown in figure 3.3. Figure 3.3 shows that the fuselage in ParFuse is slightly shorter than the reference aircraft fuselage as it was mentioned in table 3.2. The same number and type of exits are present in both fuselages but their locations are slighly altered. This is due to the difference in fuselage length as well as the difference in the seating arrangement in economy class. The nose cone shape of ParaFuse overlaps well with the nose cone shape of the reference aircraft. However there is a mismatch in the tail cone shape due to the difference in fuselage length but the shape remains similar between both fuselages.

The overlap of the fuselage cross section for first class seats is depicted in figure 3.4. The outer shape of the cross section in ParaFuse perfectly overlaps with the cross section of the reference aircraft. This was expected because both cross sections have the same heigh and width as shown in table 3.2. The seat locations match as well however the simple shape of the seats in ParaFuse does not match the complex shape of the seats in the reference aircraft. The seat width, armrest width and seat heigh are the same. However the seat back width is larger in the reference aircraft than in ParaFuse. ParaFuse cannot generate complex seat shapes resulting in the slight mismatch shown in figure 3.4. The overhead storage compartments in ParaFuse have the same height and width as the overhead storage compartments of the reference aircraft. The outer shape of the overhead storage compartments in ParaFuse is slighly different from the one in the reference aircraft. ParaFuse uses a simple rounded shape to generate the storage compartments as can be seen in figure 3.4 in orange which is similar to the shape shown in figure **??** but not exactly the same. Overhead storage compartments can have a lot of different shapes thus this simple shape was chosen to be implemented in ParaFuse. The most important features are the heigh and the width of the overhead storage compartments so that a realistic luggage volume can be derived. Finally figure 3.4 shows that the floor in ParaFuse is much thicker in ParaFuse than in the reference aircraft. As it was mentioned before, this is due to the fact that the design rule used to calculate the floor thickness for the reference aircraft is unknown thus the design rule of Torenbeek [40] was used.

The overlap of the fuselage cross section for economy class seats is depicted in figure 3.5. The outer shape of the cross section in ParaFuse overlaps well with the cross section of the reference aircraft. The seat locations match as well as the seat dimensions and the aisle width. The overhead storage compartments in ParaFuse have the same heigh and width as the overhead storage compartments of the reference aircraft and the floor in ParaFuse is much thicker than in the reference aircraft.

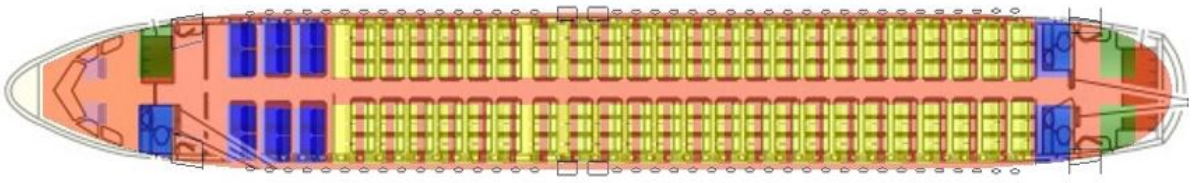

Figure 3.2: A320-200 seating arrangement overlap of reference aircraft [3] and ParaFuse

3.4. CONCLUSION

The fuselage of the Airbus A320-200 has been generated in order to gain confidence in the fuselage models generated by ParaFuse in terms of outer geometry and cabin configuration. The comparison between the

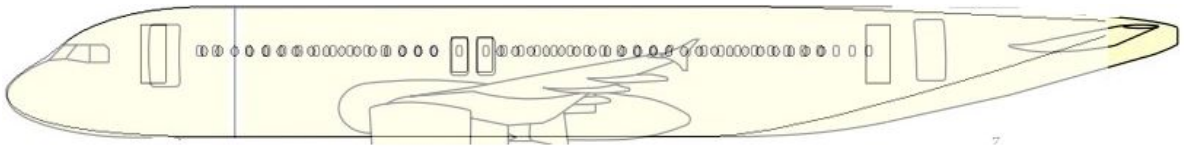

Figure 3.3: A320-200 side view overlap of reference aircraft [3] and ParaFuse

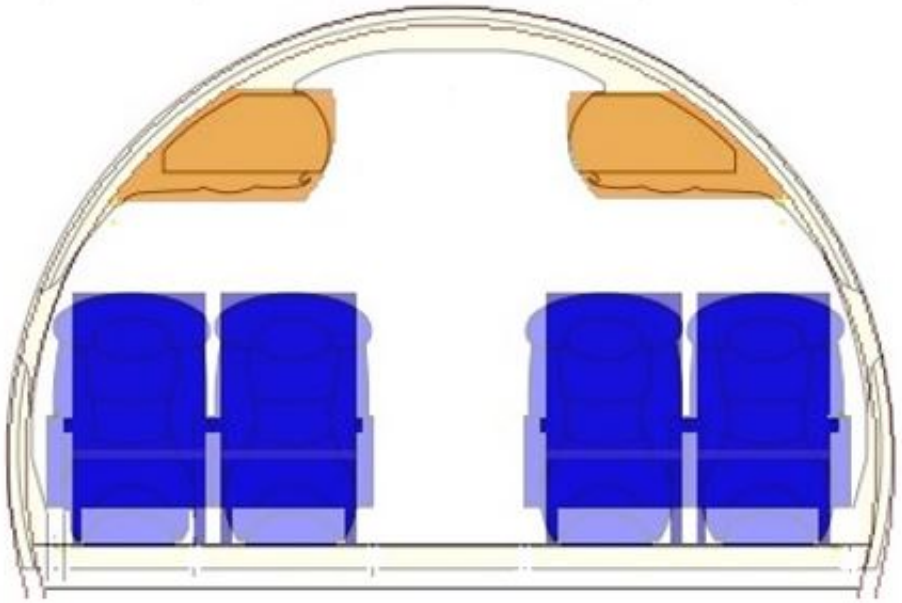

Figure 3.4: A320-200 cross section with 4 seats abreast overlap of reference aircraft [3] and ParaFuse

fuselage of the reference aircraft and the fuselage generated by ParaFuse has shown that the number of passengers, the type and number of exits, the number of lavatories and galleys remain the same. The fuselage heigh and width is also the same. However the fuselage length and the floor thickness are different in ParaFuse than for the reference aircraft. Numerous causes have been given to explain the differences observed. These causes have been summarized and categorized in table 3.3. The causes fall under the following categories: missing rule in ParaFuse, inaccurate rule in ParaFuse and inaccurate selection of input parameters.

Table 3.3: Causes of the differences between reference aircraft and ParaFuse

Missing rule	Inaccurate rule	Inaccurate selection of input parameters
Larger seat pitch at the overwing emergency exits	Floor thickness calculation [40]	Initial floor thickness [42]
Larger seat pitch between two seat classes	Simple seat shape	Nose cone shape
	Simple overhead storage compartment shape	Tail cone shape

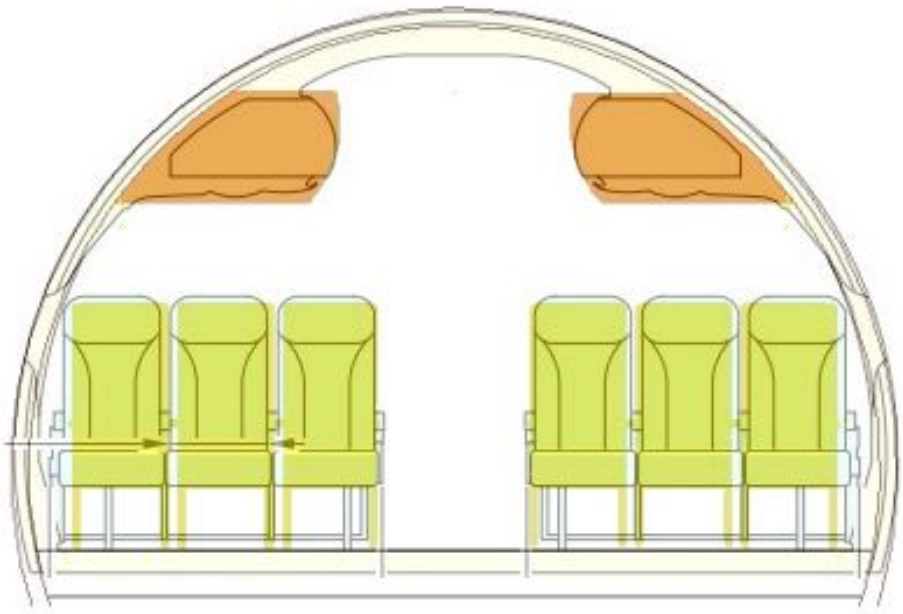

Figure 3.5: A320-200 cross section with 6 seats abreast overlap of reference aircraft [3] and ParaFuse

4

CASE STUDIES

Four cases studies have been performed in order to answer the subquestions presented in section 1.7. Each study has been performed for a medium range aircraft similar to the A320-200 presented in section 3. The fuselage performances calculated in each of the following case studies are the fuselage drag area and the fuselage weight. Section 1.6 details how the fuselage drag and weight are calculated. The cruise conditions for all the case studies are presented in table 4.1. The cruise conditions in table 4.1 are typical for a medium range aircraft such as the A320-200 and are fixed for each study.

Table 4.1: Cruise conditions for a medium range aircraft

Parameter	Symbol	Unit	Value
Altitude	h	$[m]$	11280
Cruise Mach number	M	$[-]$	0.78
Air density	ρ	$[kg/m^3]$	0.348
Speed of sound	a	$[m/s]$	295.1
Dynamic viscosity	μ	$[kg/(s.m)]$	$1.42 \cdot 10^{-5}$

4.1. CROSS SECTION STUDY

The first study aims at answering the following question:

Given a certain amount of passengers, what is the impact of varying the number of seats abreast on the fuselage performances?

The fuselage generated in ParaFuse has the same top level requirements as the A320-200 fuselage presented in table 3.1 apart from the number of seats abreast and the cross section type. In fact, this study varies the number of seats abreast and the cross section type for the same number of passengers. The fuselage is generated using the inside-out approach in ParaFuse. For each cross section type, the fuselage drag area and the fuselage weight are calculated based on data extracted from ParaFuse.

The fuselage drag area with respect to the number of seats abreast can be found in figure 4.1. The red square in figure 4.1 represents the drag area for the fuselage generated in ParaFuse in section 3. The first observation that can be made from figure 4.1 is that, for seats abreast between 6 and 9, increasing the number of seats abreast leads to an increase in fuselage drag for all cross section types. However for seats abreast between 4 and 6 the trends are different for each cross section type. The elliptical and double bubble fuselages have an increase in fuselage drag area for a number of seats abreast varying from 4 to 5, then a decrease in drag from 5 to 6 seats abreast and finally an increase in drag area from 6 to 9 seats abreast. The circular fuselage shows a decrease in drag from 4 to 6 seats abreast and then an increase until 9 seats abreast. Finally the oval fuselage shows a decrease in drag from 4 to 5 seats abreast and then an increase in drag from 5 to 9 seats abreast. The drag variations per cross section type are summarized in table 4.2.

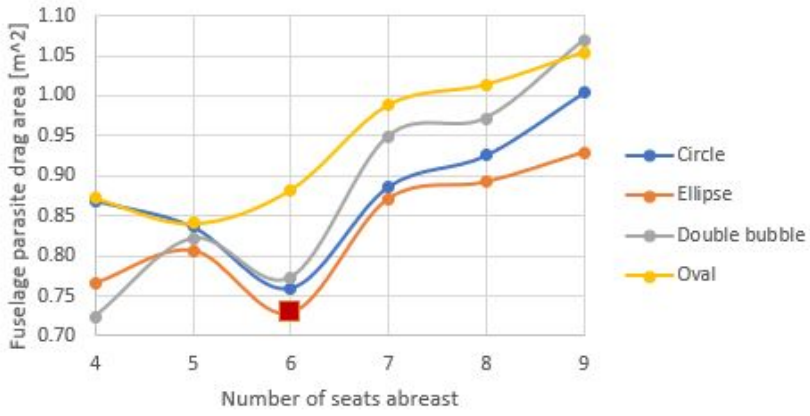

Figure 4.1: Fuselage drag area for various cross section types and number of seats abreast

Table 4.2: Drag variations per cross section type

Cross section type	Drag variation 4 to 5 nsa	Drag variation 5 to 6 nsa	Drag variation 6 to 9 nsa
Circle	↘	↘	↗
Ellipse	↗	↘	↗
Double bubble	↗	↘	↗
Oval	↘	↗	↗

The fuselage drag depends on the cruise conditions, the fuselage length, the fuselage diameter and the wetted area. These variations are presented in figures 4.4, 4.5 and 4.6. The increase in number of seats abreast leads to a reduction in fuselage length but leads to an increase in fuselage diameter. The increase in number of seats abreast leads to a reduction in the number of rows because the number of passengers remains constant. Less seat rows reduces the fuselage length which is what is observed in figure 4.4. The increase of seats abreast leads to larger rows of seats thus the fuselage width increases to accommodate the higher number of seats per row which is what is observed in figure 4.2. The fuselage height increases for the circular, double bubble or oval fuselage but remains more or less constant for the elliptical cross section as the number of seats abreast increases. Thus, the fuselage equivalent diameter increases as the number of seats abreast increases.

The variations in fuselage length and diameter lead to a decrease in fuselage slenderness when the number of seats abreast increases as figure 4.7 shows. This fuselage slenderness is then used to calculate the form factor k. A decrease in fuselage slenderness leads to an increase in form factor as figure 4.8 shows. As for the fuselage wetted area, each cross section type shows a decrease in fuselage wetted area from 4 to 6 seats abreast, an increase from 6 to 7 seats abreast, a decrease from 7 to 8 seats abreast and finally an increase from 8 to 9 seats abreast.

In order to understand the cause of the variations in fuselage drag area presented in table 4.2, the percentage of variation in form factor k and fuselage wetted area S_{wet} are compared in table 4.3. For the circular fuselage, the decrease in wetted area is larger in terms of percentage that the increase in form factor when increasing the number of seats abreast from 4 to 5. This results in a decrease in drag area as table 4.2 and figure 4.1 show. However for the elliptical fuselage, there is a larger increase in form factor than a decrease in wetted area resulting in an increase in drag area.

The variation in drag area is due to the variation in wetted area and in form factor. When the wetted area

and the form factor both increase this leads to an increase in drag area. The same conclusion is drawn when the wetted area and the form factor decrease. However when the wetted area and the form factor show different variations, the highest variation in terms of percentage has the highest influence on the variation in drag area.

Table 4.3: Variation in form factor and wetted area between 4 and 5 seats abreast

Cross section type	Parameter	4 NSA	5 NSA	Difference
Circle	$S_{wet}[m^2]$	541.72	476.55	-12.03 %
	$k[-]$	1.06	1.13	6.79 %
Ellipse	$S_{wet}[m^2]$	476.08	450.45	-5.38 %
	$k[-]$	1.05	1.14	8.85 %
Double bubble	$S_{wet}[m^2]$	517.31	471.21	-8.91 %
	$k[-]$	0.92	1.12	21.61 %
Oval	$S_{wet}[m^2]$	541.72	476.55	-12.03 %
	$k[-]$	1.06	1.13	6.79 %

When considering average values, applying the oval cross section to a medium range fuselage results in the highest drag area and applying the elliptical cross section results in the lowest drag area. For a medium range fuselage, the highest drag is reached for a double bubble cross section fuselage with 9 seats abreast and the lowest drag is reached for an elliptical cross section fuselage with 6 seats abreast. The latter fuselage is in fact the Airbus A320-200 generated in ParaFuse in section 3.

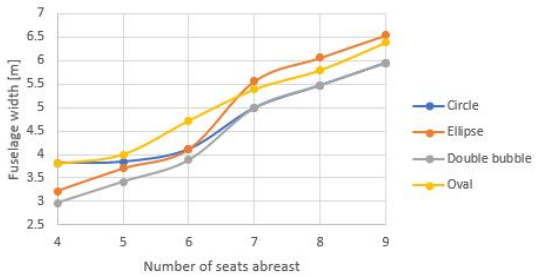

Figure 4.2: Fuselage width variation with respect to the number of seats abreast

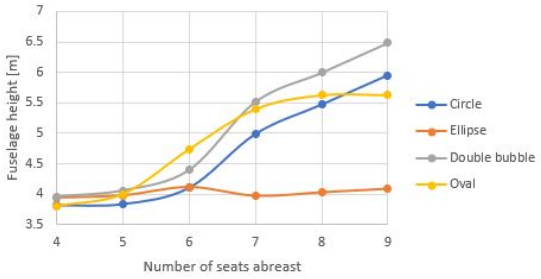

Figure 4.3: Fuselage height variation with respect to the number of seats abreast

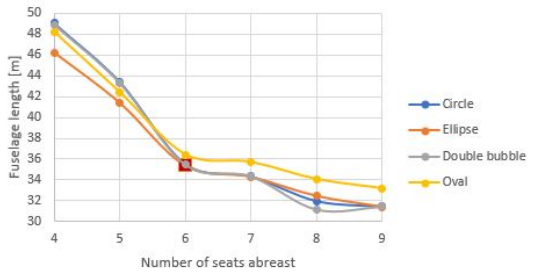

Figure 4.4: Fuselage length variation with respect to the number of seats abreast

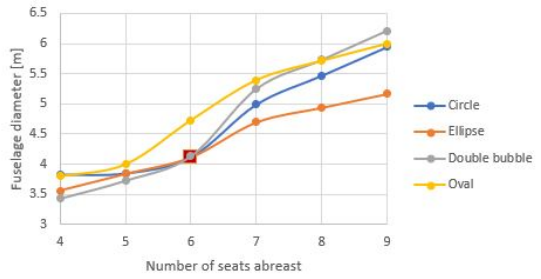

Figure 4.5: Fuselage diameter variation with respect to the number of seats abreast

The fuselage weight with respect to the number of seats abreast can be found in figure 4.9. The red square in figure 4.9 represents the fuselage generated in ParaFuse in section 3. The first observation that can be made from figure 4.9 is that the fuselage weight variation with respect to the number of seats abreast does not have a monotone trend. Between 4 and 6 seats abreast, the fuselage weight of each cross section type decreases. Between 6 and 7 seats abreast, the fuselage weight of each cross section type increases. Between 7 and 8 seats

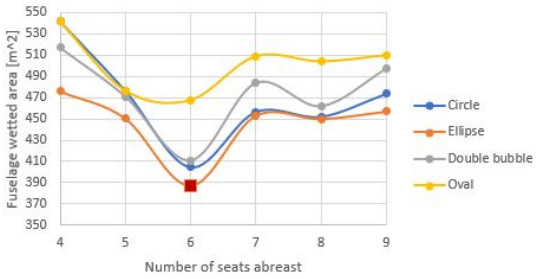

Figure 4.6: Fuselage wetted area variation with respect to the number of seats abreast

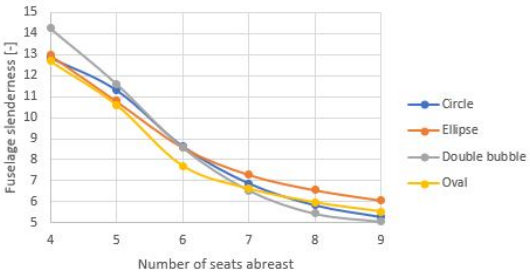

Figure 4.7: Fuselage slenderness variation with respect to the number of seats abreast

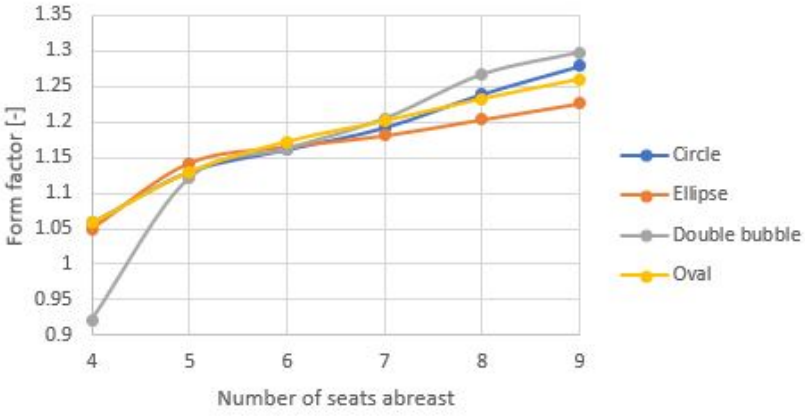

Figure 4.8: Fuselage form factor variation with respect to the number of seats abreast

abreast, the fuselage weight of each cross section type decreases. Finally, between 8 and 9 seats abreast, the fuselage weight of the oval and the elliptical fuselages decreases while the fuselage weight of the circular and the double bubble fuselages increases. The weight variations per cross section type are summarized in table 4.4.

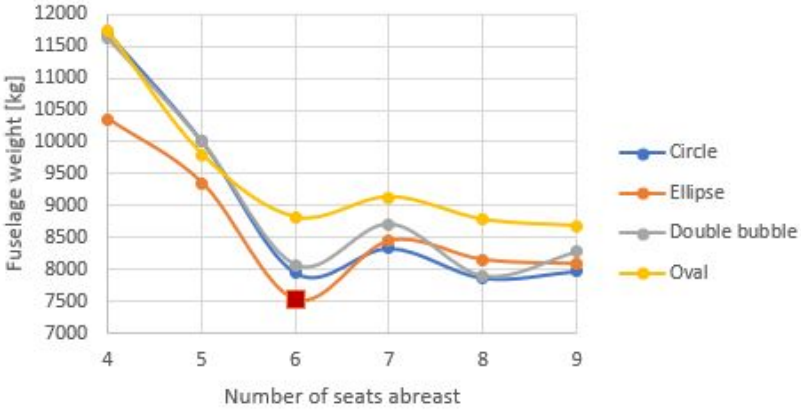

Figure 4.9: Fuselage weight variation with respect to the number of seats abreast

The fuselage weight is calculated within the Initiator either with the Class II Weight Estimation or the Class II.V Weight Estimation. As stated in section 1.6, the Class II.V Weight Estimation module of the Initiator can only calculate the weight of circular and oval cross sections. Here, the fuselage has an elliptical cross section thus the Class II Weight Estimation is used. The variations of the fuselage width, height and wetted area with respect to the number of seats abreast are presented respectively in figure 4.2, 4.3 and 4.6. The increase in

Table 4.4: Weight variations per cross section type

Cross section type	Weight variation 4 to 6 nsa	Weight variation 6 to 7 nsa	Weight variation 7 to 8 nsa	Weight variation 8 to 9 nsa
Circle	↘	↗	↘	↗
Ellipse	↘	↗	↘	↘
Double bubble	↘	↗	↘	↗
Oval	↘	↗	↘	↘

number of seats abreast leads to an increase in fuselage width and an increase in fuselage height except for the elliptical fuselage which shows an almost constant fuselage height. The fuselage weight shows the same trend as the fuselage wetted area for each cross section type. It seems thus that the fuselage wetted area variation has the highest influence on the variation in fuselage weight.

When considering average values, applying the oval cross section to a medium range fuselage leads to the highest fuselage weight and applying the elliptical cross section leads to the lowest fuselage weight. For a medium range fuselage, the highest fuselage weight is reached for an oval cross section and 4 seats abreast. The lowest fuselage weight is reached for an elliptical cross section and 6 seats abreast. The latter fuselage is in fact the A320-200 fuselage generated in ParaFuse in section 3.

The fuselage weight and the fuselage drag area have to be taken into account simultaneously to make the fuselage design choices. Thus, the drag and weight curves with respect to the fuselage slenderness are generated for each cross section type in figure 4.10, 4.11, 4.12 and 4.13. The intersection of the drag and the weight curve corresponds to the best slenderness for the fuselage in terms of fuselage performances. In order to find this intersection, polynomial trendlines of order 3 have been generated. The correlation of the trendlines varies between 0.8305 and 0.9864 which is a good indicator of the reliability of the trendline results with respect to the actual data. The intersection points of the drag and weight trendlines are summarized in table 4.5. The intersection point of the oval fuselage shows the highest drag area and weight with a slenderness of 8.7 and the intersection point of the elliptical fuselage shows the lowest drag area and weight with a slenderness of 8.5.

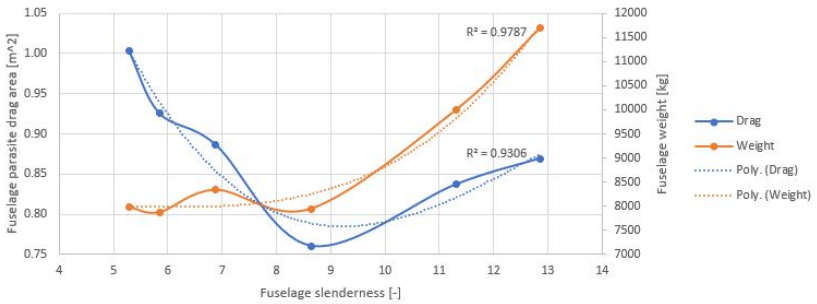

Figure 4.10: Drag area - weight curve for circular fuselage with respect to fuselage slenderness

This cross section study for a medium range aircraft with 150 passengers has shown that an increase in the number of seats abreast leads to an increase in fuselage drag area for every cross section type. On average the highest fuselage drag is reached when an oval cross section is applied to the fuselage and the lowest fuselage drag is reached for an elliptical cross section. The variation in drag area is related to the variation in wetted area and in form factor. As for the fuselage weight, the oval cross section fuselage leads to the highest fuselage weight and the circular cross section fuselage to the lowest fuselage weight on average. The fuselage weight does not follow a monotone trend when the number of seats abreast increases. The variation of the

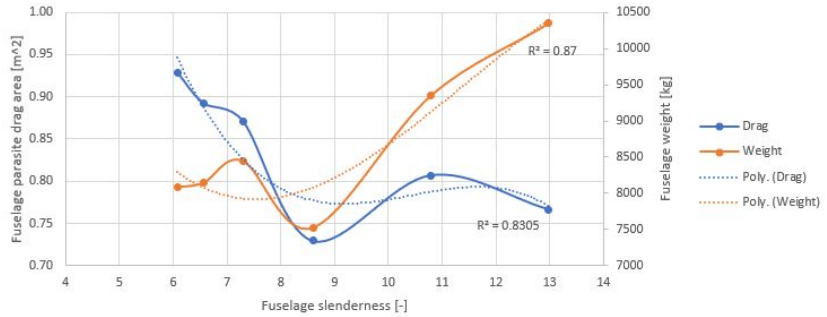

Figure 4.11: Drag area - weight curve for elliptical fuselage with respect to fuselage slenderness

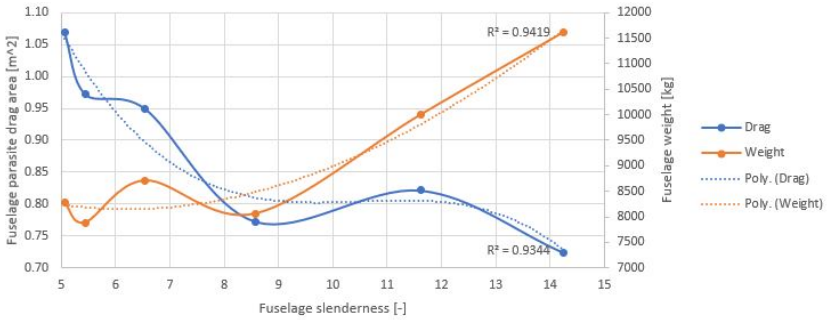

Figure 4.12: Drag area - weight curve for double bubble fuselage with respect to fuselage slenderness

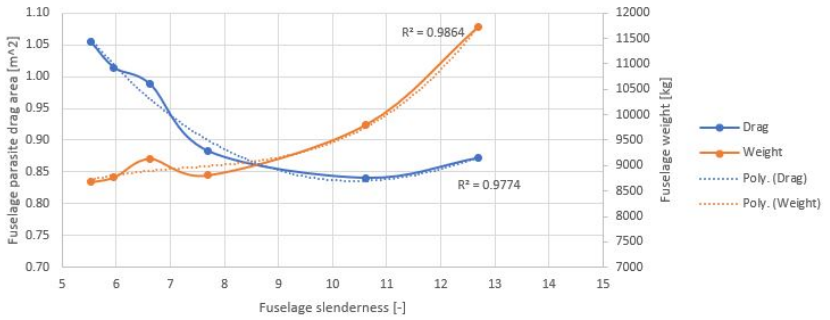

Figure 4.13: Drag area - weight curve for oval fuselage with respect to fuselage slenderness

Table 4.5: Drag area - weight curves intersection parameters

Cross section type	Slenderness [−]	Drag area [m^2]	Weight [kg]
Circle	7.5	0.82	8200
Ellipse	8.5	0.78	8100
Double bubble	8.4	0.81	8400
Oval	8.7	0.86	9100

fuselage weight seems to be following the trend of the fuselage wetted area. On average the highest fuselage weight is reached when an oval cross section is applied to the fuselage and the lowest fuselage weight is reached for an elliptical cross section. The variation in fuselage weight is related to the variation in wetted area. From this study it came out that the lowest fuselage drag area and the lowest fuselage weight were reached for the same fuselage: the medium range A320-200 fuselage with an elliptical cross section and 6 seats abreast. Finally it was also possible to draw the drag-weight curve with respect to the slenderness of the fuselage to find the optimum design point. The optimum design point with the lowest fuselage drag and weight corresponded to the elliptical fuselage while the optimum design point with the highest fuselage drag and weight corresponded to the oval fuselage. It is important to note that this optimum design point only

takes the fuselage component of the aircraft into account. A fuselage is typically more slender than what the fuselage optimum design point suggests because a more slender fuselage leads to reducing the size of the tail of the aircraft. A smaller tail leads to less weight and drag due to the tail. However the tail of the aircraft is not taken into account in this study. But the tail could be taken into account in this study by making use of the full Initiator modules.

4.2. REDUCING TURN AROUND TIME BY INCREASING THE AISLE WIDTH

This study aims at answering the following question:

What is the impact of increasing the aisle width on the fuselage drag and the fuselage weight?

Turn around time can be reduced by increasing the aisle width in the cabin for the passengers. In fact, increasing the aisle width would lead to more space available in the cabin for passengers when boarding and disembarking the aircraft. The aisle width increase would have to be such that two passengers can cross in the aisle thus avoiding the recurrent issue of passengers loading and unloading carry-on luggage into the overhead bins which results in blocking the aisle for other passengers. Turn around time would inevitably be reduced as boarding and disembarking would take less time with the increase of the aisle width. But it is still necessary to measure the impact of such a change on the fuselage drag and weight.

A typical aisle width for medium range aircraft is 64 cm like in the Airbus A320-200. In order to define which aisle width increase would allow two passengers to cross, the hip breadth of the 95th percentile US male is used. The hip breadth of the 95th percentile US male measures 40.5 cm. Thus an aisle width of 81 cm, twice the hip breadth of the 95th percentile US male, would allow for two passengers to cross. This study will thus consider two aisles widths: 64 cm and 81 cm.

For the purpose of this research, the fuselage of the medium range aircraft A320-200 is used. Table 3.1 shows the top level requirements of the fuselage. The cross section shape and the aisle width will vary during this case study. The fuselage is generated using the inside-out approach and the fuselage drag area and fuselage weight are calculated based on data extracted from ParaFuse. The aisle width increase is first going to be illustrated by showing the elliptical cross section with an aisle width of 64 cm in figure 4.14 and the elliptical cross section with an aisle width of 81 cm in figure 4.15. An overlap of figures 4.14 and 4.15 can be found in figure 4.16. This aisle width increase has a different impact on the fuselage height, width and length depending on the type of cross section used. In fact, table 4.6 shows that for an elliptical cross section, an aisle width increase results in an increase in fuselage width and length but not in height. Tables 4.7, 4.8 and 4.9 show that an incease in aisle width results in an increase in fuselage height, width and length for a circular, double bubble and oval fuselage.

The geometrical modifications of the fuselage due to the aisle width increase have been presented. These geometrical modifications have an impact on the fuselage wetted area and the form factor which in turn influence the variation of fuselage drag area and fuselage weight as described in section 4.1. Tables 4.6 to 4.9 show that the aisle width increase leads to an increase in wetted area and in form factor for all the cross section types. This forecasts an increase in fuselage drag area and in fuselage weight as it was concluded in section 4.1.

Table 4.6: Elliptical fuselage dimensions with different aisle widths

Parameter	Unit	Aisle width = 0.64m	Aisle width = 0.81m	Difference
Fuselage height	$[m]$	4.14	4.14	0.0%
Fuselage width	$[m]$	3.95	4.14	4.81%
Equivalent diameter	$[m]$	4.04	4.14	2.48 %
Fuselage length	$[m]$	35.93	36.23	0.83%
Wetted area	$[m^2]$	402.35	410.82	2.11%
Form factor	$[-]$	1.1619	1.1629	0.086 %

The results for the fuselage drag area are presented in table 4.10. An increase in aisle width leads, as it was expected, to an increase in drag area for each cross section type. The increase in drag area varies between

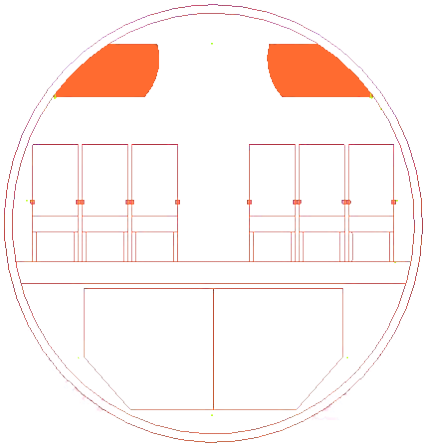

Figure 4.14: Elliptical cross section with an aisle width of 64 cm

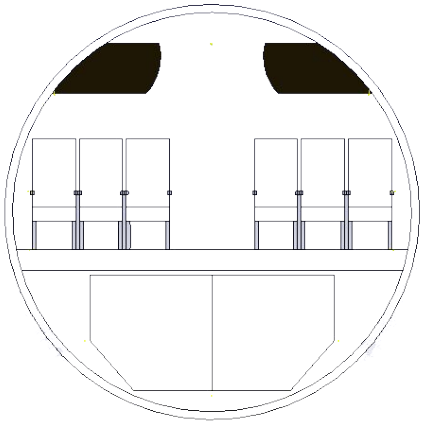

Figure 4.15: Elliptical cross section with an aisle width of 81 cm

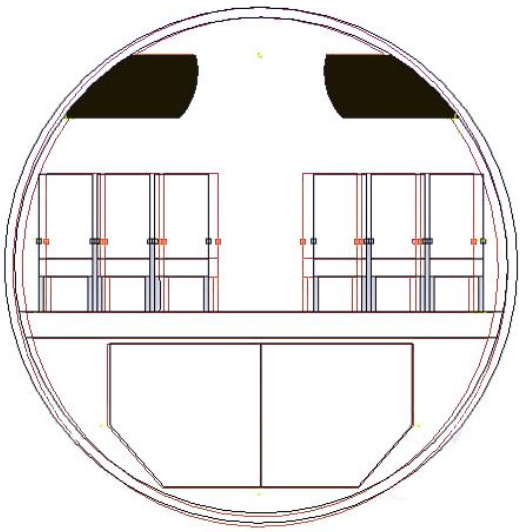

Figure 4.16: Overlap of elliptical cross section with aisle widths of 64 and 81 cm

Table 4.7: Circular fuselage dimensions with different aisle widths

Parameter	Unit	Aisle width = 0.64m	Aisle width = 0.81m	Difference
Fuselage height	$[m]$	4.11	4.19	1.95%
Fuselage width	$[m]$	4.11	4.19	1.95%
Equivalent diameter	$[m]$	4.11	4.19	1.95%
Fuselage length	$[m]$	36.75	36.77	0.05%
Wetted area	$[m^2]$	420.18	426.97	1.62%
Form factor	$[-]$	1.1595	1.1606	0.095 %

1.1% for the oval cross section and 2.6% for the circular cross section. However for each aisle width, the highest drag area is reached for the oval cross section fuselage and the lowest drag area is reached for the elliptical cross section fuselage. The value in bold in table 4.10 shows the lowest drag area which corresponds to the fuselage generated in section 3.

The results for the fuselage weight are presented in table 4.11. As for the drag area, an increase in aisle width results in an increase in fuselage weight. The increase in weight varies between 0.96% for the circular cross section and 1.7% for the double bubble cross section. For each aisle width, the highest weight is reached

Table 4.8: Double bubble fuselage dimensions with different aisle widths

Parameter	Unit	Aisle width = 0.64m	Aisle width = 0.81m	Difference
Fuselage height	$[m]$	4.4	4.52	2.73%
Fuselage width	$[m]$	3.88	4.00	3.09%
Equivalent diameter	$[m]$	4.13	4.25	2.91%
Fuselage length	$[m]$	36.66	36.71	0.14%
Wetted area	$[m^2]$	426.62	437.74	2.61%
Form factor	$[-]$	1.1599	1.1616	0.15 %

Table 4.9: Oval fuselage dimensions with different aisle widths

Parameter	Unit	Aisle width = 0.64m	Aisle width = 0.81m	Difference
Fuselage height	$[m]$	4.74	4.80	1.27%
Fuselage width	$[m]$	4.72	4.78	1.27%
Equivalent diameter	$[m]$	4.73	4.79	1.27%
Fuselage length	$[m]$	38.55	38.70	0.39%
Wetted area	$[m^2]$	499.01	506.89	1.58%
Form factor	$[-]$	1.1662	1.167	0.069%

Table 4.10: Fuselage drag area results for an increased aisle width

Cross section type	Aisle width = 0.64m	Aisle width = 0.81m	Difference
Circle	0.78 m^2	0.80 m^2	2.6%
Ellipse	**0.76** m^2	0.77 m^2	1.3%
Double bubble	0.80 m^2	0.82 m^2	2.5%
Oval	0.93 m^2	0.94 m^2	1.1%

for the oval cross section fuselage and the lowest weight is reached for the elliptical cross section fuselage. The value in bold in table 4.11 shows the lowest fuselage weight which corresponds to the fuselage generated in section 3.

Table 4.11: Fuselage weight results for an increased aisle width

Cross section type	Aisle width = 0.64m	Aisle width = 0.81m	Difference
Circle	8313 kg	8393 kg	0.96%
Ellipse	**7887** kg	8014 kg	1.6%
Double bubble	8436 kg	8577 kg	1.7%
Oval	9525 kg	9645 kg	1.3%

An increase in aisle width leads to an increase in fuselage wetted area and form factor thus leading to an increase in fuselage drag area and in fuselage weight. Reducing turn around time seems to come at a cost in terms of fuselage performance for medium range aircraft.

4.3. INCREASING PASSENGER'S COMFORT BY SHIFTING CARGO HOLD VOLUME TO OVERHEAD BINS

This study aims at answering the following question:

What is the impact of shifting cargo hold volume to overhead bins on the fuselage performances?

There is a need to increase the overhead bin volume so that each passenger can bring at least two carry-on luggage in the cabin. This would in fact increase passenger's comfort as passengers with two carry-on luggage would not have to check one in. In fact, passengers tend to bring luggage in the cabin rather than checking it

to go into the cargo holds on continental flights. Thus, it would be interesting to look at the impact of shifting a portion of the cargo hold volume into the overhead bins on the fuselage drag and weight.

Before performing this study, the portion of cargo hold volume that should be shifted to the overhead bins needs to be defined. The cross section of the reference aircraft from section 3 is generated. It can be found in figure 4.17. A carry-on luggage has been drawn in figure 4.17 and is represented by a blue rectangle. Figure 4.17 shows that the overhead bins can fit one carry-on luggage. The question that needs to be asked now is: how much volume needs to be shifted from the cargo holds to the overhead bins so that the overhead bins can fit two carry-on luggage on top of each other? This study is performed for a medium range aircraft with 150 passengers. A standard carry-on luggage has a size of 55x35x25 cm thus a volume of 0.048 m^3. 150 carry-on luggage corresponds to 7.2 m^3. But it is not enough to conclude that 7.2 m^3 should be shifted because the overhead bins also need a minimum height to fit two carry-on luggage on top of each other. The height of the initial overhead bins in figure 4.17 measures 50 cm. These overhead bins cannot fit two carry-on luggage thus the height must be increased by the breadth of a carry-on luggage: 25 cm. The shift of cargo hold volume to the overhead bins will be performed by shifting 7.2 m^3 to the overhead bins with a minimum overhead bin height of 75 cm.

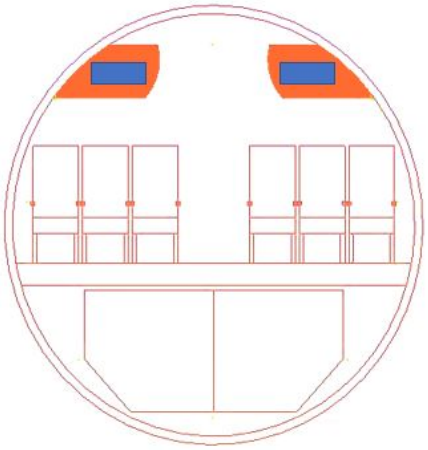

Figure 4.17: Elliptical cross section fitting one carry-on luggage in overhead bins

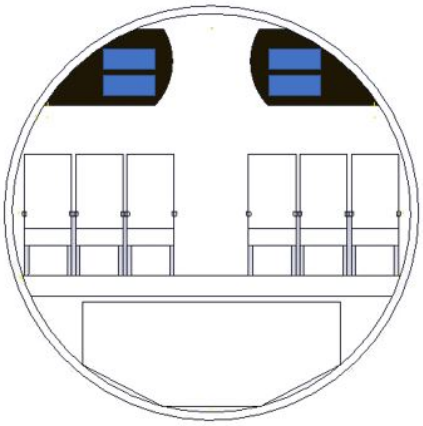

Figure 4.18: Elliptical cross section fittin two carry-on luggage in overhead bins

This study is again performed with the top level requirements presented in table 3.1. The cross section shape is varied during the study. The cargo is defined as bulk and not containerized. Reducing the cargo hold volume results in a lower cargo hold height. If the cargo hold type is containerized, a lower height results in a different ULD type. A bulk cargo allows more flexibility to perform this study. The shift of cargo hold volume to the overhead bins has a the same impact on the fuselage height and width for all the cross sections but has a different impact on the fuselage length depending on the type of cross section used. In fact, the cargo hold volume shift to the overhead bins leads to a decrease in fuselage width and height for all the cross sections as tables 4.12, 4.13, 4.14 and 4.15 show. Tables 4.12 and 4.14 show that the volume shift leads to a slightly longer fuselage for an elliptical and double bubble cross section. Finally tables 4.13 and 4.15 show that the fuselage length is slightly reduced for a circular and an oval fuselage when the volume shift occurs.

The geometrical modifications of the fuselage due to the cargo hold volume shift to the overhead bins have been presented. These geometrical modifications have an impact on the fuselage wetted area and form factor which in turn influence the variation of fuselage drag area and fuselage weight as described in section 4.1. Tables 4.12 to 4.15 show that the cargo hold volume shift to the overhead bins leads to a decrease in wetted area and in form factor for all the cross section types. This forecasts a decrease in fuselage drag area and in fuselage weight as it was concluded in section 4.1.

The results for the fuselage drag area are presented in table 4.16. The volume shift results in a lower fuselage drag area for each cross section type. The reduction of fuselage drag area varies between 2.02% for the elliptical cross section and 3.71% for the oval cross section. For each case presented in table 4.16, the high-

Table 4.12: Elliptical fuselage dimensions with cargo hold volume shift

Parameter	Unit	Reference case	Cargo hold volume shift	Difference
Fuselage height	$[m]$	4.14	3.88	-6.28%
Fuselage width	$[m]$	3.95	3.88	-1.77%
Equivalent diameter	$[m]$	4.04	3.88	-3.96%
Fuselage length	$[m]$	35.93	36.04	0.31%
Wetted area	$[m^2]$	402.35	389.43	-3.21%
Form factor	$[-]$	1.1619	1.1573	-0.40%

Table 4.13: Circular fuselage dimensions with cargo hold volume shift

Parameter	Unit	Reference case	Cargo hold volume shift	Difference
Fuselage height	$[m]$	4.11	3.88	-5.60%
Fuselage width	$[m]$	4.11	3.88	-5.60%
Equivalent diameter	$[m]$	4.11	3.88	-5.60%
Fuselage length	$[m]$	36.75	36.66	-0.24%
Wetted area	$[m^2]$	420.18	389.43	-7.32%
Form factor	$[-]$	1.1595	1.1563	-0.28%

Table 4.14: Double bubble fuselage dimensions with cargo hold volume shift

Parameter	Unit	Reference case	Cargo hold volume shift	Difference
Fuselage height	$[m]$	4.4	4.2	-4.55%
Fuselage width	$[m]$	3.88	3.86	-0.52%
Equivalent diameter	$[m]$	4.13	4.03	-2.42%
Fuselage length	$[m]$	36.66	36.71	0.14%
Wetted area	$[m^2]$	426.62	402.54	-5.64%
Form factor	$[-]$	1.1599	1.1580	-0.16%

Table 4.15: Oval fuselage dimensions with cargo hold volume shift

Parameter	Unit	Reference case	Cargo hold volume shift	Difference
Fuselage height	$[m]$	4.74	4.54	-4.22%
Fuselage width	$[m]$	4.72	4.51	-4.45%
Equivalent diameter	$[m]$	4.73	4.52	-4.44%
Fuselage length	$[m]$	38.55	38.33	-0.57%
Wetted area	$[m^2]$	499.01	476.22	-4.57%
Form factor	$[-]$	1.1662	1.1630	-0.27%

est drag area is reached for the oval cross section and the lowest drag area is reached for the elliptical cross section. The value in bold in table 4.16 shows the lowest drag area which corresponds to the elliptical cross section with a cargo hold volume shift to the overhead bins.

Table 4.16: Fuselage drag area results when shifting cargo hold volume into overhead bins

Cross section type	Reference case	Cargo hold volume shift	Difference
Circle	0.760 m^2	0.738 m^2	-2.89%
Ellipse	0.742 m^2	**0.727** m^2	-2.02%
Double bubble	0.795 m^2	0.770 m^2	-3.14%
Oval	0.916 m^2	0.882 m^2	-3.71%

The results for the fuselage weight are presented in table 4.17. This volume shift results in a lower fuselage weight for each cross section type. The reduction of fuselage weight varies between 0.40% for the elliptical

cross section and 2.99% for the oval cross section. For each case presented in table 4.17, the highest fuselage weight is reached for the oval cross section and the lowest fuselage weight is reached for the elliptical cross section. The value in bold in table 4.16 shows the lowest fuselage weight which corresponds to the elliptical cross section with a cargo hold volume shift to the overhead bins.

Table 4.17: Fuselage weight results when shifting cargo hold volume into overhead bins

Cross section type	Reference case	Cargo hold volume shift	Difference
Circle	8150 kg	7993 kg	-1.93%
Ellipse	7841 kg	**7810** kg	-0.40%
Double bubble	8436 kg	8323 kg	-1.34%
Oval	9491 kg	9207 kg	-2.99%

The cross section and the side view of this fuselage can be found respectively in figures 4.20 and 4.23. These figures are accompagnied by the cross section and the side view of the A320-200 fuselage, shown in figures 4.19 and 4.22. An overlap of figures 4.19 and 4.20 can be found in figure 4.21. The smaller fuselage height and width for the new cross section are clearly visible in figure 4.21. Moreover, the larger overhead bins and the smaller cargo holds are depicted in figure 4.21. An overlap of figures 4.22 and 4.23 can be found in figure 4.24. This overlap shown clearly the smaller fuselage height and the larger fuselage length for the fuselage depicted in figure 4.23 compared to the A320-200 fuselage depicted in figure 4.22.

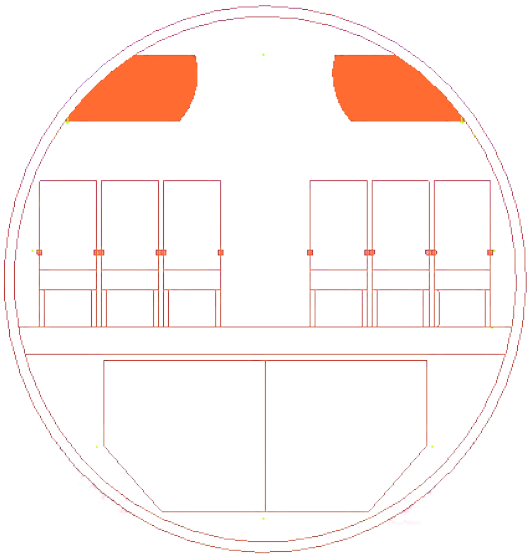

Figure 4.19: Cross section of the A320-200 fuselage

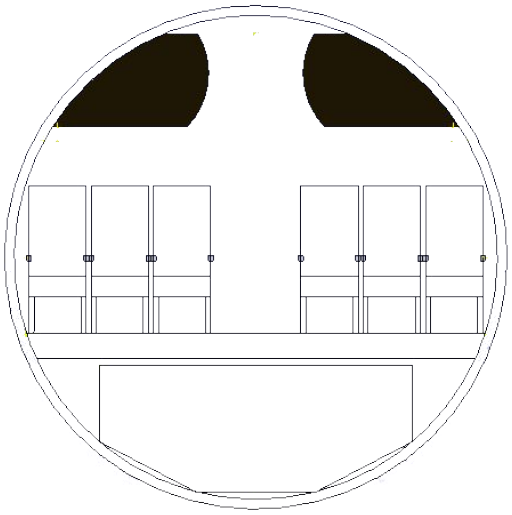

Figure 4.20: Cross section of the best fuselage with a shift of the cargo hold volume to the overhead bins

It can be concluded from this study that the shift of cargo hold volume to the overhead bins leads to a decrease in fuselage wetted area and form factor thus leading to a decrease in fuselage drag area and fuselage weight for each cross section type. The best cross section type, meaning the cross section type leading to the lowest fuselage drag area and the lowest fuselage weight, is the elliptical cross section. Shifting cargo hold volume to the overhead bins results in a lower drag area and weight than the A320-200 fuselage presented in section 3.

4.4. COMBINING THE SHIFT OF CARGO HOLD VOLUME AND THE INCREASE IN AISLE WIDTH

This study aims at answering the following question:

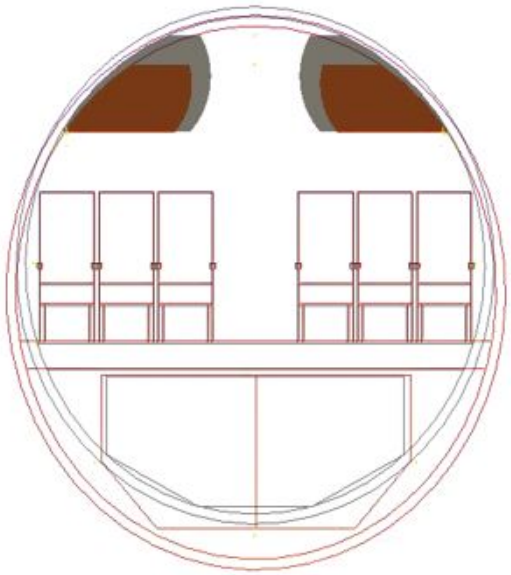

Figure 4.21: Overlap of A320-200 cross section with cross section with cargo hold volume shift

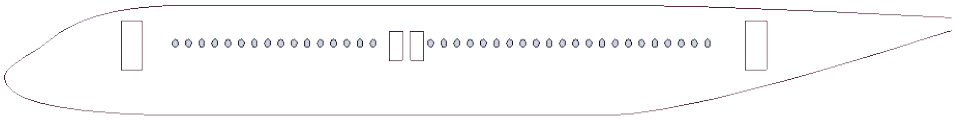

Figure 4.22: Side view of the A320-200 fuselage

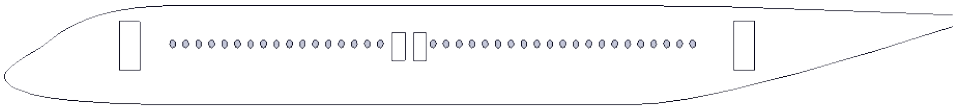

Figure 4.23: Side view of the best fuselage with a shift of the cargo hold volume to the overhead bins

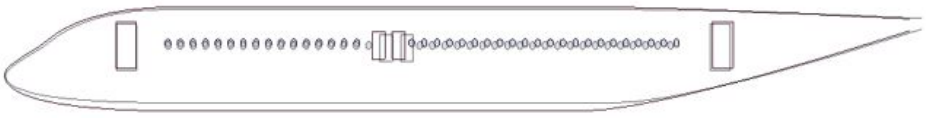

Figure 4.24: Overlap of A320-200 side view with side view with cargo hold volume shift

How are the fuselage performances impacted by increasing the aisle width and shifting cargo hold volume to overhead bins?

So far it has been concluded that an aisle width increase results in higher fuselage drag area and higher fuselage weight whereas a shift of cargo hold volume to the overhead bins results in lower fuselage drag area and lower fuselage weight. It would be interesting to see the impact of making both modifications simultaneously. It is the goal of this case study.

The study is performed using the top level requirements presented in table 3.1. The aisle width is going to be increased, the cross section shape varied and the cargo type is changed to bulk to have a more flexible geometry when removing cargo hold volume. The number of passengers, seats abreast and the percentage of passengers in first class is fixed. Combining the cargo hold volume shift with the aisle width increase has a different impact on the fuselage height, width and lenght depending on the type of cross section used. These

results are show in tables 4.18, 4.19, 4.20 and 4.21. It leads to a decrease in fuselage height for the elliptical, circular and oval fuselages but to an increase in fuselage height for the double bubble fuselage. It leads to an increase in fuselage width for the elliptical and the double bubble fuselages but to a decrease in fuselage width for the circular and oval fuselages. Finally, it leads to an increase in fuselage length for the elliptical and the double bubble fuselages but to a decrease in fuselage length for the circular and the oval fuselages.

The geometrical modifications of the fuselage due to the cargo hold volume shift to the overhead bins combined with the aisle width increase have been presented. These geometrical modifications have an impact on the fuselage wetted area and form factor which in turn influence the variation of fuselage drag area and fuselage weight as described in section 4.1. Tables 4.18 to 4.21 show that the cargo hold volume shift to the overhead bins leads to a decrease in wetted area and in form factor for the elliptical, circular and oval fuselages but leads to an increase in wetted area and in form factor for the double bubble fuselage. This forecasts a decrease in fuselage drag area and in fuselage weight for the elliptical, circular and oval fuselages but to an increase in fuselage drag area and in fuselage weight for the double bubble fuselage.

Table 4.18: Elliptical fuselage dimensions with aisle width increase and cargo hold volume shift

Parameter	Unit	Reference case	Geometrical modifications	Difference
Fuselage height	$[m]$	4.14	4.00	-3.38%
Fuselage width	$[m]$	3.95	4.00	1.27%
Equivalent diameter	$[m]$	4.04	4.00	-0.99%
Fuselage length	$[m]$	35.93	36.13	0.56%
Wetted area	$[m^2]$	402.35	400.79	-0.39%
Form factor	$[-]$	1.1619	1.1589	-0.26%

Table 4.19: Circular fuselage dimensions with aisle width increase and cargo hold volume shift

Parameter	Unit	Reference case	Geometrical modifications	Difference
Fuselage height	$[m]$	4.11	4.00	-2.68%
Fuselage width	$[m]$	4.11	4.00	-2.68%
Equivalent diameter	$[m]$	4.11	4.00	-2.68%
Fuselage length	$[m]$	36.75	36.71	-0.11%
Wetted area	$[m^2]$	420.18	408.00	-2.90%
Form factor	$[-]$	1.1595	1.1580	-0.13%

Table 4.20: Double bubble fuselage dimensions with aisle width increase and cargo hold volume shift

Parameter	Unit	Reference case	Geometrical modifications	Difference
Fuselage height	$[m]$	4.4	4.52	2.73%
Fuselage width	$[m]$	3.88	4.00	3.09%
Equivalent diameter	$[m]$	4.13	4.25	2.91%
Fuselage length	$[m]$	36.66	36.71	0.14%
Wetted area	$[m^2]$	426.62	437.74	2.61%
Form factor	$[-]$	1.1599	1.1616	0.15%

The results for the fuselage drag area are presented in table 4.22. It shows that combining the aisle width increase with the cargo hold volume shift to the overhead bins results in a lower fuselage drag area for the circular, the elliptical and the oval cross section but results in a higher fuselage drag area for the double bubble cross section. The lowest fuselage drag area is reached for the elliptical cross section and the highest fuselage drag area is reached for the oval cross section in both cases. The value in bold in table 4.22 shows the lowest fuselage drag area of the case study which corresponds to the elliptical cross section with a larger aisle width, more volume in overhead bins and less volume in the cargo holds.

Table 4.21: Oval fuselage dimensions with aisle width increase and cargo hold volume shift

Parameter	Unit	Reference case	Geometrical modifications	Difference
Fuselage height	$[m]$	4.74	4.55	-4.01%
Fuselage width	$[m]$	4.72	4.52	-4.24%
Equivalent diameter	$[m]$	4.73	4.53	-4.23%
Fuselage length	$[m]$	38.55	37.54	-2.62%
Wetted area	$[m^2]$	499.01	465.63	-6.69%
Form factor	$[-]$	1.1662	1.1648	-0.12%

Table 4.22: Fuselage drag area results when combining aisle width increase and cargo hold volume shift

Cross section type	Reference case	Geometrical modifications	Difference
Circle	0.760 m^2	0.759 m^2	-0.13%
Ellipse	0.742 m^2	**0.731** m^2	-1.48%
Double bubble	0.795 m^2	0.817 m^2	2.77%
Oval	0.916 m^2	0.868 m^2	-5.24%

The results for the fuselage weight are presented in table 4.23. It shows that combining the aisle width increase with the cargo hold volume shift to the overhead bins results in a lower fuselage weight for the circular, elliptical and oval cross sections but results in a higher fuselage weight for the double bubble cross section. The lowest fuselage weight is reached for the elliptical cross section and the highest fuselage weight is reached for the oval cross section in both cases. The value in bold in table 4.22 shows the lowest fuselage weight of the case study which corresponds to the elliptical cross section with a larger aisle width, more volume in overhead bins and less volume in the cargo holds.

Table 4.23: Fuselage weight results when combining aisle width increase and cargo hold volume shift

Cross section type	Reference case	Geometrical modifications	Difference
Circle	8150 kg	8135 kg	-0.18%
Ellipse	7841 kg	**7822** kg	-0.24%
Double bubble	8436 kg	8577 kg	1.67%
Oval	9491 kg	8952 kg	-5.68%

The cross section and the side view of this fuselage can be found respectively in figures 4.26 and 4.29. These figures are accompagnied by the cross section and the side view of the A320-200 fuselage, shown in figures 4.25 and 4.28. An overlap of figures 4.25 and 4.26 can be found in figure 4.27. The smaller fuselage height and width for the new cross section are clearly visible in figure 4.27. Moreover, the larger overhead bins and the smaller cargo holds are depicted in figure 4.27. Finally, the larger aisle width for the new cross section can be observed. An overlap of figures 4.28 and 4.29 can be found in figure 4.30. This overlap shows the smaller fuselage height and the larger fuselage length for the fuselage depicted in figure 4.29 compared to the A320-200 fuselage depicted in figure 4.28.

It can be concluded that increasing passenger's comfort and shifting cargo hold volume to overhead bins results in lower fuselage drag area and fuselage weight for the circular, elliptical and oval cross sections but results in higher fuselage drag area and fuselage weight for the double bubble cross section. The best fuselage configuration of the study is the elliptical cross section fuselage with a larger aisle width and the shift of cargo hold volume to the overhead bins.

4.5. CONCLUSION

This set of case studies has shown the impact of fulfilling some of the requirements for the future of air travel. Circular, elliptical and double bubble cross sections have been applied to a medium range conventional fuselage of the A320-200 type to show the impact of increasing the aisle width and shifting cargo hold volume to the overhead bins on the fuselage drag area and the fuselage weight. A fourth cross section has also been

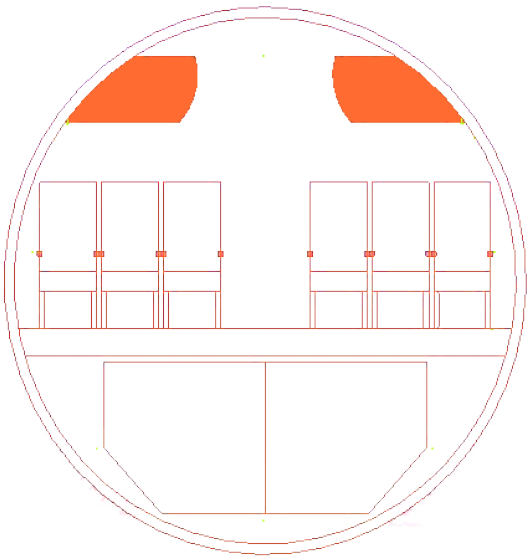

Figure 4.25: Cross section of the A320-200 fuselage

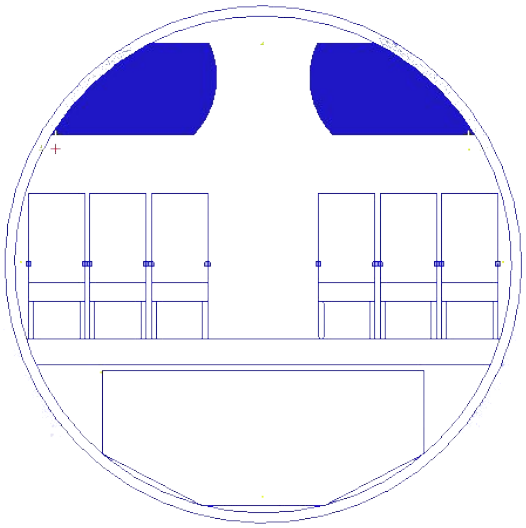

Figure 4.26: Cross section of the best fuselage with a shift of the cargo hold volume to the overhead bins and an aisle width increase

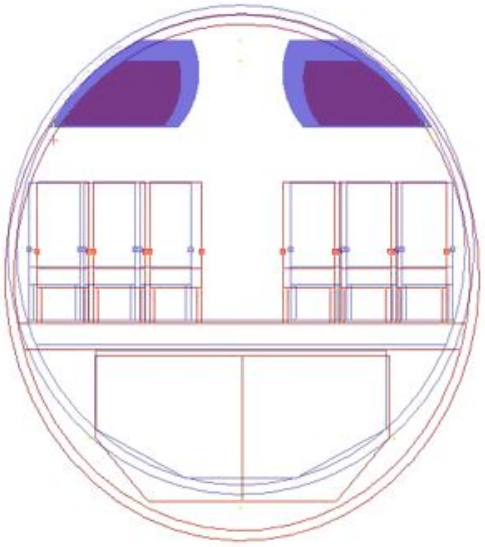

Figure 4.27: Overlap of A320-200 cross section with cross section with cargo hold volume shift and aisle width increase

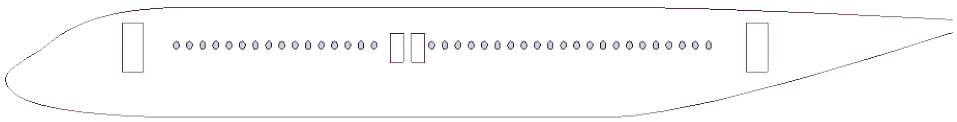

Figure 4.28: Side view of the A320-200 fuselage

applied to the conventional fuselage: the oval cross section. This cross section was designed to be applied to fuselage with a large amount of seats abreast (higher than 10 seats abreast). From the case studies presented here, the oval fuselage results in higher fuselage drag area and weight than a circular, elliptical or double bubble fuselage. The best fuselage cross section resulting in the lowest fuselage drag area and the lowest fuselage weight is the elliptical cross section. Only increasing the aisle width results in an increase in fuselage drag area and fuselage weight whereas only shifting cargo hold volume to the overhead bins results in a decrease

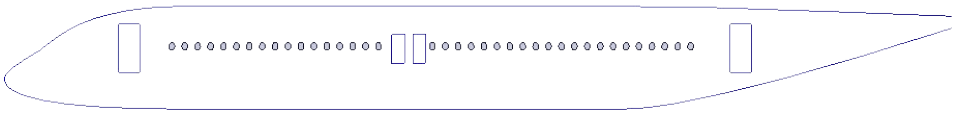

Figure 4.29: Side view of the best fuselage with a shift of the cargo hold volume to the overhead bins and an aisle width increase

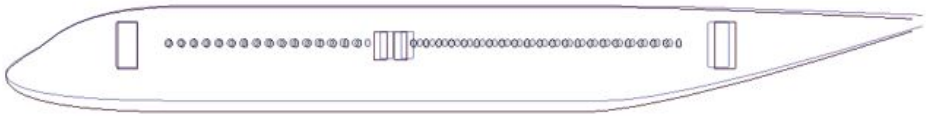

Figure 4.30: Overlap of A320-200 side view with side view with cargo hold volume shift and an aisle width increase

in fuselage drag area and fuselage weight. A combination of the two geometry modifications results in a decrease in fuselage drag area and fuselage weight for the circular, elliptical and oval cross section fuselages but results in an increase in fuselage drag area and fuselage weight for the double bubble cross section fuselage. It seems that applying the elliptical cross section to a medium range aircraft fuselage gives the best results in terms of fuselage performances. It also seems to be the best cross section to use when modifying the fuselage to meet the requirements for the future of air travel.

The focus of the case studies presented was on conventional fuselages. An unconventional cross section, the oval cross section, was also studied along side the conventional cross sections (circle, ellipse and double bubble). But what would happen to the fuselage performances if an unconventional fuselage were to be studied for the same requirements for the future of air travel? How would the fuselage performances be impacted? This is the purpose of the next section: the Prandtl Plane fuselage.

5

THE PRANDTL PLANE FUSELAGE

The Prandtl Plane is now being studied as part of a Horizon 2020 project funded by the European Commission. The main goal of this project is to 'confer to present aircraft like the Airbus 320 or Boeing 737 the payload capacity of bigger airplanes, such as A330/B767' [1]. This project aims at increasing the payload capacity of medium range aircraft without altering the fuselage length or the wingspan. The particular wing system of the Prandtl Plane falls out of the scope of this thesis project because this study focuses on the fuselage. However it is important to mention that the wing system of the Prandtl Plane enables the increase in payload capacity which results in a smaller increase in wingspan than a conventional aircraft. In fact, an increase in payload in a commercial aircraft leads to an increase in wingspan because the extra payload leads to additional weight which has to be supported by the wings. The wing system of the Prandtl Plane called the box shaped wings makes use of a front wing and a rear wing both generating positive lift. The Prandtl Plane configuration can then be seen as a low wing span configuration as described in chapter 1 which means that an increase in payload capacity would lead to a smaller increase in wingspan for the Prandtl Plane than for a conventional fuselage.

A report for advisors [10] of the Parsifal project was published presenting the results of their activities so far. The report shows the outer geometry and cabin configuration of single deck and double deck fuselages with various fuselage lengths. The purpose of the study in this master thesis is three fold:

- Regenerate the fuselages' outer geometry and cabin configuration in ParaFuse starting from the same payload requirements used in the Parsifal report [10],
- Generate different cabin configurations using the outside-in approach of ParaFuse to show other cabin configurations than the high capacity configuration presented in the Parsifal report [10],
- Apply different cross sections to the fuselages to observe the impact on the fuselage performances,
- Increase the aisle width and shift a portion of cargo hold volume into the overhead bins to observe the impact on the fuselage performances.

5.1. GENERATE PRANDTL PLANE'S FUSELAGES IN PARAFUSE

The generation of the fuselages described in the Parsifal report [10] is performed using the inside-out approach of ParaFuse. Five Prandtl Plane fuselages are described in the Parsifal report [10]: three single deck fuselages with a different number of passengers and two double deck fuselages with a different number of passengers. The inputs used to generate the single deck fuselages are described in table 5.1. The inputs used to generate the double deck fuselages are described in table 5.2.

[1] www.parsifalproject.eu

5.1.1. GENERATION OF SINGLE DECK PRANDTL PLANE FUSELAGES

The results for the cross section of the single deck Prandtl Plane fuselages extracted from ParaFuse can be found in table 5.4. The results presented in table 5.4 can be applied to the three single deck fuselages with different number of passengers. The cross section generated in ParaFuse results in a slightly lower fuselage height but a quite larger fuselage width. The floor thickness and the cross sectional area are not known for the reference fuselage but are given in ParaFuse. The differences observed for the fuselage height and width are firstly due to the constraints of the main cabin cross section. These constraints, which are used to determine the main cross section in the inside-out approach, are the floor point extremes, the side wall clearances, the aisle height, the eye clearance constraints and the cargo extreme points. As can be seen in figure 5.1, six constraints are active and are depicted by red, orange and green bullets. The other constraint points are not active and are depicted by yellow crosses. The active constraints correspond to the eye clearance constraints on the starboard and port sides of the fuselage and the cargo extreme points. The cargo extreme points are defined by the shape and size of the unit load device LD3-45. The eye clearance constraints are defined by two inputs. The values of these inputs are given in table 5.3. The sitting eye height corresponds to a measurement from buttocks to eyes of the 95th percentile US male [41]. The eye clearance radius is given by Torenbeek in [40] page 71. The values of these inputs used for the reference aircraft A320-200 are not known thus default values had to be chosen. An increase in sitting eye height and a decrease in eye clearance radius could lead to a higher fuselage height and a lower fuselage width in ParaFuse in order to get a better match with the cross section dimensions. Other causes explain the difference in fuselage height and width. These causes will be detailed below thanks to the observation made from the overlap presented in figure 5.4.

Table 5.1: Input parameters to generate single deck Prandtl Plane fuselages in ParaFuse using the inside-out approach

Parameter	Value	Unit
Number of passengers	{248, 280, 316}	[−]
Aisle width	0.70	[m]
Aisle height	2.108	[m]
Cargo type	Containerized	[−]
ULD type	LD3-45	[−]
Cross section shape	Ellipse	[−]
Number of seats abreast	8	[−]
Seat width	0.457	[m]
Seat height	0.991	[m]

Table 5.2: Input parameters to generate double deck Prandtl Plane fuselages in ParaFuse using the inside-out approach

Parameter	Value	Unit
Number of passengers	{318, 350}	[−]
Aisle width	0.75	[m]
Aisle height	2.108	[m]
Cargo type	Containerized	[−]
ULD type	LD3-45	[−]
Cross section shape	Ellipse	[−]
Number of seats abreast - lower deck	6	[−]
Number of seats abreast - upper deck	6	[−]
Seat width	0.457	[m]
Seat height	0.991	[m]

Table 5.3: Inputs used to calculate the eye clearance constraints

Input	Unit	Value
Sitting eye height [41]	[m]	0.89
Eye clearance constraint [40]	[m]	0.25

Both cross sections (of the reference aircraft and of the fuselage generated in ParaFuse) can be found in

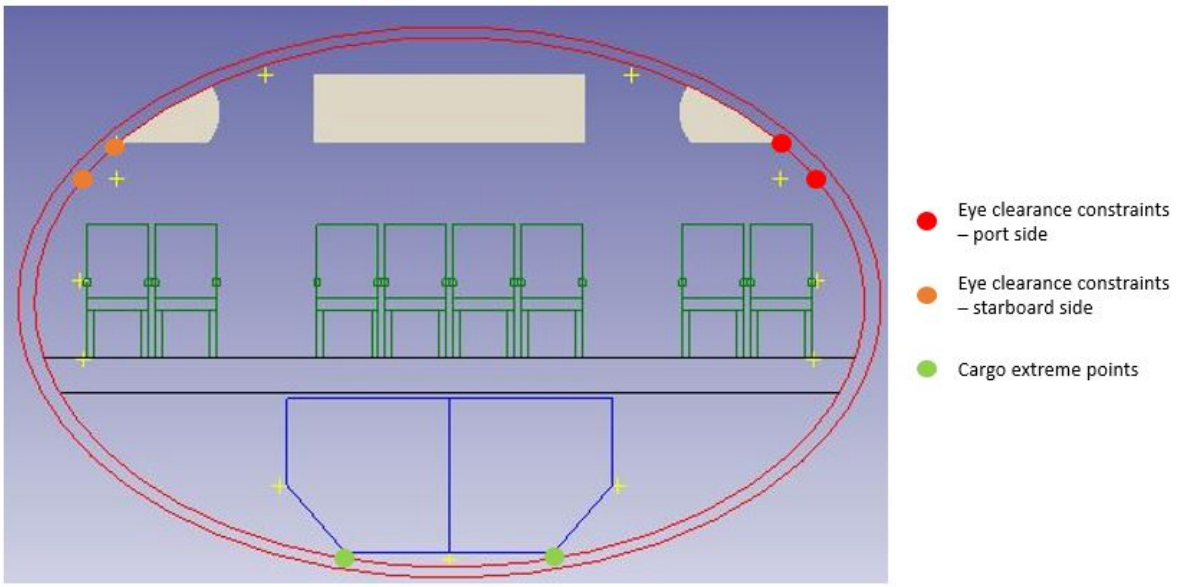

Figure 5.1: Active constraints of the main cross section of the single deck Prandtl Plane fuselage generated in ParaFuse

figures 5.2 and 5.3. An overlap of both cross sections can be found in figure 5.4. Both cross sections have been overlapped with respect to the floor location. Thus, the first observation that can be made is that the seats have the same height. The seats have the same width as well although on the overlap it seems that the widths are different. This is due to the fact that ParaFuse takes the armrest into account whereas the Parsifal report [10] only drew simple rectangles for the seats without taking the armrest into account. The aisle width also seems larger in ParaFuse than in the reference fuselage. The aisle width is in fact slightly larger due to the armrests which are taken into account to satisfy the aisle width given as input. The second observation is about the floor thickness which is larger in ParaFuse than in the report. In ParaFuse, the floor thickness is calculated based on the equivalent diameter of the cross section [40]. However there is no mention of the floor thickness calculation in the Parsifal report. Having a larger floor thickness in ParaFuse than in the Parsifal report makes sense because the equivalent diameter in ParaFuse is larger than in the Parsifal report as table 5.4 shows. The cargo hold has the same size and shape but is placed lower in ParaFuse than in the reference fuselage due to the thicker floor. Finally, the overhead bins generated in ParaFuse fit in the space drawn in the report dedicated to the overhead bins.

As stated previously, the cross sectional area is not given in the Parsifal report [10]. In ParaFuse however, the cross sectional area is given and corresponds to 19.20 m^2. If the cross section in the Parsifal report is considered an ellipse, then the cross sectional area can be calculated with the width and height and corresponds then to 16.87 m^2. However by overlapping the cross section of figure 5.2 with an ellipse generated in ParaFuse with a width of 5.155 m and a height of 4.166 m, both cross sections do not overlap as figure 5.5 shows. Figure 5.5 shows that the ellipse in blue with the same height and width as the cross section in the report [10] has a lower cross sectional area than the cross section in the Parsifal report. Only a qualitative conclusion can be given with respect to the cross sectional area of the cross section in the Parsifal report. It can be concluded here that the elliptical cross section is not the best cross section to describe the Prandtl Plane cross section of the Parsifal report. It is thus important here to make a recommendation: the cross section could be defined as a 'free form' cross section [9] which makes use of a Class function/ Shape function transformation (CST) method proposed by Kulfan ([36], [37]). This study will keep the elliptical cross section so that the fuselage performances can be calculated as in chapter 4.

The results for the single deck Prandtl Plane fuselage with 248 pasengers can be found in table 5.5. The fuselage length is slightly larger in ParaFuse than in the report [10]. There is the same number of passengers which is what was expected as the number of passengers is given as input. The number of exits and the type of exits is given in ParaFuse but there is no mention of this in the report. The number and type of exits is directly derived from the number of passengers: 248 passengers leads to needing 8 exits of type 'B'. The same

Table 5.4: Characteristics of cross section of single deck Prandtl Plane fuselages extracted from report [10] and from ParaFuse

Parameter	Unit	Reference aircraft [10]	ParaFuse aircraft	Difference
Fuselage height	$[m]$	4.166	4.104	-1.49%
Fuselage width	$[m]$	5.155	6.444	25.0%
Equivalent diameter	$[m]$	4.634	5.143	11%
Floor thickness	$[m]$	-	0.257	-
Cross sectional area	$[m^2]$	-	19.20	-

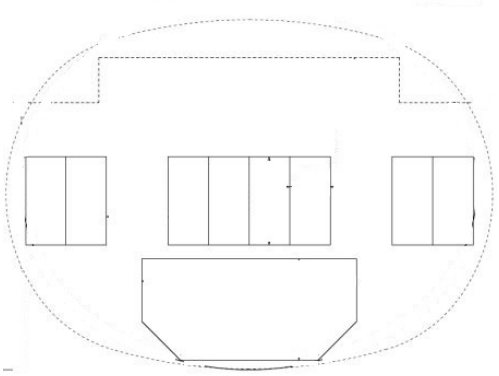

Figure 5.2: Cross section of the single deck Prandtl Plane fuselage [10]

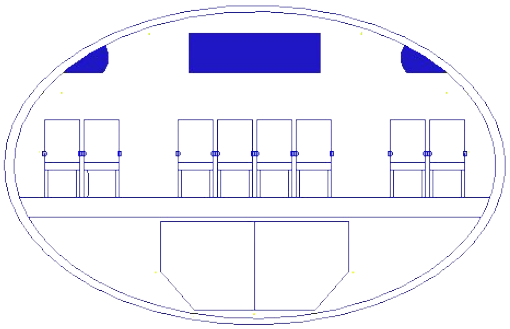

Figure 5.3: Cross section of the single deck Prandtl Plane fuselage generated in ParaFuse

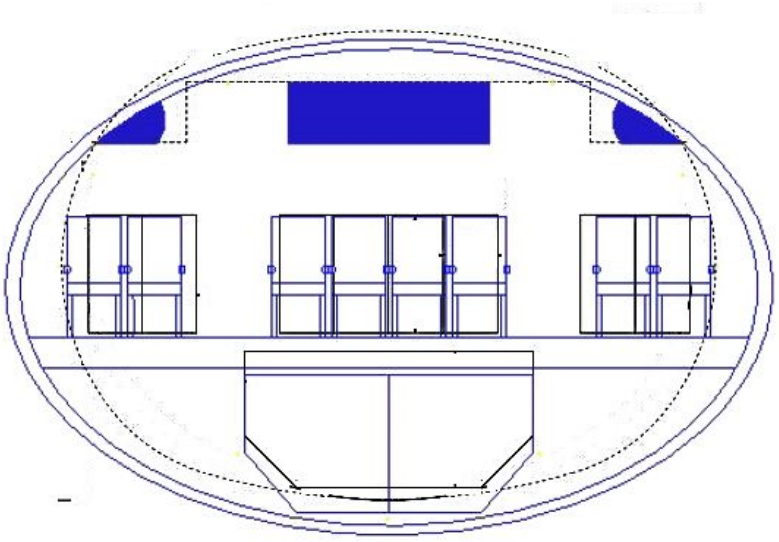

Figure 5.4: Overlap of cross sections from report [10] and generated in ParaFuse

goes for the number of lavatories and galleys: 4 lavatories and 3 galleys are necessary for 248 passengers. A top view of the fuselage can be found from the report in figure 5.6. A top view of the fuselage generated in ParaFuse can be found in figure 5.7. An overlap of figures 5.6 and 5.7 can be found in figure 5.8. The main observation that can be made is that the report did not take into account space for the emergency exits. This could be an explanation for why the fuselage is longer in ParaFuse than in the report. Also, the report does not make the distinction between lavatories and galleys. It only allocates a certain amount of space to both. ParaFuse gives a more detailed description. On the overlap in figure 5.8, it is observed that the fuselage in ParaFuse is in fact larger and longer than the fuselage in the report.

The results for the single deck Prandtl Plane fuselage with 280 pasengers can be found in table 5.6. The fuselage length is larger in ParaFuse than in the report [10]. There is the same number of passengers which is

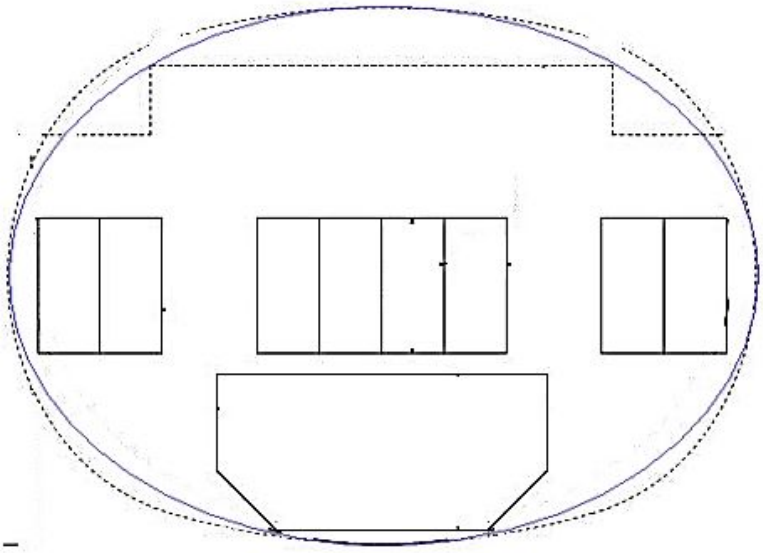

Figure 5.5: Overlap of cross section from report [10] with mathematical ellipse with same height and width

Table 5.5: Single deck Prandtl Plane fuselage characteristics for 248 passengers extracted from report [10] and from ParaFuse

Parameter	Unit	Reference aircraft [10]	ParaFuse aircraft	Difference
Fuselage length	$[m]$	36	37.05	2.91%
Number of passengers	[−]	248	248	0 %
Exit type and number	[−]	-	['B', 8]	-
Lavatories	[−]	-	4	-
Galleys	[−]	-	3	-

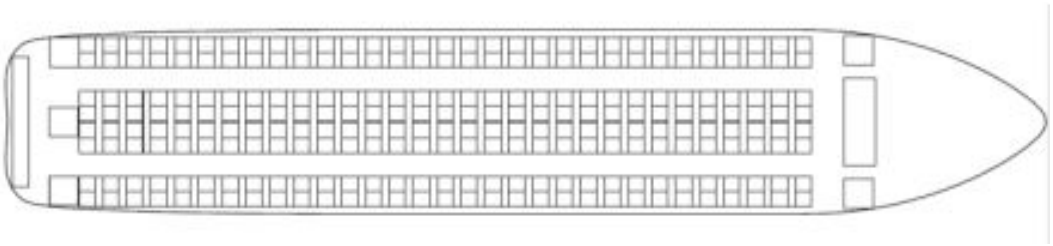

Figure 5.6: Top view of fuselage with 248 passengers [10]

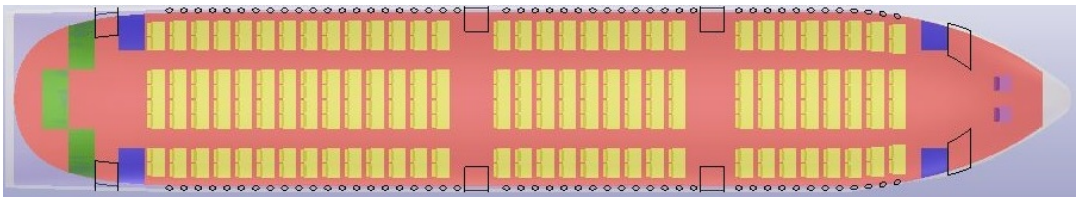

Figure 5.7: Top view of fuselage with 248 passengers in ParaFuse

what was expected as the number of passengers is given as input. The number of exits and the type of exits is given in ParaFuse but there is no mention of this in the report. The number and type of exits is directly derived from the number of passengers: 280 passengers leads to needing 8 exits of type 'B'. The same goes for the number of lavatories and galleys: 5 lavatories and 3 galleys are necessary for 280 passengers. A top view of the fuselage can be found from the report in figure 5.9. A top view of the fuselage generated in ParaFuse can be found in figure 5.10. An overlap of figures 5.9 and 5.10 can be found in figure 5.11. The main observation that can be made is that the report did not take into account space for the emergency exits. This could be an

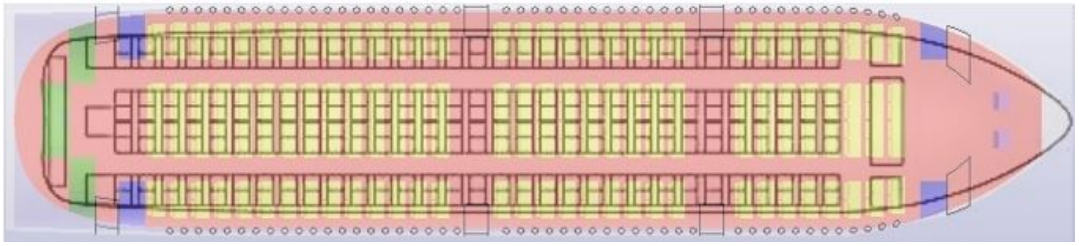

Figure 5.8: Overlap of top views of fuselage with 248 passengers from [10] and in ParaFuse

explanation for why the fuselage is longer in ParaFuse than in the report. Also, the report does not make the distinction between lavatories and galleys. It only allocates a certain amount of space to both. ParaFuse gives a more detailed description. On the overlap, it is observed that the fuselage in ParaFuse is in fact larger than the fuselage in the report.

Table 5.6: Single deck Prandtl Plane fuselage characteristics for 280 passengers extracted from report [10] and from ParaFuse

Parameter	Unit	Reference aircraft [10]	ParaFuse aircraft	Difference
Fuselage length	$[m]$	39	41.35	6.04%
Number of passengers	[−]	280	280	0 %
Exit type and number	[−]	-	[‘B’, 8]	-
Lavatories	[−]	-	5	-
Galleys	[−]	-	3	-

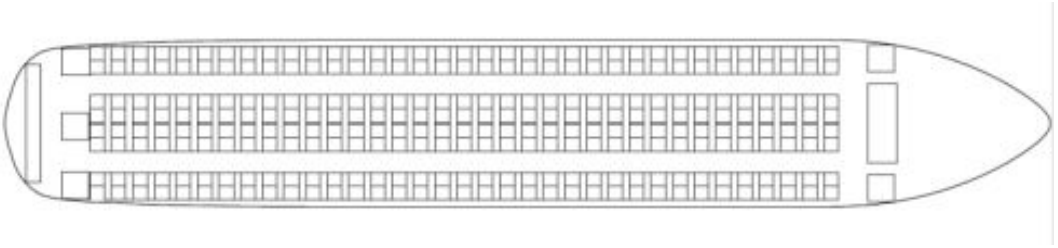

Figure 5.9: Top view of fuselage with 280 passengers [10]

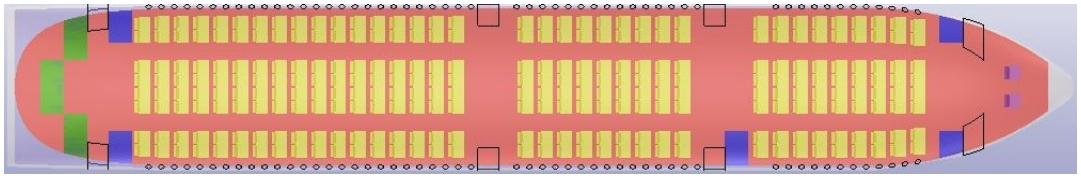

Figure 5.10: Top view of fuselage with 280 passengers in ParaFuse

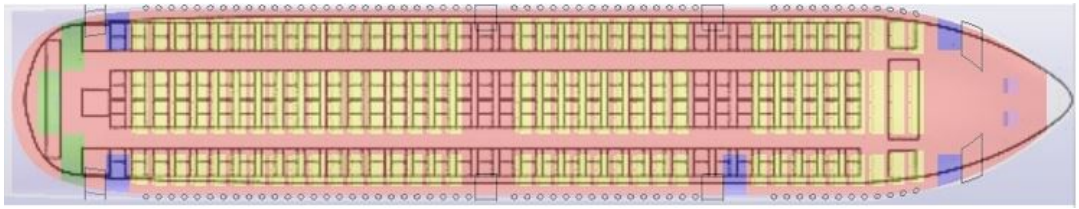

Figure 5.11: Overlap of top views of fuselage with 280 passengers from [10] and in ParaFuse

The results for the single deck Prandtl Plane fuselage with 316 pasengers can be found in table 5.7. Before

commenting on the results, an important observation has to be made: the number of passengers is not 316 passengers as stated in the Parsifal report [10] but rather 312 passengers. There are in fact 39 rows of 8 seats which results in 312 passengers as figure 5.12 shows. The fuselage length is larger in ParaFuse than in the report [10]. The number of passengers is the same in ParaFuse as in the report. If the number of passengers given to ParaFuse has been 316 and not 312, the total number of passengers in ParaFuse would have been 320. This is due to the fact that ParaFuse can fill incomplete rows. 316 passengers would lead to 39 rows of 8 seats abreast and one row of 4 seats abreast. ParaFuse would have completed the last row thus increasing the number of passengers to 320. The number of exits and the type of exits is given in ParaFuse but there is no mention of this in the report. The number and type of exits is directly derived from the number of passengers: 312 passengers leads to needing 6 exits of type 'A' which are larger than type 'B' exits. The same goes for the number of lavatories and galleys: 5 lavatories and 3 galleys are necessary for 320 passengers. A top view of the fuselage can be found from the report in figure 5.12. A top view of the fuselage generated in ParaFuse can be found in figure 5.13. An overlap of figures 5.12 and 5.13 can be found in figure 5.14. The main observation that can be made is that the report did not take into account space for the emergency exits. This could be an explanation for why the fuselage is longer in ParaFuse than in the report. Also, the report does not make the distinction between lavatories and galleys. It only allocates a certain amount of space to both. ParaFuse gives a more detailed description. On the overlap in figure 5.14, it is observed that the fuselage in ParaFuse is in fact larger and longer than the fuselage in the report.

Table 5.7: Single deck Prandtl Plane fuselage characteristics for 312 passengers extracted from report [10] and from ParaFuse

Parameter	Unit	Reference aircraft [10]	ParaFuse aircraft	Difference
Fuselage length	$[m]$	42	45.55	8.45%
Number of passengers	[−]	312	312	0.0 %
Exit type and number	[−]	-	['A', 6]	-
Lavatories	[−]	-	5	-
Galleys	[−]	-	3	-

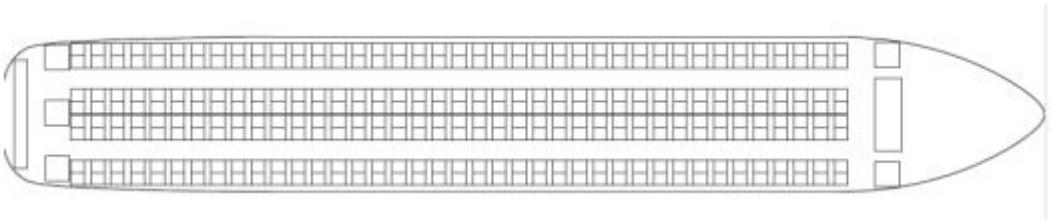

Figure 5.12: Top view of fuselage with 312 passengers [10]

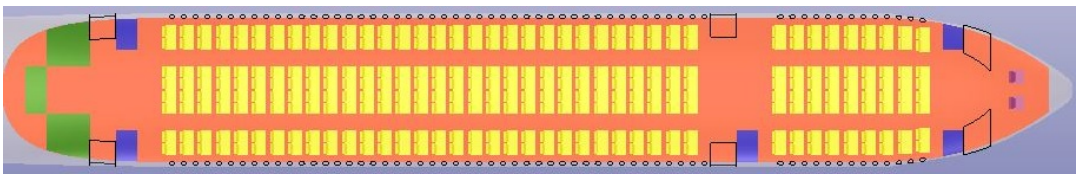

Figure 5.13: Top view of fuselage with 312 passengers in ParaFuse

5.1.2. GENERATION OF DOUBLE DECK PRANDTL PLANE FUSELAGES

The results for the cross section of the double deck Prandtl Plane fuselages extracted from ParaFuse can be found in table 5.8. The results presented in table 5.8 can be applied to the two double deck fuselages with different number of passengers. The cross section generated in ParaFuse results in a larger fuselage width and height than in the report [10]. The cross section of the report and the cross section of ParaFuse can be found in figures 5.16 and 5.17. The floor thickness and the cross sectional area are not known for the reference fuselage but are given in ParaFuse. The differences observed for the fuselage height and width are again due

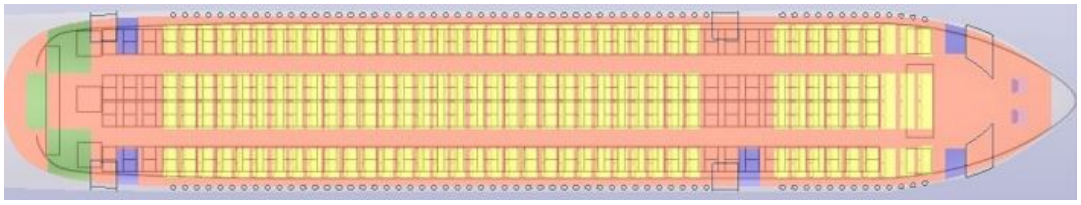

Figure 5.14: Overlap of top views of fuselage with 312 passengers from [10] and in ParaFuse

to the constraints of the main cabin cross section as for the single deck cross section in section 5.1.1. Figure 5.15 shows the active constraints of the double deck cross section. The active constraints are depicted by red, orange and green bullets. The other constraint points are inactiv and depicted by yellow crosses. The active constraints correspond to two of the four eye clearance constraints on the starboard and the port sides of the fuselage and the cargo extreme points. The cargo extreme points are defined by the shape and size of the unit load device LD3-45. The eye clearance constraints are defined by the sitting eye height and the eye clearance radius, both defined in table 5.3.

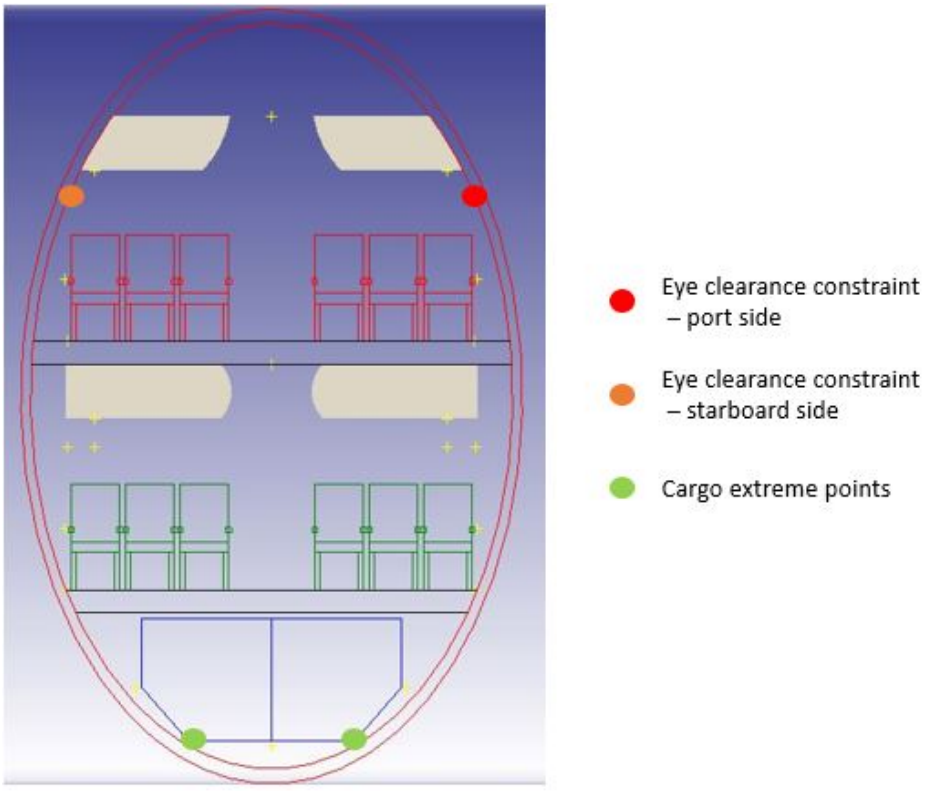

Figure 5.15: Active constraints of the main cross section of the double deck Prandtl Plane fuselage generated in ParaFuse

An overlap of both cross sections can be found in figure 5.18. Both cross sections have been overlapped with respect to the lower deck's floor location. The larger fuselage width and height can be observed in figure 5.17. The larger equivalent diameter of the cross section leads to a thicker floor which is observed in figure 5.17. The seats have the same height as can be seen on the lower deck but their width seems to be different. This is due to the fact that ParaFuse takes the armrests into account. The aisle width also seems larger in ParaFuse due to the armrests present. The cargo hold has the same size and shape but is placed lower in ParaFuse due to the thicker floor. The overhead bins generated in ParaFuse fit in the space drawn on the lower deck in the report. It is important to note that ParaFuse makes sure that there is enough space between two overhead bins to open both doors at the same time. The space allocated to the overhead bins in the Parsifal report would not allow for both overhead bin doors to open simultaneously. This is why the overhead bins in ParaFuse are slightly shorter than in the report. The upper floor is located higher in ParaFuse thus there is a

mismatch with the overhead bins on the upper floor. This cross section is used to generate two double deck fuselages with 318 passengers and 350 passengers.

As stated previously, the cross sectional area is not given in the Parsifal report [10]. In ParaFuse however, the cross sectional area is given and corresponds to 24.60 m^2 as table 5.8 shows. If the cross section in the report is considered elliptical, the cross sectional area can be computed and corresponds then to 18.88 m^2. However by overlapping the cross section of figure 5.16 with an ellipse generated in ParaFuse using the outside-in approach with a width of 3.932 m and a height of 6.113 m, both cross sections do not overlap as figure 5.19 shows. Figure 5.19 shows that the double deck cross section in the Parsifal report has a higher cross sectional area than the elliptical cross section with the same height and width (depicted in blue in figure 5.19). Again, only a qualitative conclusion can be drawn with respect to the cross sectional area of the cross section in the report. Like in section 5.1.1, the elliptical cross section is not the best cross section to describe the Prandtl Plane double deck cross section. A free from cross section defined by CST coefficients would be more appropriate. This study will keep the elliptical cross section though as for the single deck cross section.

Table 5.8: Characteristics of cross section of single deck Prandtl Plane fuselages extracted from report [10] and from ParaFuse

Parameter	Unit	Reference aircraft [10]	ParaFuse aircraft	Difference
Fuselage height	$[m]$	6.113	7.243	18.48%
Fuselage width	$[m]$	3.932	4.678	18.97%
Equivalent diameter	$[m]$	4.903	5.821	18.72%
Floor thickness	$[m]$	-	0.217	-
Cross sectional area	$[m^2]$	-	24.60	-

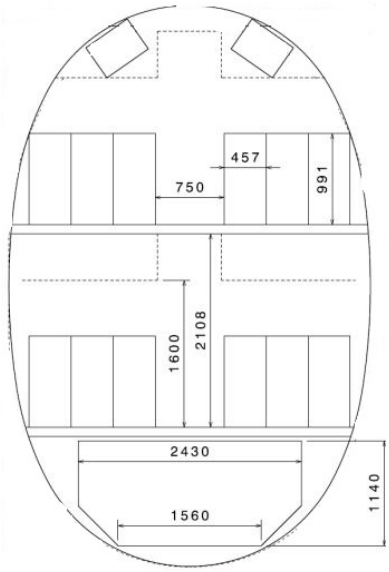

Figure 5.16: Cross section of the double deck Prandtl Plane fuselage [10]

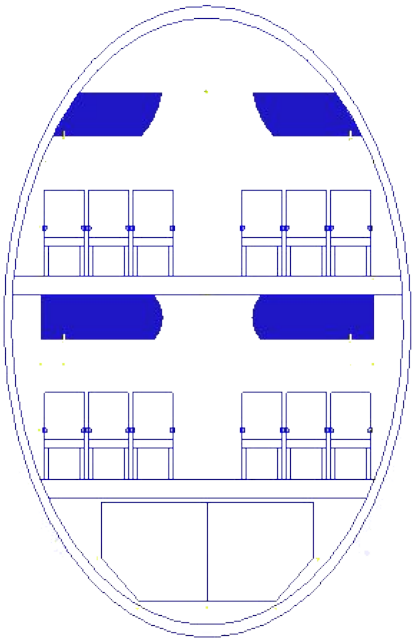

Figure 5.17: Cross section of the double deck Prandtl Plane fuselage generated in ParaFuse

The results for the double deck Prandtl Plane fuselage with 318 passengers can be found in table 5.9. The fuselage length is smaller in ParaFuse than for the reference aircraft. The total number of passengers is slightly larger due to the possibility of ParaFuse to fill incomplete rows of seats. In fact there is no possibility to check the actual number of passengers in the fuselage like in section 5.1.1 because the top view of this fuselage is not drawn. The number of passengers on each deck is not given in the report [10] however this data is available in ParaFuse. The number of passengers on each deck enables the calculation of the number of exits and

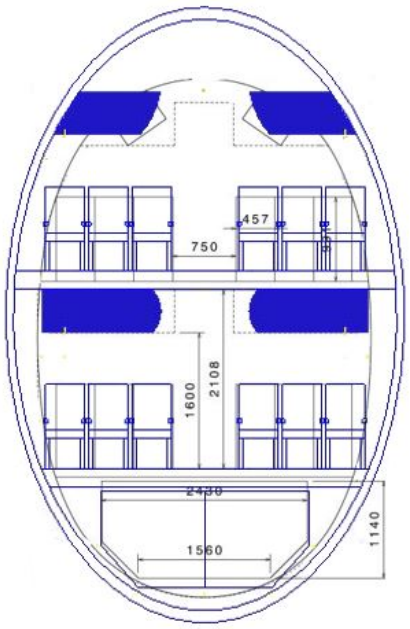

Figure 5.18: Overlap of cross sections from report [10] and generated in ParaFuse

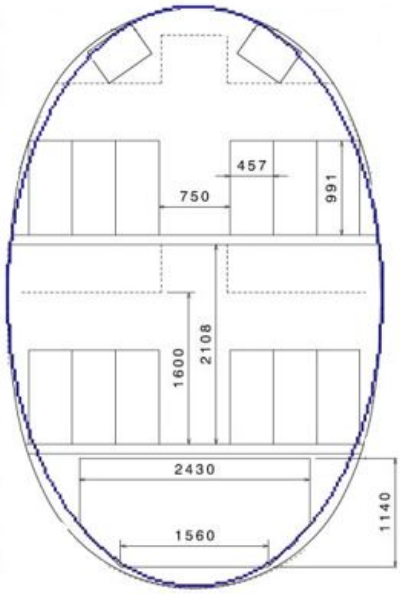

Figure 5.19: Overlap of cross section from report [10] with mathematical ellipse with same height and width

their types, the number of lavatories and the number of galleys per deck. There are four exits type '1' and four exits type '3', four lavatories and two galleys on each deck. A top view of the lower deck can be found in figure 5.20 and a top view of the upper deck can be found in figure 5.21. As can be seen in figure 5.21, there are no seats in the nose cone in order to accomodate for stairs to connect both decks, as well as coat stowage and other stowage present for example in the nose cone of the Airbus A380 [3].

The results for the double deck Prandtl Plane fuselage with 350 passengers can be found in table 5.10. The fuselage length is smaller in ParaFuse than for the reference aircraft. The total number of passengers is slightly larger due to the possibility of ParaFuse to fill incomplete rows of seats. The number of passengers on each deck is not given in the report [10] however this data is available in ParaFuse. The number of passengers

Table 5.9: Double deck Prandtl Plane fuselage characteristics for 318 passengers extracted from report [10] and from ParaFuse

Parameter	Unit	Reference aircraft [10]	ParaFuse aircraft	Difference
Fuselage length	$[m]$	36	34.59	-3.92%
Passengers lower deck	[−]	-	166	-
Passengers upper deck	[−]	-	154	-
Total number of passengers	[−]	318	320	0.63 %
Exit type and number	[−]	-	['1', 8], ['3', 8]	-
Lavatories	[−]	-	8	-
Galleys	[−]	-	4	-

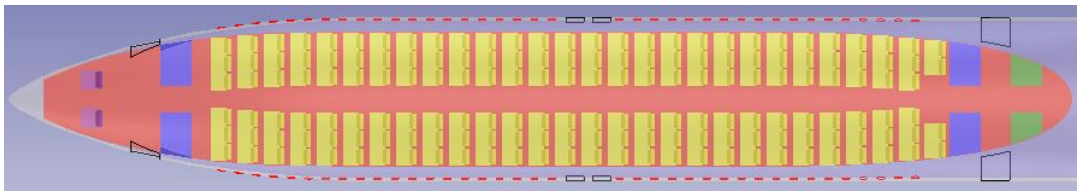

Figure 5.20: Top view of lower deck of fuselage with 320 passengers, generated in ParaFuse

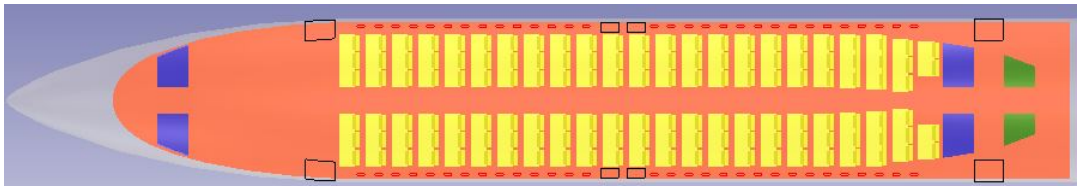

Figure 5.21: Top view of upper deck of fuselage with 320 passengers, generated in ParaFuse

on each deck enables the calculation of the number of exits and their types, the number of lavatories and the number of galleys per deck. There are four exits type '1' and four exits type '3', four lavatories and two galleys on each deck. A top view of the lower deck can be found in figure 5.22 and a top view of the upper deck can be found in figure 5.23. As for the previous double deck fuselage, it can be seen in figure 5.23 that there are no seats in the nose cone in order to accomodate for stairs to connect both decks, as well as coat stowage and other stowage.

Table 5.10: Double deck Prandtl Plane fuselage characteristics for 350 passengers extracted from report [10] and from ParaFuse

Parameter	Unit	Reference aircraft [10]	ParaFuse aircraft	Difference
Fuselage length	$[m]$	42	38.42	-8.52%
Passengers lower deck	[−]	-	180	-
Passengers upper deck	[−]	-	174	-
Total number of passengers	[−]	350	354	1.14%
Exit type and number	[−]	-	['1', 8], ['3', 8]	-
Lavatories	[−]	-	8	-
Galleys	[−]	-	4	-

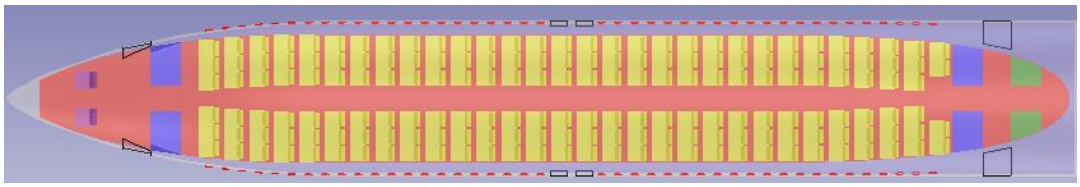

Figure 5.22: Top view of lower deck of fuselage with 354 passengers, generated in ParaFuse

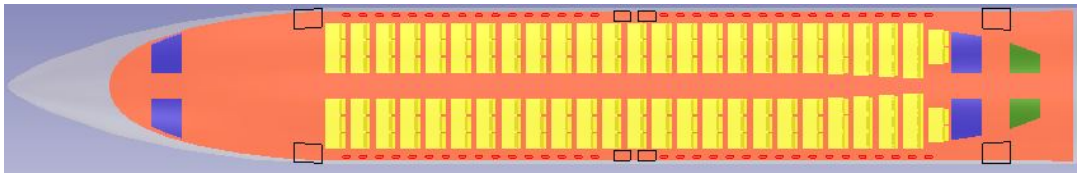

Figure 5.23: Top view of upper deck of fuselage with 354 passengers, generated in ParaFuse

5.2. POSSIBLE CABIN CONFIGURATIONS FOR PRANDTL PLANE FUSELAGES

The report of the Parsifal project [10] shows the initial definition of two fuselage designs: a single deck and a double deck fuselage configuration. Both configurations have been designed at high capacity, meaning that there is only one seat class present: the economy class. ParaFuse enables the generation of different cabin configurations by fixing the outer geometry of a fuselage. This method is called the outside-in method. The various cabin configurations that are going to be generated are:

- One seat class: full economy class,
- Two seat classes: first and economy class,
- Three seat classes: first, premium economy and economy class,
- Four seat classes: first, business, premium economy and economy class.

The report [10] only gives the dimensions of the economy seat. Table 5.11 gives the seat pitch and width of the first class, business class, premium economy class and economy class seats. The economy class seat dimensions are taken from report [10]. The first, business and premium economy class seat dimensions are taken from De Jonge's Master thesis [9] for short range flights. The four cabin configurations are going to be generated for a single deck fuselage. The outer dimensions of the single deck fuselage are described in table 5.12. These dimensions are taken from tables 5.4 and 5.5.

Table 5.11: Seat dimensions for Prandtl Plane cabin configurations [10], [9]

	Seat pitch $[m]$	Seat width $[m]$
Economy class	0.76	0.457
Premium economy class	0.97	0.48
Business class	0.98	0.51
First class	0.98	0.51

Table 5.12: Fuselage dimensions for Prandtl Plane cabin configurations

Fuselage length $[m]$	Fuselage height $[m]$	Fuselage width $[m]$
37.05	4.104	6.444

The four cabin configurations are shown in figures 5.24, 5.25, 5.26 and 5.27. The yellow seats correspond to the economy class, the orange seats to the premium economy class, the green seats to the business class and the blue seats to the first class. The number of passengers per class and the total number of passengers for each cabin configuration can be found in table 5.13. Each cabin configuration has a different number of passengers. Increasing the number of classes inevitably reduces the total number of passengers because the economy class seats have the lowest seat pitch and seat width as table 5.11 shows.

The cabin configurations generated here are just a few examples of the cabin configuration possibilities for this single deck fuselage. ParaFuse can generate fuselages with one to four different seat classes which gives a lot of flexibility in terms of cabin configuration.

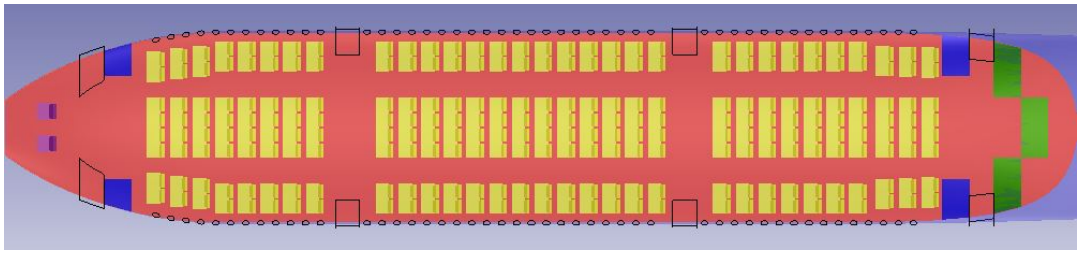

Figure 5.24: Top view of single deck fuselage with one seat class

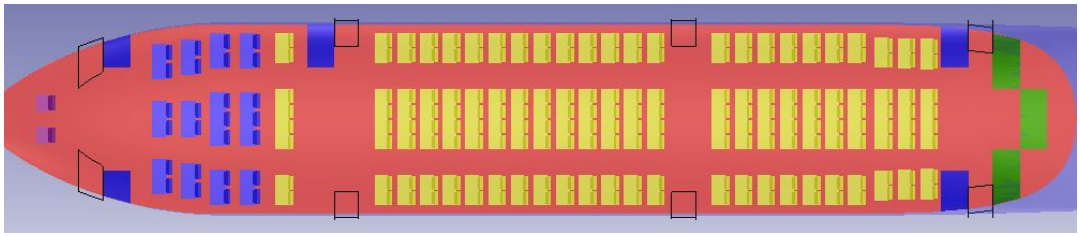

Figure 5.25: Top view of single deck fuselage with two seat class

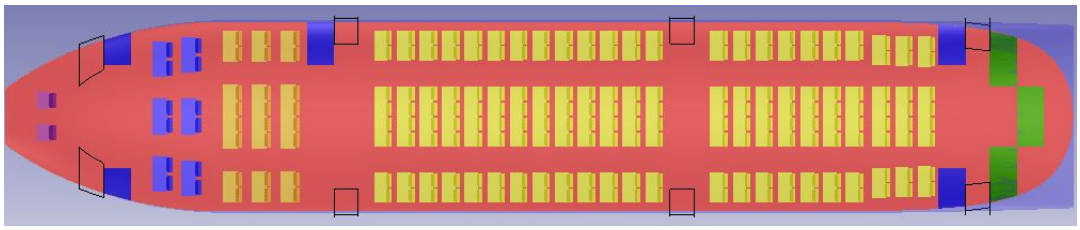

Figure 5.26: Top view of single deck fuselage with three seat class

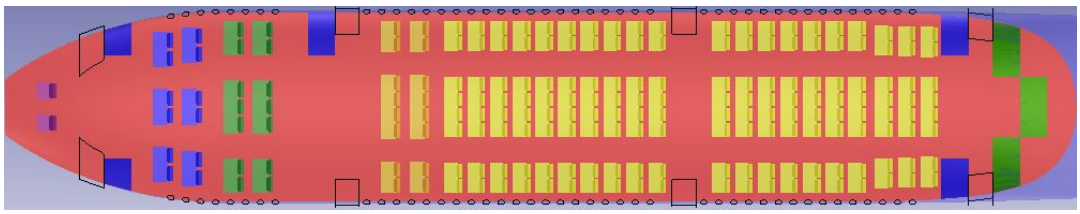

Figure 5.27: Top view of single deck fuselage with four seat class

Table 5.13: Number of passengers per cabin configuration

Cabin configuration	First pax	Business pax	Premium economy pax	Economy pax	Total pax
One seat class	0	0	0	248	248
Two seat classes	26	0	0	192	218
Three seat classes	12	0	24	184	220
Four seat classes	12	14	16	160	202

5.3. CASE STUDIES ON AIRCRAFT PERFORMANCES

Three case studies have been performed in order to answer the subquestions presented in section 1.7 for the Prandtl Plane. Each study has been performed for the single deck fuselage with 248 passengers in economy class presented in figure 5.7. The fuselage performances calculated in each of the following case studies are the fuselage drag area and the fuselage weight.

5.3.1. REDUCING TURN AROUND TIME BY INCREASING THE AISLE WIDTH

This study aims at answering the following question:

What is the impact of increasing the aisle width on the fuselage drag and the fuselage weight?

The study performed is the same as the one performed in section 4.2. During this study, the cross section shape and the aisle width will vary. The fuselage is generated using the inside-out approach and the fuselage drag area and fuselage weight are calculated based on data extracted from ParaFuse.

The aisle width increase has a different impact on the fuselage height, width and length depending on the cross section type used. In fact, tables 5.14 and 5.15 show that an increase in aisle width results in an increase in fuselage height width and length for a circular and an elliptical fuselage. However, table 5.16 shows that an increase in aisle width results in an increase in fuselage width but a slight decrease in fuselage length. It has no impact on the fuselage height.

The geometrical modifications of the fuselage due to the aisle width increase have been presented. These geometrical modifications have an impact on the fuselage wetted area and the form factor which in turn influence the variation of fuselage drag area and fuselage weight as described in section 1.6. Tables 5.14 to 5.16 show that the aisle with increase leads to an increase in wetted area and in form factor for all the cross section types. This forecasts an increase in fuselage drag area and in fuselage weight as it was concluded in section 4.1.

Table 5.14: Circular fuselage dimensions with different aisle widths

Parameter	Unit	Aisle width = 0.70m	Aisle width = 0.81m	Difference
Fuselage height	$[m]$	6.44	6.64	3.11%
Fuselage width	$[m]$	6.44	6.64	3.11%
Equivalent diameter	$[m]$	6.44	6.64	3.11%
Fuselage length	$[m]$	37.82	38.02	0.53%
Wetted area	$[m^2]$	592.34	626.32	5.74%
Form factor	$[-]$	1.2375	1.2466	0.74 %

Table 5.15: Elliptical fuselage dimensions with different aisle widths

Parameter	Unit	Aisle width = 0.70m	Aisle width = 0.81m	Difference
Fuselage height	$[m]$	4.1	4.13	0.73%
Fuselage width	$[m]$	6.44	6.64	3.11%
Equivalent diameter	$[m]$	5.14	5.24	1.91%
Fuselage length	$[m]$	37.04	37.14	0.27%
Wetted area	$[m^2]$	587.67	601.95	2.43%
Form factor	$[-]$	1.1828	1.1859	0.26%

Table 5.16: Oval fuselage dimensions with different aisle widths

Parameter	Unit	Aisle width = 0.70m	Aisle width = 0.81m	Difference
Fuselage height	$[m]$	5.66	5.66	0.0%
Fuselage width	$[m]$	6.23	6.48	4.01%
Equivalent diameter	$[m]$	5.94	6.06	1.99%
Fuselage length	$[m]$	38.81	38.52	-0.75%
Wetted area	$[m^2]$	645.34	683.57	5.92%
Form factor	$[-]$	1.2046	1.2121	0.62%

The results for the fuselage drag area are presented in table 5.17. An increase in aisle width leads to an increase in drag area for each cross section type. The increase in drag area varies between 1.79% for the elliptical cross section and 6.84% for the circular cross section. However for each aisle width, the highest drag

area is reached for the oval cross section fuselage and the lowest drag area is reached for the elliptical cross section fuselage. The value in bold in table 5.17 shows the lowest drag area which corresponds to the Prandtl Plane fuselage generated in figure 5.7.

Table 5.17: Fuselage drag area results for an increased aisle width for Prandtl Plane fuselage

Cross section type	Aisle width = 0.70m	Aisle width = 0.81m	Difference
Circle	1.17 m^2	1.25 m^2	6.84%
Ellipse	**1.12** m^2	1.14 m^2	1.79%
Oval	1.24 m^2	1.32 m^2	6.45%

The results for the fuselage weight are presented in table 5.18. As for the drag area, an increase in aisle width results in an increase in fuselage weight. The increase in weight varies between 1.81% for the elliptical cross section and 6.4% for the oval cross section. For each aisle width, the highest weight is reached for the oval cross section fuselage and the lowest weight is reached for the circular cross section fuselage. The value in bold in table 5.18 shows the lowest fuselage weight which corresponds to the Prandtl Plane fuselage with a circular cross section and an aisle width of 0.70 meters.

Table 5.18: Fuselage weight results for an increased aisle width for Prandtl Plane fuselage

Cross section type	Aisle width = 0.70m	Aisle width = 0.81m	Difference
Circle	**10028** kg	10559 kg	5.30%
Ellipse	10981 kg	11180 kg	1.81%
Oval	11567 kg	12266 kg	6.04%

Before concluding on this case study, it is important to remember that the elliptical cross section described in this study is different from the 'quasi-elliptical' cross section drawn in the Parsifal report [10]. For the same fuselage length, applying this 'quasi-elliptical' cross section would result in a lower wetted area. The fuselage would also have a higher slenderness because the equivalent diameter is lower for the same fuselage length thus leading to a lower form factor. The difference in wetted area and in form factor would lead to a lower fuselage drag area. The difference in wetted area alone would lead to a lower fuselage weight. However, using this 'quasi-elliptical' cross section would lead this study to the same conclusion that an aisle width increase leads to a higher fuselage drag area and a higher fuselage weight.

As for the conventional fuselage, an increase in aisle width leads to an increase in fuselage drag area and in fuselage weight for the Prandtl Plane fuselage. Increasing passenger's comfort seems to come at a cost in terms of aircraft performance for medium range aircraft (conventional and Prandtl Plane).

5.3.2. INCREASING PASSENGER'S COMFORT BY SHIFTING CARGO HOLD VOLUME TO OVERHEAD BINS

This study aims at answering the following question:

What is the impact of shifting cargo hold volume to overhead bins on the fuselage performances?

The same study is performed as in section 4.3. The cross section shape is again varied in this study. The cargo is defined as bulk and not containerized. An important feature of the Prandtl Plane fuselage is that the cargo hold is continuous and not divided into a forward and an aft cargo hold as in conventional fuselages. The bulk cargo in this study has the same height and width as the ULD LD3-45.

The shift of cargo hold volume to the overhead bins has the same impact on the fuselage height and width for all the cross sections but has a different impact on the fuselage length depending on the type of cross section used. In factor, the cargo hold volume shift to the overhead bins leads ot a decrease in fuselage width and height for all the cross sections as tables 5.19 to 5.21 show. Tables 5.19 and 5.21 show that the volume shift

leads to a slightly shorter fuselage for a circular and an oval fuselage. Table 5.20 on the other hand shows that the fuselage length is slightly longer for an elliptical fuselage when the volume shift occurs.

The geometrical modifications of the fuselage due to the cargo hold volume shift to the overhead bins have been presented. These geometrical modifications have an impact on the fuselage wetted area and form factor which in turn influence the variation of fuselage drag area and fuselage weight as described in section 4.1. Tables 5.19 to 5.21 show that the cargo hold volume shift to the overhead bins leads to a decrease in wetted area and in form facto for all the cross section types. This forecasts a decrease in fuselage drag area and in fuselage weight as it was concluded in section 4.1.

Table 5.19: Circular fuselage dimensions with different aisle widths

Parameter	Unit	Reference case	Cargo hold volume shift	Difference
Fuselage height	$[m]$	6.62	6.31	-4.68%
Fuselage width	$[m]$	6.62	6.31	-4.68%
Equivalent diameter	$[m]$	6.62	6.31	-4.68%
Fuselage length	$[m]$	38.72	38.55	-0.44%
Wetted area	$[m^2]$	620.68	592.41	-4.55%
Form factor	$[-]$	1.2389	1.2243	-1.18%

Table 5.20: Elliptical fuselage dimensions with different aisle widths

Parameter	Unit	Reference case	Cargo hold volume shift	Difference
Fuselage height	$[m]$	4.06	3.9	-3.94%
Fuselage width	$[m]$	6.62	6.31	-4.68%
Equivalent diameter	$[m]$	5.18	4.96	-4.31%
Fuselage length	$[m]$	37.28	38.04	2.04%
Wetted area	$[m^2]$	599.63	586.71	-2.15%
Form factor	$[-]$	1.1832	1.173	-0.86%

Table 5.21: Oval fuselage dimensions with different aisle widths

Parameter	Unit	Reference case	Cargo hold volume shift	Difference
Fuselage height	$[m]$	5.62	5.39	-4.09%
Fuselage width	$[m]$	6.49	6.31	-1.69%
Equivalent diameter	$[m]$	6.04	5.86	-2.90%
Fuselage length	$[m]$	38.56	37.86	-1.82%
Wetted area	$[m^2]$	682.76	651.19	-4.62%
Form factor	$[-]$	1.211	1.2079	-0.26%

The results for the fuselage drag area are presented in table 5.22. This volume shift results in a lower fuselage drag area for each cross section type. The reduction of fuselage drag area varies between 3.43% for the elliptical cross section and 5.64% for the circular cross section. For each case presented in table 5.22, the highest drag area is reached for the oval cross section and the lowest drag area is reached for the elliptical cross section. The value in bold in table 5.22 shows the lowest drag area which corresponds to the elliptical fuselage with a cargo hold volume shift to the overhead bins. The cross section of this fuselage can be found in figure 5.29. This cross section is accompagnied by the cross section of the Prandtl Plane prior to the volume shift in figure 5.28. An overlap of figures 5.28 and 5.29 can be found in figure 5.30. The smaller fuselage height and width for the new fuselage are clearly visible in figure 5.30. Moreover, the larger overhead bins and the smaller cargo holds for the new fuselage are shown in figure 5.30.

The results for the fuselage weight are presented in table 5.23. This volume shift results in a lower fuselage weight for each cross section type. The reduction of fuselage weight varies between 0.37% for the elliptical

Table 5.22: Fuselage drag area results when shifting cargo hold volume into overhead bins for Prandtl Plane fuselage

Cross section type	Reference case	Cargo hold volume shift	Difference
Circle	1.223 m^2	1.154 m^2	-5.64%
Ellipse	1.137 m^2	**1.098** m^2	-3.43%
Oval	1.316 m^2	1.256 m^2	-4.56%

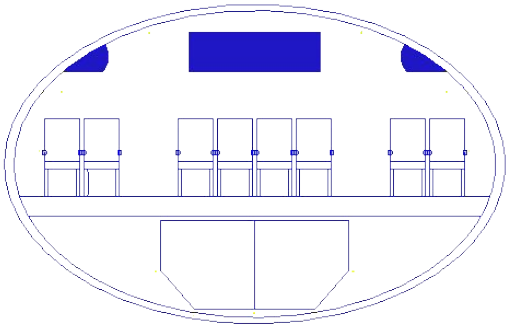

Figure 5.28: Cross section of the Prandtl Plane in ParaFuse

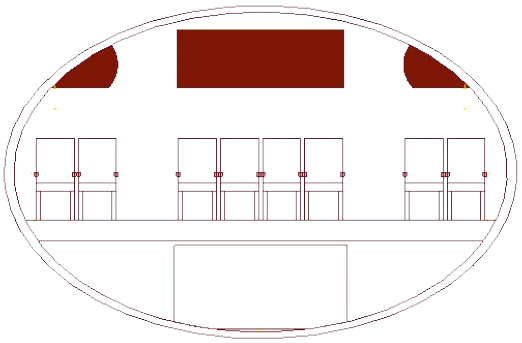

Figure 5.29: Cross section of the best Prandtl Plane fuselage in terms of drag area with a shift of the cargo hold volume to the overhead bins

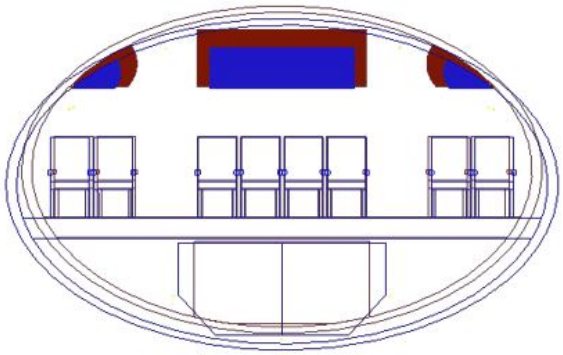

Figure 5.30: Overlap of Prandtl Plane elliptical cross section with elliptical cross section with cargo hold volume shift

cross section and 4.17% for the oval cross section. For each case presented in table 5.23, the highest fuselage weight is reached for the oval cross section and the lowest fuselage weight is reached for the circular cross section. The value in bold in table 5.23 shows the lowest fuselage weight which corresponds to the circular cross section with a cargo hold volume shift to the overhead bins.

Table 5.23: Fuselage weight results when shifting cargo hold volume into overhead bins for Prandtl Plane fuselage

Cross section type	Reference case	Cargo hold volume shift	Difference
Circle	10461 kg	**10132** kg	-3.15%
Ellipse	11175 kg	11134 kg	-0.37%
Oval	12264 kg	11753 kg	-4.17%

It can be concluded from this study that the shift of cargo hold volume to the overhead bins has an impact on the fuselage drag area and the fuselage weight. In fact, this volume shift results in a lower fuselage drag area and a lower fuselage weight for each cross section type. The best cross section regarding the fuselage drag area is the elliptical cross section. Regarding the fuselage weight, the best cross section is the circular cross section.

5.3.3. COMBINING THE SHIFT OF CARGO HOLD VOLUME TO OVERHEAD BINS AND THE INCREASE IN AISLE WIDTH

This study aims at answering the following question:

How are the fuselage performances impacted by increasing the aisle width and shifting cargo hold volume to overhead bins?

In this study, the aisle width is going to be increased, the cross section shape varied and the cargo type is changed to bulk to have a more flexible geometry when removing cargo hold volume. This study is performed as the study in section 4.4. Combining the cargo hold volume shift with the aisle width increase has a the same impact on the fuselage height but has a different impact on the fuselage width and length depending on the type of cross section used. These results are presented in tables 5.24, 5.25 and 5.26. It leads to a a decrease in fuselage height for all the cross section types. It leads to a decrease in fuselage width for the circular and the elliptical fuselages but to an increase in fuselage width for the oval cross section. Finally it leads to an increase in fuselage length for the circular and elliptical fuselages but to a decrease in fuselage length for the oval fuselage.

The geometrical modifications of the fuselage due to the cargo hold volume shift to the overhead bins combined with the aisle width increase have been presented. These geometrical modifications have an impact on the fuselage wetted area and form factor which in turn influence the variation of fuselage drag area and fuselage weight as described in section 4.1. Table 5.24 shows that the aisle width increase and the cargo hold volume shift result in a lower wetted area and a lower form factor for the circular fuselage. Table 5.25 shows that these modifications result in a slightly higher wetted area but a lower form factor. The decrease in form factor is more important in percentage than the increase in wetted area. Finally, table 5.26 shows that these modifications result in a lower wetted area but a slightly higher form factor. In this case, the decrease in wetted area is more important in percentage than the increase in form factor. This all forecasts a decrease in fuselage drag area and in fuselage weight for all the fuselages.

Table 5.24: Circular fuselage dimensions with aisle width increase and cargo hold volume shift

Parameter	Unit	Reference case	Geometrical modifications	Difference
Fuselage height	$[m]$	6.62	6.55	-1.06%
Fuselage width	$[m]$	6.62	6.55	-1.06%
Equivalent diameter	$[m]$	6.62	6.55	-1.06%
Fuselage length	$[m]$	38.72	38.86	0.36%
Wetted area	$[m^2]$	620.68	610.2	-1.69%
Form factor	$[-]$	1.2389	1.234	-0.40%

Table 5.25: Elliptical fuselage dimensions with aisle width increase and cargo hold volume shift

Parameter	Unit	Reference case	Geometrical modifications	Difference
Fuselage height	$[m]$	4.06	3.9	-3.94%
Fuselage width	$[m]$	6.62	6.55	-1.06%
Equivalent diameter	$[m]$	5.18	5.05	-2.51%
Fuselage length	$[m]$	37.28	38.12	2.25%
Wetted area	$[m^2]$	599.63	602.18	0.43%
Form factor	$[-]$	1.1832	1.1754	-0.66%

The results for the fuselage drag area are presented in table 5.27. It shows that combining the aisle width increase with the cargo hold volume shift to the overhead bins results in a lower fuselage drag area for each cross section type. The reduction in fuselage drag area varies between 0.70% for the elliptical cross section and 2.21% for the circular cross section. The lowest fuselage drag area is reached for the elliptical cross section and the highest fuselage drag area is reached for the oval cross section in both cases. The value in bold in table 5.27 shows the lowest fuselage drag area of the case study which corresponds to the elliptical cross

Table 5.26: Oval fuselage dimensions with aisle width increase and cargo hold volume shift

Parameter	Unit	Reference case	Geometrical modifications	Difference
Fuselage height	$[m]$	5.62	5.41	-3.74%
Fuselage width	$[m]$	6.49	6.62	2.00%
Equivalent diameter	$[m]$	6.04	5.98	-0.91%
Fuselage length	$[m]$	38.56	37.96	-1.56%
Wetted area	$[m^2]$	682.76	666.55	-2.37%
Form factor	$[-]$	1.211	1.2129	0.16%

section with a larger aisle width, more volume in overhead bins and less volume in the cargo holds. The cross section of this fuselage can be found in figure 5.32. This cross section is accompagnied by the cross section of the Prandtl Plane prior to the volume shift and the aisle width increase in figure 5.31. An overlap of figures **??** and 5.32 can be found in figure 5.33. The smaller fuselage height and width for the new fuselage are clearly visible in figure 5.33. Moreover, the larger overhead bins and the smaller cargo holds for the new fuselage are shown in figure 5.33. Finally, the slight increase in aisle width in observable.

Table 5.27: Fuselage drag area results when combining aisle width increase and cargo hold volume shift for Prandtl Plane fuselage

Cross section type	Reference case	Geometrical modifications	Difference
Circle	1.223 m^2	1.196 m^2	-2.21%
Ellipse	1.137 m^2	**1.129** m^2	-0.70%
Oval	1.316 m^2	1.291 m^2	-1.90%

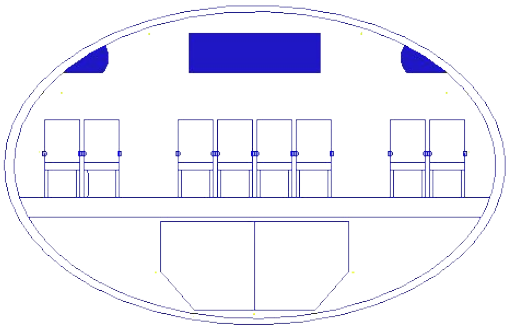

Figure 5.31: Elliptical cross section of the Prandtl Plane in Para-Fuse

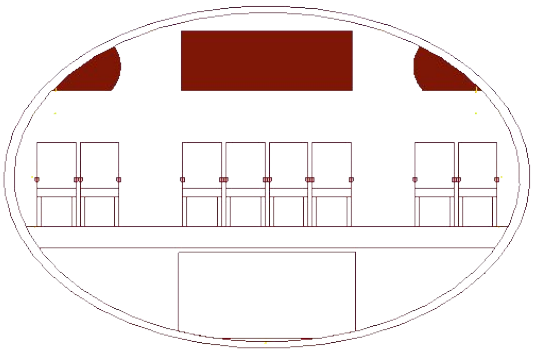

Figure 5.32: Cross section of the best Prandtl Plane fuselage in terms of drag area with a shift of the cargo hold volume to the overhead bins and aisle width increase

The results for the fuselage weight are presented in table 5.28. It shows that combining the aisle width increase with the cargo hold volume shift to the overhead bins results in a lower fuselage weight for the circular and oval cross sections but results in a higher fuselage weight for the elliptical cross section. The lowest fuselage weight is reached for the circular cross section and the highest fuselage weight is reached for the oval cross section in both cases. The value in bold in table 5.27 shows the lowest fuselage weight of the case study which corresponds to the circular cross section with a larger aisle width, more volume in overhead bins and less volume in the cargo holds.

It can be concluded that increasing passenger's comfort and shifting cargo hold volume to overhead bins results in lower fuselage drag area for the circular, elliptical and oval cross sections. It also results in lower fuselage weight for the circular and oval cross sections but results in higher fuselage weight for the elliptical cross section.

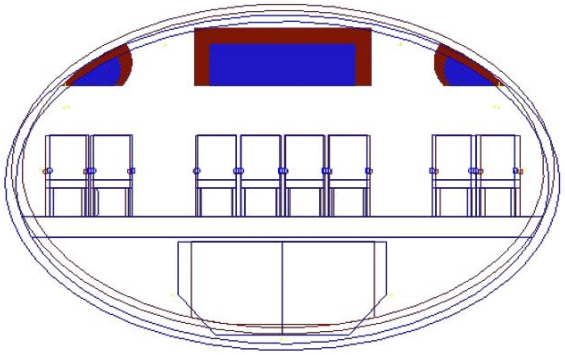

Figure 5.33: Overlap of Prandtl Plane elliptical cross section with elliptical cross section with cargo hold volume shift and aisle width increase

Table 5.28: Fuselage weight results when combining aisle width increase and cargo hold volume shift for Prandtl Plane fuselage

Cross section type	Reference case	Geometrical modifications	Difference
Circle	10461 kg	**10304** kg	-1.50%
Ellipse	11175 kg	11355 kg	1.61%
Oval	12264 kg	11955 kg	-2.52%

5.4. COMPARISON CONVENTIONAL FUSELAGE WITH PRANDTL PLANE FUSELAGE

The goal of this section is to show the main differences in terms of aircraft performances between a medium range conventional fuselage similar to the A320-200 and a Prandtl Plane fuselage. The main fuselage dimensions and passenger capacity are presented in table 5.29. The Prandtl Plane fuselage contains 65.3% more passengers than the conventional fuselage for a fuselage length only 4.56% larger. The fuselage height is relatively similar but the fuselage width is 56.79% larger for the Prandtl Plane fuselage due to the higher number of seats abreast.

Table 5.29: Fuselage dimensions and passenger capacity for conventional and Prandtl Plane fuselages

	Conventional fuselage	Prandtl Plane fuselage	Difference
Number of passengers	150	248	65.3%
Number of seats abreast	6	8	33.3%
Fuselage height	4.12 m	4.104 m	-0.38%
Fuselage width	4.11 m	6.444 m	56.79%
Fuselage length	35.36 m	37.05 m	4.56%

Each fuselage has been studied in the previous sections in terms of aircraft performances when increasing aisle width and shifting cargo hold volume to the overhead bins. Table 5.30 shows the best configuration in terms of fuselage drag area and fuselage weight for each case study per fuselage type. The first observation that can be made from these results is that the conventional fuselage has a lower fuselage drag area and a lower fuselage weight than the Prandtl Plane fuselage. This is due to the higher number of passengers and number of seats abreast of the Prandtl Plane fuselage which lead to a higher fuselage width which leads to a higher wetted area as both fuselages have approximatively the same fuselage length. The three values in bold correspond to a circular cross section whereas all the other results correspond to an elliptical cross section.

The conventional fuselage and the Prandtl Plane fuselage do not have the same payload capacity. Thus, in order to perform a proper comparison between the fuselage performances of the conventional and the Prandtl Plane fuselages, the values from table 5.30 are divided by the number of passengers of each fuselage. The results are presented in table 5.31. These results show that overall the drag area per passenger and the fuselage weight per passenger is lower for the Prandtl Plane than for the conventional fuselage.

Table 5.30: Fuselage performances comparison

Case study	Aircraft performance type	Conventional fuselage	Prandtl Plane fuselage
Reference fuselage	drag area [m^2]	0.76	1.12
	Fuselage weight [kg]	7887	10981
Increase aisle width	drag area [m^2]	0.76	1.12
	Fuselage weight [kg]	7887	**10028**
Shifting cargo hold volume	drag area [m^2]	0.727	1.098
	Fuselage weight [kg]	7810	**10132**
Increase aisle width and shifting cargo volume	drag area [m^2]	0.731	1.129
	Fuselage weight [kg]	7822	**10304**

Table 5.31: Fuselage performances comparison per passenger

Case study	Aircraft performance type	Conventional fuselage	Prandtl Plane fuselage
Reference fuselage	drag area [m^2]	$5.07 \cdot 10^{-3}$	$4.52 \cdot 10^{-3}$
	Fuselage weight [kg]	52.58	44.28
Increase aisle width	drag area [m^2]	$5.07 \cdot 10^{-3}$	$4.52 \cdot 10^{-3}$
	Fuselage weight [kg]	52.58	**40.45**
Shifting cargo hold volume	drag area [m^2]	$4.85 \cdot 10^{-3}$	$4.43 \cdot 10^{-3}$
	Fuselage weight [kg]	52.07	**40.44**
Increase aisle width and shifting cargo volume	drag area [m^2]	$4.87 \cdot 10^{-3}$	$4.55 \cdot 10^{-3}$
	Fuselage weight [kg]	52.15	**41.55**

For a medium range conventional aircraft, the best fuselage cross section is the elliptical cross section. However, for a Prandtl Plane fuselage with the same fuselage length, the best fuselage cross section is the elliptical one if one considers only the drag area but it is the circular cross section if one considers only the fuselage weight. Again it is important to remember that the elliptical cross section differs from the 'quasi-elliptical' cross section in the Parsifal report [10]. For each case study, the drag area per passenger and the fuselage weight per passenger is lower for a Prandtl Plane fuselage configuration than for a conventional fuselage configuation.

6

CONCLUSIONS & RECOMMENDATIONS

6.1. CONCLUSIONS

Due to the rapid increase in air travel expected in the years to come, requirements have been set to be tackled by the Aerospace industry. Within Europe, the focus is mainly turned to short and medium haul flights which are used to connect countries and regions. For short and medium haul flights, important requirements to be tackled are the reduction in turnaround time and the increase in passenger comfort. Turnaround time could be reduced by increasing the aisle width of the fuselage and passenger comfort could be increased by allowing passengers to bring two carry-on luggage instead of one.

The goal of this master thesis is the development of an advanced design tool that supports the conceptual design of conventional and novel fuselages to enable the investigation of such fuselages meeting the requirements of future air travel. The development of ParaFuse will allow to perform a fuselage performance study. Hence, this thesis project aims at answering the following question: to what extend can the turnaround time be reduced and passenger's comfort be enhanced by conventional and novel fuselages? What would be the opportunities offered by a Prandtl Plane configuration on the reduction of turn around time and enhancement of passenger's comfort?

The advanced design tool that has been developed in this thesis project is called ParaFuse. It is a Knowledge Based Engineering application that generates parametric fuselage models. ParaFuse has been extended in order to generate oval fuselages and double deck fuselages. It has also been improved to generate more realistic size and shape of the overhead storage compartments and continuous cargo holds for the Prandtl Plane fuselage. This new ParaFuse, called ParaFuse 2.0, has then been coupled to the Initiator in order to get the weight of the fuselage generated in ParaFuse. All this work performed has allowed to perform numerous case studies on fuselage performances.

This thesis project first answered this question: what is the impact of varying the number of seats abreast on the fuselage performances while maintaining the same number of passengers? An increase in the number of seats abreast leads to an increase in fuselage parasite drag area for every cross section type. On average the highest fuselage drag is reached when an oval cross section is applied to the fuselage and the lowest fuselage drag is reached for an elliptical cross section. As for the fuselage weight, the oval cross section fuselage leads to the highest fuselage weight and the circular cross section fuselage to the lowest fuselage weight on average. The fuselage weight does not follow a monotone trend when the number of seats abreast increases. From this study it came out that the lowest fuselage parasite drag area and the lowest fuselage weight were reached for the same fuselage: the medium range A320-200 fuselage with an elliptical cross section and 6 seats abreast.

Then this master thesis answered the following question: What is the impact of increasing the aisle width on the fuselage drag and the fuselage weight? The turn around time could be reduced by increasing the aisle width. For conventional and Prandtl Plane fuselages, an increase in aisle width results in an increase in fuselage parasite drag area and in an increase in fuselage weight. Of all the cross section types, the oval cross section leads to the highest fuselage drag area and weight. But the elliptical cross section leads to the lowest

fuselage drag and weight.

Furthermore, another question was answered: Does the shift of cargo hold volume to overhead bins have an impact on the fuselage drag and weight? It was found that this cargo hold volume shift leads to a decrease in fuselage drag area and fuselage weight for conventional and Prandtl Plane fuselages. The lowest fuselage drag area is reached for elliptical cross section for both fuselages but the lowest fuselage weight is reached for an elliptical cross section for a conventional fuselage and is reached for a circular cross section for a Prandtl Plange fuselage.

Finally, this master thesis combined both previous studies and looked at the impact on the aircraft performances. Combining the aisle width increase and the cargo volume shift leads to a decrease in fuselage parasite drag area and in fuselage weight for a conventional fuselage and a Prandtl Plane fuselage except for the fuselage weight of an elliptical cross section Prandtl Plane fuselage.

Fulfilling the requirements of the future of air travel in terms of passenger comfort and turn around time can come at a cost and lead to higher fuselage weight and drag. Combining the fulfilment of different requirements can lead to a reduction of the fuselage weight and drag as it was shown. The oval fuselage does not have any advantages for a medium range fuselage which was expected as it was defined for wide fuselages with a high passenger capacity such as the Blended Wing Body. Per passenger, the Prandtl Plane fuselage has a lower fuselage drag and weight than a conventional fuselage.

6.2. RECOMMENDATIONS

The recommendations that follow this thesis work are divided into three groups: recommendations for the development of ParaFuse, for the case studies presented in this master thesis and for future possible case studies. The recommendations for the further development of ParaFuse are:

- ParaFuse 2.0 currently runs with ParaPy 1.0.7. A new version of ParaPy has been released. ParaFuse should be made compatible with the new version of ParaPy: ParaPy 2.0.
- ParaFuse 2.0 can only generate single and twin aisle fuselages. Now that the oval fuselage has been implemented, it would be interesting to implement the possibility to generate fuselages with more than two aisles which would be a step closer to generating Blended Wing Bodies in ParaFuse.
- The double deck fuselage is generated in the inside-out approach. It would be interesting to implement the double deck fuselage in the outside-in approach as well.
- In case of a double deck aircraft, there is currently no staggering of the emergency exits. However, two emergency exits cannot be positioned on top of each other in case of a double deck aircraft because it is very inconvenient structurally. Having two emergency exits on top of each other introduces two weaknesses in a fuselage frame instead of one where the exits are located. Also, it is not feasible to have two emergency slides on top of each other. A proper rule for staggering of the exits in case of a double deck aircraft should be introduced.
- Again in case of a double deck aircraft, the assumption of no passenger seats in the nose cone has been made. This assumption should be removed. Instead, a proper calculation of the space needed for stairs, coat stoware, additional stowage and crew resting should be performed. After this calculation is performed, it would be possible to fit a few rows of seats within the nose cone thus possibly reducing the space needed on the upper deck thus possibly reducing the fuselage length.

The recommendations for the case studies presented in this master thesis are:

- The assumption was made that the cross section of the Airbus A320-200 was elliptical. This was based on the information found in the Aircraft Characteristics Airport and Maintenance Planning. Another source, the Airbus Standard Specification issue 8 from 20th June 2011, shows that the cross section of the Airbus A320-200 is double bubble. This cross section is shown in figure 6.1. Another verification of the model could be performed using the double bubble cross section.
- It would be interesting to use a Class Function/Shape Function transformation method to generate the 'quasi-elliptical' cross section of the Parsifal report [10] using a free-form cross section in ParaFuse.

- Another possibility to generate the 'quasi-elliptical' cross section of the Parsifal report [10] would be to use the oval cross section and removing the internal box. In fact, this 'quasi-elliptical' cross section is designed with a top, a bottom and two side arcs like the oval cross section. A new definition of the oval cross section would be needed because currently the generation of the four arcs is based on the position of the corners of the box.

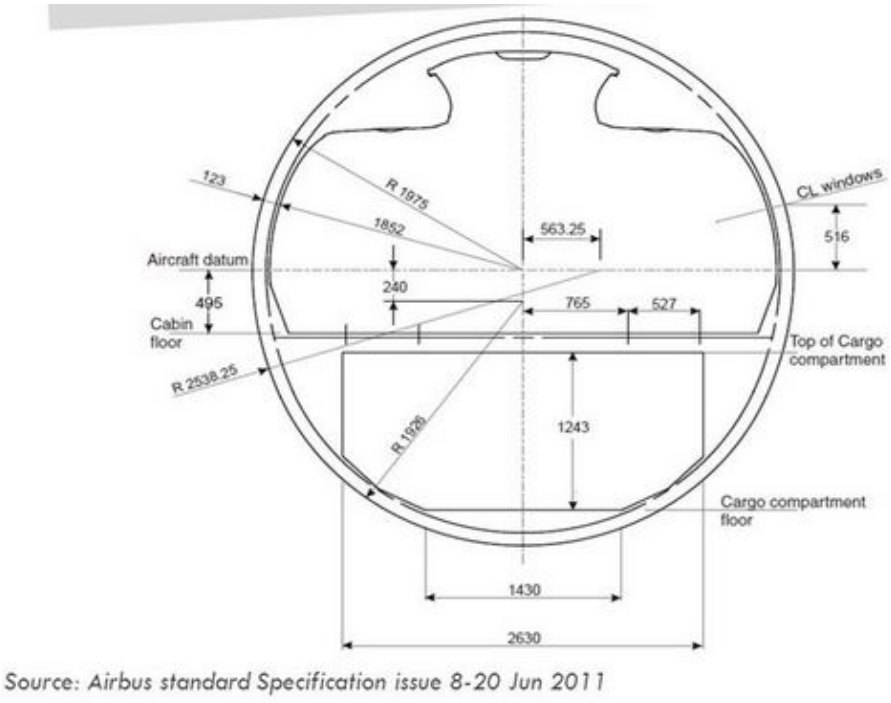

Figure 6.1: A320-200 double bubble cross section

The recommendations for future possible case studies are:

- A hypothesis has been made in this thesis project: the fact that an increase in aisle width reduces the boarding and disembarking time. A recurrent issue while boarding and disembarking a plane has been used to support this hypothesis: the aisle being blocked while a passenger is loading a carry-on luggage in the overhead storage compartments. A proper study on the turnaround time should be perfomed with the aisle width increase to measure quantitatively the impact of such an increase on the turnaround time.
- This thesis project has been focused on the fuselage component of an aircraft. The drag and weight have only been calculated for the fuselage hence there is no insight on the overall aircraft performances. The study performed in this master thesis project should be extended to an overall aircraft performance study. This could be performed thanks to the coupling of ParaFuse to the Initiator.
- An assumption was made that passengers do not only want to bring more carry-on luggage in short-medium flights but they also check-in their luggage less and less. No study was found that had gathered data about the number of carry-on luggage and the number of check-in luggage per flight. Thus, a proper study on the number of carry-on luggage and check-in luggage per flight over the last few years would help quantify what is the ratio of carry-on luggage versus check-in luggage and what is the exact trend for the years to come.

BIBLIOGRAPHY

[1] P. Kokus, M. Hepting, and A. Leipold, *Long-term performance of the global air transport system in special consideration of sustainability issues,* Deutscher Luft- und Raumfahrtkongress , 1 (2013).

[2] A. Frediani, E. Rizzo, and C. Bottoni, *A 250 Passenger PrandtlPlane transport aircraft preliminary design,* Vol. 84 (Aerotecnica Missili & Spazio, 2016) pp. 152–163.

[3] Airbus, *Aircraft Characteristics Airport and Maintenance Planning* (2005).

[4] K. Schmidt, *A Semi-Analytical Weight Estimation Method for Oval Fuselages in Novel Aircraft Configurations* (MSc thesis, Delft University of Technology, 2014) pp. 1–20.

[5] R. Cavallaro and L. Demasi, *Challenges, ideas, and innovations of joined-wing configurations: a concept from the past, an opportunity for the future,* Progress in Aerospace Sciences **87**, 1 (2016).

[6] D. Schrage, T. Beltracchi, L. Berke, A. Dodd, L. Niedling, and J. Sobieszczanski-Sobieski, *Aiaa technical committee on multidisciplinary design optimization (mdo) white paper on current state of the art,* AIAA Paper MDO Technical Committee Report (1991).

[7] J. Schut and M. Van Tooren, *Design" Feasilization" Using Knowledge-Based Engineering and Optimization Techniques,* Vol. 44 (Journal of Aircraft, 2007) pp. 1776–1786.

[8] M. Hoogreef, *The Oval Fuselage* (MSc thesis, Delft University of Technology, 2012).

[9] R. de Jonge, *Development of a Knowledge-Based Engineering Application to Support Conceptual Fuselage Sizing and Cabin Configuration* (MSc thesis, Delft University of Technology, 2017).

[10] PARSIFAL, *Report for advisors* (2017).

[11] T. Reilly, *The st. petersburg-tampa airboat line: 90 days that changed the world of aviation,* Tampa Bay History **18**, 18 (1996).

[12] International Air Transport Association, *Air Passenger Forecasts Global Report* (2016) pp. 1–4.

[13] M. Darecki, C. Edelstenne, T. Enders, E. Fernandez, P. Hartman, J. Herteman, M. Kerkloh, I. King, P. Ky, and M. Mathieu, *Flightpath 2050 Europes Vision for Aviation* (2011).

[14] R. Elmendorp, R. Vos, and G. La Rocca, *A conceptual design and analysis method for conventional and unconventional airplanes,* 29th Congress of the International Council of the Aeronautical Sciences , 1 (2014).

[15] G. Buttazzo and A. Frediani, *Variational Analysis and Aerospace Engineering: Mathematical Challenges for Aerospace Design: Contributions from a Workshop Held at the School of Mathematics in Erice, Italy,* Vol. 66 (Springer Science & Business Media, 2012).

[16] D. More and R. Sharma, *The turnaround time of an aircraft: a competitive weapon for an airline company,* Decision **41**, 489 (2014).

[17] J. A. Authorities, *Joint aviation requirements. jar-25. large aeroplanes,* Civil Aviation Authority Printing & Publication Services, Greville House **37** (1994).

[18] A. Frediani, L. Balis Crema, G. Chiocchia, G. Ghiringhelli, and L. Morino, *Development of an innovative configuration for transport aircraft; a project of five Italian universities* (XVII Congresso Nazionale AIDAA, 2003) pp. 2089–2104.

[19] E. Torenbeek, *Innovative configurations and advanced concepts for future civil aircraft* (2005) p. 661.

[20] E. Torenbeek, *Advanced aircraft design: Conceptual design, technology and optimization of subsonic civil airplanes* (John Wiley & Sons, 2013).

[21] A. Frediani, *The prandtl wing,* Von Kárman Institute for Fluid Dynamics: VKI Lecture Series: Innovative Configurations and Advanced Concepts for Future Civil Transport Aircraft. Rhode St-Genèse: Von Kárman Institute for Fluid Dynamics (2005).

[22] G. La Rocca, *Knowledge based engineering techniques to support aircraft design and optimization* (Ph.D. thesis, Delft University of Technology, 2011).

[23] Certification Specifications, *Acceptable Means of Compliance for Large Aeroplanes*, Vol. 11 (2011).

[24] R. Vos, F. Geuskens, and M. Hoogreef, *A new structural design concept for blended wing body cabins* (American Institute of Aeronautics and Astronautics (AIAA), 2012).

[25] A. Frediani, M. Gasperini, G. Saporito, and A. Rimondi, *Development of a prandtlplane aircraft configuration,* in *XVII Congresso Nazionale AIDAA (17th National Congress AIDAA), Roma* (2003) pp. 2089–2104.

[26] E. Rizzo, *Optimization Methods Applied to the preliminary design of innovative, non conventional aircraft configurations* (2009) p. 154.

[27] P. Thiede, *Aerodynamic Drag Reduction Technologies: Proceedings of the CEAS/DragNet European Drag Reduction Conference, 19–21 June 2000, Potsdam, Germany*, Vol. 76 (Springer Science & Business Media, 2013).

[28] L. Prandtl, *Induced drag of multiplanes,* National Advisory Commitee for Aeronautics **NACA-TN-182** (1924).

[29] J. Sobieszczanski-Sobieski and R. Haftka, *Multidisciplinary aerospace design optimization: survey of recent developments,* Structural optimization **14**, 1 (1997).

[30] C. Chapman and M. Pinfold, *Design engineering - a need to rethink the solution using knowledge based engineering*, Vol. 12 (Knowledge-based systems, 1999) pp. 257–267.

[31] P. Sainter, K. Oldham, and A. Larkin, *Achieving benefits from knowledge-based engineering systems in the longer term as well as in the short term* (Proceedings of: 6th International Conference on Concurrent Enterprising, 2000).

[32] C. Chapman and M. Pinfold, *The application of a knowledge based engineering approach to the rapid design and analysis of an automotive structure*, Vol. 32 (Advances in Engineering Software, 2001) pp. 903–912.

[33] D. Cooper and G. La Rocca, *Knowledge-based techniques for developing engineering applications in the 21st century* (7th AIAA ATIO Conference, Belfast, Northern Ireland, 2007).

[34] N. Milton, *Knowledge Technologies* (Advanced Engineering Informatics, 2010).

[35] J. Sobieszczanski-Sobieski, A. Morris, and M. van Tooren, *Multidisciplinary design optimization supported by knowledge based engineering* (John Wiley & Sons, 2015).

[36] B. M. Kulfan, *Universal parametric geometry representation method,* Journal of Aircraft **45**, 142 (2008).

[37] B. M. Kulfan, *Recent extensions and applications of the 'cst'universal parametric geometry representation method,* The Aeronautical Journal **114**, 157 (2010).

[38] I. Kroo and R. Shevell, *Aircraft design: Synthesis and analysis* (Desktop Aeronautics Inc., Textbook Version 0.99, 2001).

[39] T. Von Karma, *Turbulence and skin friction,* Journal of the Aeronautical Sciences (2012).

[40] E. Torenbeek, *Synthesis of subsonic airplane design: an introduction to the preliminary design of subsonic general aviation and transport aircraft, with emphasis on layout, aerodynamic design, propulsion and performance* (Springer Science & Business Media, 2013).

[41] R. L. Huston, *Principles of biomechanics. 2009,* ed: CRC Press Taylor & Francis Group (2004).

[42] M. Nita and D. Scholz, *From preliminary aircraft cabin design to cabin optimization* (Deutscher Luft- und Raumfahrtkongress, 2010).

A

UML DIAGRAM OF PARAFUSE

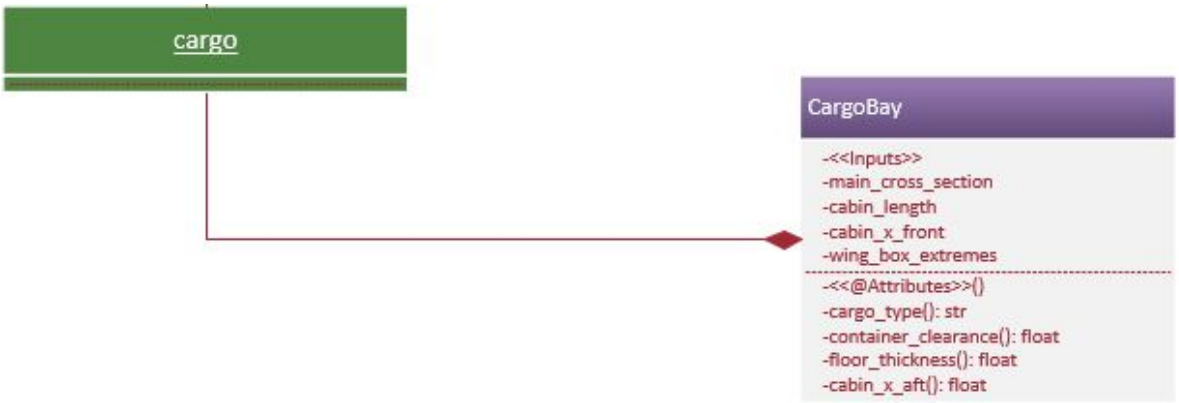

Figure A.1: Screenshot of UML diagram of class CargoBay of ParaFuse

B

ADDITIONAL IMPROVEMENTS MADE TO PARAFUSE

B.0.1. ELLIPSE CROSS SECTION IN OUTSIDE-IN APPROACH

The outside-in approach only supported circular cross sections thus the elliptical cross section was added to this approach to enlarge its capabilities and the possibilities for comparisons. To do so, the class Ellipse is used in ParaFuse. The class Ellipse requires a major radius and a minor radius which are provided by the user as inputs in the outside-in approach.

B.0.2. EQUIVALENT DIAMETER

Following the definition of the oval cross section and the elliptical cross section, a new parameter has been defined in ParaFuse: the equivalent diameter. Indeed, the diameter of the cross section is a very important parameter to determine the tail cone and nose cone lengths. These lengths are defined by the fineness of the cone and the diameter of the main cross section, as can be seen in equation B.1.

$$l = fineness * d \tag{B.1}$$

However, in case of an oval, an elliptical or a double bubble cross section, the diameter cannot be defined as the maximum width of the cross section as the diameter is not constant along the cross section. Thus, an equivalent diameter has been implemented in ParaFuse and is defined as follows:

$$d_{equivalent} = \sqrt{w_{max} * h_{max}} \tag{B.2}$$

with $d_{equivalent}$ the equivalent diameter, w_{max} the maximum width of the cross section and h_{max} the maximum height.

The equivalent diameter is also used for calculating the floor thickness during the main cross section optimization. Indeed, the floor thickness is dependent on the diameter of the main cross section. However, in case of a horizontally enlarged fuselage, the diameter (meant as the maximum width) is particularly large compared to the maximum height thus an abnormally large floor would be present. Again, in case of a vertically enlarged fuselage, the maximum width is smaller than the maximum height resulting in a too thin floor.

B.0.3. CABIN WINDOWS

The size of the cabin windows is based on the A330/A340 windows. The inputs are default but can be modified by the user in the input file if necessary. Also, the cabin windows are placed according to the fuselage frames and are independent of the seat locations. A fuselage frame has a typical length of 50 cm thus this default input has been chosen. Again, as for the dimensions of the cabin windows, this fuselage frame length can be modified by the user of the KBE application.

B.0.4. CPACS COMPATIBILITY

In order to make ParaFuse CPACS compatible, the location of a large amount of inputs had to be changed. Indeed, before this thesis project, in order to run ParaFuse, a total of six input files had to be chosen:

- main input file,
- exit data input file,
- monument data input file,
- seat data input file,
- uld data input file,
- visibility data input file.

A default name for each of these input files was hardcoded in the application thus making it very difficult for the user to modify each input file. This is why the first step towards making ParaFuse CPACS compatible was to create a unique input file containing all the data necessary for the run of ParaFuse. The next step was to identify the input which were present in the CPACS documentation [1]. ParaFuse runs now with a unique CPACS input file.

[1] www.cpacs.de